EXPLORING IOT-BASED APPLICATIONS IN POWER SYSTEMS MONITORING, DEMAND SIDE MANAGEMENT AND PROTECTION

by

LONG ZHAO

DISSERTATION

Submitted in partial fulfillment of the requirements
for the degree of Doctor of Philosophy at
The University of Texas at Arlington
August, 2020

Arlington, Texas

Supervising Committee:

Dr. Wei-Jen Lee, Supervising Professor
Dr. David A Wetz
Dr. Ali Davoudi
Dr. Ramtin Madani
Dr. Rasool Kenarangui
Dr.William E. Dillon, Graduate Advisor

ABSTRACT

EXPLORING IOT-BASED APPLICATIONS IN POWER SYSTEMS

MONITORING, DEMAND SIDE MANAGEMENT AND PROTECTION

Long Zhao, Ph.D.

The University of Texas at Arlington, 2020

Supervising Professor: Wei-Jen Lee

The Internet-of-Things (IoT) concept allows objects to share data through wired or wireless connections for communication purposes. Currently, IoT has been involved with the development of smart grids in many applications. In this article-based dissertation, IoT applications in power systems are presented in 7 published research papers.

In the first three papers, the developments of the IoT-based monitoring system are presented. Power substation monitoring for the petrochemical facility is discussed in the first paper. Internal design and detection mechanisms are emphasized in this research. The second paper presents the communication and task allocations for a generic power substation monitoring system. The third paper shows a holistic monitoring system for wind turbine considering both Subsynchronous Control Interaction detection and condition monitoring.

The fourth and fifth papers presented a study for demand-side management (DSM) at the residential level and commercial level respectively. Comparing with traditional power meters, smart meters can provide much more detailed information that can be applied in IoT applications such as DSM. In the fourth paper, the research is to examine the key reasons for the underlying ineffectiveness/effectiveness of one type of DSM programs at the residential level using real residential

smart meter data. In the fifth paper, the potential of DSM for commercial consumers is analyzed considering energy storage based on real smart meter data of commercial consumers.

In the sixth paper, a new approach for arc flash fault detection by using the spectrum of the light is developed in this research. By examining the spectrum of the light, arc flash can be accurately and quickly detected. This research is being extended for arcing fault type identification with IoT technology to improve the current arc flash protection operation and provide more detailed information for system operators, and it is presented in the last paper.

ACKNOWLEDGEMENTS

I would like to express my deepest appreciation to my supervising professor Dr. Wei-Jen Lee for his consistent support, guidance, and overall insights in this filed which have made my Ph.D. studies an inspiring experience for me.

I would also like to extend my gratitude to my dissertation defense committee members, Dr. David A. Wetz, Dr. Ali Davoudi, Dr. Ramtin Madani, Dr. Rasool Kenarangui, and Dr. William Dillon for their instructive guidelines and constructive comments on my dissertation. Meanwhile, I would like to thank Dr. Zhiyong yang for his help during my Ph.D. studies especially in the Interdisciplinary research we have done.

I would also like to thank my lab mates and good friends from the Energy Systems Research Center (ESRC) Dr. Igor B. M. Matsuo, Mr. Yuhao Zhou, Dr. Shiuan-Hau Rao, Dr. Kun-Long Chen, Dr. Franklin L. Quilumba, Dr. Farshid Salehi and Dr. Suratsavadee Koonlaboon Korkua who have provided creative and constructive research ideas. With their supports, we, therefore, could have transformed our research results into high-quality publications.

DEDICATION

I dedicate this work to my Supervising Professor, Dr. Wei-Jen Lee, he has not only showed me how to be an outstanding researcher and a great faculty member in the education system but also demonstrate how to be a person with integrity, courage, patience, and confidence in his daily life. Without his help, I am not able to achieve what I have achieved.

I dedicate this work to my family especially to my parents Mingliang Zhao and Fengyun Lv. I am extremely grateful for their endless support and love. I also want to dedicate this work to my grandfather Anshan Zhao who is no longer with us today. I hope I have made him proud.

I would like to dedicate this work to Dr. Yaowu Hao. Without his help, I would not have the chance to meet my advisor Dr. Lee and join his research group. I also want to dedicate this work to my American family and friends from Wichita, Kansas. Without their unending support and inspiration, I would not be able to finish this dissertation.

TABLE OF CONTENT

ABSTRACT ii

ACKNOWLEDGEMENTS v

DEDICATION vi

TABLE OF CONTENT vii

LIST OF FIGURES xii

LIST OF TABLES xvii

CHAPTER 1 1

1.1 BACKGROUND 2

1.2 SUMMARY OF PUBLICATIONS 2

1.3 REFERENCE 4

CHAPTER 2 6

2.1 INTRODUCTION 8

2.2 STRUCTURE AND FUNCTIONS OF THE MONITORING SYSTEM 11

2.2.1 Hardware Configuration 12

2.2.2 Event-Triggering Mechanisms and Recording Functions 13

2.3 SUBSYNCHRONOUS OSCILLATION MONITORING 16

2.4 IN-LAB MONITORING SYSTEM TEST 17

2.5 CONCLUSION 22

2.6 REFERENCES 22

CHAPTER 3 26
3.1 INTRODUCTION 28
3.2 FRAMEWORK OF THE IIOT-BASED MONITORING SYSTEM 30
3.2.1 Data Acquisition 32
3.2.2 Timestamps and Synchronization 33
3.2.3 Data Display 34
3.2.4 Data Logging 35
3.3 DATA COMMUNICATION AND PROCESSING 36
3.3.1 Tag Communication method 37
3.3.2 Stream Communication method 37
3.3.3 File Transfer Protocol (FTP) 38
3.3.4 Publish-Subscribe Pattern (PSP) 38
3.4 CYBERSECURITY OF THE SYSTEM 39
3.5 IN-FIELD TEST AND APPLICATION 40
3.6 NOVELTY OF THE DEVELOPED MONITORING SYSTEM 41
3.7 CONCLUSION 42
3.8 REFERENCE 42
CHAPTER 4 47
4.1 INTRODUCTION 49
4.2 STRUCTURE OF THE MONITORING SYSTEM 51

4.3 OPERATION OF THE MONITORING SYSTEM 52
4.3.1 Data Acquisition 52
4.3.2 Data Processing 54
4.3.3 Data Logging 54
4.4 SSCI DETECTION AND CONDITION MONITORING OF THE WIND TURBINES 54
4.4.1 SSCI Detection 55
4.4.2 Condition Monitoring of Wind Turbines 55
4.5 IN-LAB MONITORING SYSTEM TEST 57
4.5.1 SSCI Detection 57
4.5.2 Fault Detection of Induction Machine 58
4.6 CONCLUSION 62
4.7 REFERENCES 62
CHAPTER 5 65
5.1 INTRODUCTION 67
5.2 TOU IN A DEVELOPING COUNTRY (SHANGHAI, CHINA) 69
5.2.1 VR for Different Income Levels 70
5.2.2 VR for Different Housing Sizes 71
5.2.3 VR for Different Number of Residents in One House 73
5.2.4 VR for All Customers 74
5.3 THE NEED OF EFFECTIVE TIME-OF-USE (TOU) PROGRAMS 75

5.4 SIGNIFICANCE OF ZERO-PRICE AND ZERO-PRICING TOU IN TEXAS 78
5.4.1 Zero-Price 78
5.4.2 Zero-Pricing TOU in Texas 79
5.5 ASSESSMENT OF ZERO-PRICING BENEFITS 81
5.5.1 Benefits for Residential Customers 81
5.5.2 Benefits for Utility Companies 83
5.6 CONCLUSION 85
5.7 REFERENCES 85
CHAPTER 6 90
6.1 INTRODUCTION 92
6.2 RESEARCH STRUCTURE AND METHODOLOGIES 95
6.3 DEMAND ANALYSIS OF COMMERCIAL CONSUMERS 96
6.3.1 Power Consumption of Commercial Consumers 97
6.3.2 Peak Power Consumption Percentage 99
6.3.3 PDF of Derivatives of Daily Load Profile 101
6.4 FINANCIAL ANALYSIS OF THE DSM PROGRAM 104
6.5 HYBRID DSM PROGRAM 107
6.6 CONCLUSION 111
6.7 REFERENCES 111
CHAPTER 7 114

7.1 INTRODUCTION 116
7.2 ARC FLASH SPECTRUM MEASUREMENT 117
7.2.1 Arc Flash Test 117
7.2.2 Spectrum Measurement 119
7.3 ARC FLASH DETECTION ALGORITHM 126
7.3.1 The Derivative of Spectral Lines of Arc Flashes 126
7.3.2 The Derivative of Spectral Lines of Ambient Light Sources 129
7.3.3 General Regression Neural Network (GRNN) 131
7.4 CONCLUSIONS 134
7.5 REFERENCES 134
CHAPTER 8 137
8.1 CONCLUSION 138
8.2 THE FUTURE RESEARCH DIRECTION 139

LIST OF FIGURES

Figure Page

Fig. 2.1 Oscilloscope record of a subsynchronous event 9

Fig. 2.2 Real-Time web-based monitoring system 11

Fig. 2.3 Structure of DAQ controllers 12

Fig. 2.4 DAQ controller 13

Fig. 2.5 In-Lab system setup 17

Fig. 2.6 Raw data of voltage 17

Fig. 2.7 RMS value of voltage 18

Fig. 2.8 Frequency of the power system 18

Fig. 2.9 Voltage, frequency, and power monitoring panel 18

Fig. 2.10 Power Osccilation Monitoring Mechanism 19

Fig. 2.11 Circuit Breaker Status 19

Fig. 2.12 60Hz 120Vrms signal plus 37.5Hz 12Vrms SSO signal 20

Fig. 2.13 FFT of the demodulated signal 20

Fig. 2.14 Variable Autotransformer 21

Fig. 3.1 FPGA Embedded Controller 31

Fig. 3.2 Framework of IoT-Based Real-time Monitoring system 32

Fig. 3.3 Synchronization and Timestamping Process 34

Fig. 3.4 Data Synchronization and Logging 34

Fig. 3.5 HMI of the Monitoring System 35

Fig. 3.6 Stream Communication on the Controller 38

Fig. 3.7 Cybersecurity Setup of the System 39

Fig. 3.8 Installation at the Substation. 40

Fig. 3.9 Recorded Voltage Fault Event Data 41

Fig. 4.1 Structure of a Holistic IoT-Based health monitoring system 52

Fig. 4.2 The FPGA-CPU hybrid controller with input modules 53

Fig. 4.3 FPGA-CPU hybrid controller operation 54

Fig. 4.4 SSCI detection process on the hybrid controller 55

Fig. 4.5 Process of the wind turbine vibration analysis scheme 56

Fig. 4.6 SSCI Testing Simulation 57

Fig. 4.7 Flywheel Design for Rotor Imbalance 58

Fig. 4.8 Tri-axial Accelerometer Measurement on the Motor Housing 58

Fig. 4.9 The System Setup for Rotor Imbalance Test 59

Fig. 4.10 Crest Factor for Different Load Masses 60

Fig. 4.11 The FFT of the Vibration Signal with Different Masses for Each Axis 61

Fig. 4.12 Front Panel of the IoT-Based Multipurpose Monitoring System 61

Fig. 5.1 PDF of VR for customers whose income is less than 3,000USD per year 71

Fig. 5.2 PDF of VR for customers whose income is greater than 36,000RUSD per year 71

Fig. 5.3 PDF of VR for customers whose housing size is less than 10 m^2 72

Fig. 5.4 PDF of VR for customers whose housing size is greater than 150 m^2 72

Fig. 5.5 PDF of VR for A House Having 1 Resident 73

Fig. 5.6 PDF of VR for A House Having 5 Residents 74

Fig. 5.7 PDF of Valley Ratio for Residential Customers in Shanghai 74

Fig. 5.8 The percentage of customers whose VR is greater than 50% 75

Fig. 5.9 Locational Marginal Price (LMP) of ERCOT at 11:15, Oct. 08, 2012 77

Fig. 5.10 CAISO Net Generation and Average Hourly Price 77

Fig. 5.11 Monthly usage of customer A 80

Fig. 5.12 Monthly usage of customer B 80

Fig. 5.13 PDF of Valley Ratio for Residential Customers in NYC 83

Fig. 5.14 Customer B's Hourly Load Profile for a Week in August 84

Fig. 6.1 Monthly Consumption Pattern of a Customer 93

Fig. 6.2 Hourly Consumption Pattern of a Customer 94

Fig. 6.3 Breakdown of the Consumption of a Customer 94

Fig. 6.4 PDF of Daily Power Consumption for all Consumers in June (2012-2014) 97

Fig. 6.5 PDF of Daily Power Consumption for all Consumers in July (2012-2014) 97

Fig. 6.6 PDF of Daily Power Consumption for all Consumers in August (2012-2014) 98

Fig. 6.7 PDF of Daily Power Consumption for all Consumers in September (2012-2014) 98

Fig. 6.8 PR of June (2012-2014) 99

Fig. 6.9 PR of July (2012-2014) 100

Fig. 6.10 PR of August (2012-2014) 100

Fig. 6.11 PR of September (2012-2014) 101

Fig. 6.12 PDF of *dp* in June (2012-2014) 102

Fig. 6.13 PDF of *dp* in July (2012-2014) 102

Fig. 6.14 PDF of *dp* in August (2012-2014) 103

Fig. 6.15 PDF of *dp* in September (2012-2014) 103

Fig. 6.16 PDF of DIC in June (2012-2014) 105

Fig. 6.17 PDF of DIC in July (2012-2014) 105

Fig. 6.18 PDF of DIC in August (2012-2014) 106

Fig. 6.19 PDF of DIC in September (2012-2014) 106

Fig. 6.20 Daily Financial Savings in June (2012-2014) 109

Fig. 6.21 Daily Financial Savings in July (2012-2014) 109

Fig. 6.22 Daily Financial Savings in August (2012-2014) 110
Fig. 6.23 Daily Financial Savings in September (2012-2014) 110
Fig. 7.1 Arc Flash Spectrum Measurement Station 118
Fig. 7.2 Coaxial Optical Fiber Sensor 118
Fig. 7.3 Arc Flash 119
Fig. 7.4 Spectral Line of Experiment 1 120
Fig. 7.5 Spectral Line of Experiment 2 120
Fig. 7.6 Spectral Line of Experiment 3 121
Fig. 7.7 Spectral Line of Experiment 4 122
Fig. 7.8 Light Spectrum [12] 123
Fig. 7.9 Spectral Line of Arc Flash for All Experiments 123
Fig. 7.10 Nitrogen Spectrum Between 300 nm and 400 nm in dry air at 1013hPa 124
Fig. 7.11 Spectral Line of LED Light 124
Fig. 7.12 Spectral Line of Fluorescent Light 125
Fig. 7.13 Spectral Line of Daylight 125
Fig. 7.14 The Derivative of Y in Experiment 1 127
Fig. 7.15 The Derivative of Y in Experiment 2 127
Fig. 7.16 The Derivative of Y in Experiment 3 128
Fig. 7.17 The Derivative of Y in Experiment 4 128
Fig. 7.18 The Derivative of Y of LED 129
Fig. 7.19 The Derivative of Y of Fluorescent 129
Fig. 7.20 The Derivative of Y of Sunshine 130
Fig. 7.21 The Derivative of Y of Indirect Daylight 1 130
Fig. 7.22 The Derivative of Y of Indirect Daylight 2 131

Fig. 7.23 Derivative of Y from 300 nm to 400 nm 132

Fig. 7.24 Filtered Derivative of Y from 300 nm to 400 nm 132

Fig. 7.25 GRNN Training Process 133

Fig. 7.26 Detection Process with GRNN 133

LIST OF TABLES

Table Page

TABLE 2 - 1. FPGA Utilization 10

TABLE 2 - 2. Data Type and Data Rate of Each Module on DAQ Controllers 13

TABLE 2 - 3. Power Detection Triggering and Recording Mechanisms 15

TABLE 2 - 4. Recorded Raw Voltage Data (2000S/s) 21

TABLE 3 - 1. Data Acquisition Modules and Sampling Rates 33

TABLE 3 - 2. One Phase of Voltage Data Logging File 36

TABLE 4 - 1. Input Data Type and Rates of Input Modules 53

TABLE 4 - 2. RMS VALUES OF THE VIBRATION SIGNAL 59

TABLE 5 - 1. TIME-OF-USE RATES IN SHANGHAI 69

TABLE 5 - 2. Profile of Residential Data in Shanghai 69

TABLE 5 - 3. Average Valley Ratio for Different Income Levels 70

TABLE 5 - 4. Average Valley Ratio for Different Housing Sizes 72

TABLE 5 - 5. VR for different number of residents 73

TABLE 5 - 6. Profile of Customer A and B 80

TABLE 5 - 7. Monthly Percentage of Bill Savings 81

TABLE 5 - 8. Assumed Zero-Pricing Rates in Shanghai 81

TABLE 5 - 9. Average Bill Savings Annually for each customer in Shanghai in USD 82

TABLE 5 - 10. Profile of Residential Data in NYC 82

TABLE 5 - 11. Average Bill Savings Annually for each customer in NYC 83

TABLE 5 - 12. Savings on Transmission Charge in 2017 for The Utility Company 85

TABLE 6 - 1. Commercial Consumers TOU Delivery Rates 96

TABLE 6 - 2. Commercial Consumers Standard Delivery Rates 104

TABLE 7 - 1. Arc Flash Experiment 119

CHAPTER 1.

INTRODUCTION

1.1 BACKGROUND

In the document “Towards a definition of the internet of things” published by IEEE Internet of Things (IoT), IoT has been defined differently in different professional organizations. The initial idea and rudiment of the origin of IoT were proposed to promote RFID. At that time, the term “IoT” did not exist. With the development of Internet and network communication, the concept of IoT was formalized and utilized by the Auto-ID Center at MIT in 1999. Since then, IoT has been largely used and implemented in various fields. Within different scientific areas and organizations, IoT has been defined as slightly different with specific focuses. IEEE defines IoT as “A network of items—each embedded with sensors—which are connected to the Internet.” The United Nations specialized agency for information and communication technologies ITU defines IoT as a network that is “Available anywhere, anytime, by anything and anyone.” In the definition of The Internet Engineering Task Force (IETF), IoT is described as an object that could communicate seamlessly. The National Institute of Standards and Technology (NIST) refers to Cyber-physical systems (CPS) as the IoT which connects devices or systems in different areas to provide a communication platform. Organization for the Advanced of Structured Information Standards (OASIS) describes IoT as “System where the internet is connected to the physical world via ubiquitous sensors.” Therefore, IoT could be generalized as a platform that provides a communication capability to transfer and to store the data among different objects [1].

In power systems, IoT is considered one of the most critical components to transform the current power grid into a smart grid. In the publication of [2] “Review of Internet of Things in Electric Power and Energy Systems”, benefits of IoT for power systems are summarized below:

- Reliability, resiliency, adaptability, and energy efficiency can be improved using IoT.
- Communication protocols in the system can be lessened.
- The operation can be enhanced with more information provided by IoT.
- IoT provides a platform for demand-side management.
- Sensing capabilities can be improved.
- Scalability and interoperability can be enhanced.
- Mitigate damages from natural disasters.
- Avoid physical attacks.

1.2 SUMMARY OF PUBLICATIONS

Currently, IoT can be applied in different areas within power systems. To utilize the platform of IoT, this dissertation explores the application of IoT from three different perspectives including monitoring,

demand-side management, and protection. In this dissertation, seven published research papers are presented.

In Chapters 2, 3, and 4, different applications of IoT-based monitoring systems are discussed.

In Chapter 2, the paper titled “Development of a real-time web-based monitoring system for the substation of petrochemical facilities.” The paper was published in IEEE Transactions on Industry Applications in 2019. As the first author of this paper, I finished the structure and the function design of the monitoring system. Dr. Igor Matsuo and Dr. Farshid Salehi worked on the subsynchronous oscillation monitoring part. Mr. Yuhao Zhou helped us with the in-lab testing and provided some ideas on the paper writing. Our advisor Dr. Wei-Jen Lee provided the core idea of this development and helped us with the equipment we need in the development. This paper shows that a complete monitoring system for power substations at petrochemical facilities can be designed using the IoT platform.

In Chapter 3, the paper titled “Design of an Industrial IoT-based monitoring system for power substations” is presented. This paper was published in IEEE Transactions on Industry Applications in 2019. In this monitoring system, I developed functions of data acquisition, timestamps and synchronization, and data display. Dr. Igor Matsuo worked on the feature of data logging. In data communication and processing, I implemented the tag communication method, Stream communication method, and publish-subscribe pattern in this development. Dr. Igor Matsuo implemented a file transfer protocol for data logging development. Mr. Yuhao Zhou provided constructive ideas on Cybersecurity of the system. As the advisor, Dr. Wei-Jen Lee provided valuable suggestions on this design. He also helped us with the system installation in the field. Comparing with the previous monitoring system design for power substation at petrochemical facilities, this paper is extended research of Chapter 2. Provided overall construction of the monitoring system for a power substation. especially different communication protocols are considered to optimize the performance of an IoT-based monitoring system.

In Chapter 4, the paper “The design of a remote online Holistic monitoring system for a wind turbine” is presented. This paper was published in IEEE Transactions on Industry Applications in 2020. As the first author, I adopted a previous development for wind turbine condition monitoring which was done by the co-author Dr. Suratsavadee Koonlaboon Korkua and implemented on a new IoT platform with an additional monitoring function. Co-author Mr. Yuhao Zhou provided information on internal wind turbine design. Co-author Dr. Igor Matsuo developed SSCI detection and data logging in this system. Our advisor Dr. Wei-Jen Lee provided insightful knowledge on this topic and helped us with all the equipment we need. Based on the first two developed IoT-based monitoring systems we developed, this IoT monitoring

platform is applied to wind turbine considering both condition monitoring and SSCI monitoring. This paper again shows the wide application of IoT-based monitoring systems in power systems.

In Chapters 5 and 6, the application of DSM is analyzed at residential and industrial levels respectively using real smart meter data. These two studies are preliminary studies for IoT-based DSM for different types of consumers.

In Chapter 5, the paper named “The impact of time of use (TOU) rate structure on consumption patterns of the residential customers” is included. This paper was published in IEEE Transactions on Industry Applications in 2017. As the first author, I analyzed smart meter data and provided the analysis results of this research. The co-author Dr. Zhiyong Yang provided smart meter data from Shanghai, China, and zero-price background from a marketing perspective. Dr. Wei-Jen Lee pointed out the direction of this research in the beginning and provided the smart meter data from New York City. This study result shows that the special pricing mechanism has a significant impact on the effectiveness of DSM at the residential level. considering the increasing penetration of renewable energy resources, the special pricing mechanism can be considered for IoT-based DSM (Real-time pricing) and smart home in the future.

In Chapter 6, the paper titled “Potential of the commercial sector to participate in the demand side management program” is shown. As the first author of this paper, I did data analysis with real smart meter data of commercial consumers collected from New York City. Mr. Yuhao Zhou helped me with data cleaning and arrangement. Dr. Franklin L. Quilumba helped me with data understanding and analytic ideas. Dr. Wei-Jen Lee provided constructive suggestions and revised the paper. This study shows the financial evaluation results and feasibility of DSM considering energy storage for commercial consumers. As the preliminary study of IoT-based DSM, this study provides a practical view of DSM on commercial consumers.

In Chapter 7, a preliminary study of IoT application in power system protection is presented.

In Chapter 7, the paper titled “Using the spectrum of the light for high speed arcing fault detection” is included. As the first author of this paper, I finished all experiments and did data analysis. Co-author Yuhao Zhou helped me with General Regression Neural Network. Dr. Kun-Long Chen helped me set up a spectrum measurement station. Dr. Shiuan-Hau Rau provided test materials. Dr. Wei-Jen Lee shared the idea of arcing fault detection using spectrum and provided insightful knowledge in arc flash. Based on the results of this study, this approach has been extended for fault type identification which is also published in paper [3].

1.3 REFERENCE

[1] R. Minerva, A. Biru, and D. Rotondi, “Towards a definition of the internet of things (ToT),” Telecom Italia S.p.A, May. 27, 2015. Accessed: March. 17, 2020[Online]. Available:

http://iot.ieee.org/images/files/pdf/IEEE_IoT_Towards_Definition_Internet_of_Things_Revision1_27MAY15.pdf

[2] G. Bedi, G. K. Venayagamoorthy, R. Singh, R. R. Brooks, K. Wang, "Review of internet of things (IoT) in electric power and energy systems," *IEEE IoT. J*, vol. 5, pp. 847-870, Apr. 2018

CHAPTER 2.

DEVELOPMENT OF A REAL-TIME WEB-BASED MONITORING SYSTEM FOR THE SUBSTATION OF PETROCHEMICAL FACILITIES

DEVELOPMENT OF A REAL-TIME WEB-BASED MONITORING SYSTEM FOR THE SUBSTATION OF PETROCHEMICAL FACILITIES[1]

Long Zhao, Igor Matsuo, Farshid Salehi, Yuhao Zhou, Wei-Jen Lee

L. Zhao, I. Matsuo, F. Salehi, Y. Zhou. and W. Lee, "Development of a Real-Time Web-Based Power Monitoring System for the Substation of Petrochemical Facilities," *IEEE Trans. Ind. Appl.,* vol. 55, Jan/Feb. 2019. pp. 43-50.

DEVELOPMENT OF A REAL-TIME WEB-BASED POWER MONITORING SYSTEM FOR THE SUBSTATION OF PETROCHEMICAL FACILITIES

Long Zhao Igor Matsuo Farshid Salehi Yuhao Zhou* Wei-Jen Lee

Student Member, IEEE Student Member, IEEE Student Member, IEEE Student Member, IEEE Fellow, IEEE

University of Texas at Arlington, 701 S Nedderman Dr, Arlington, TX 76019, USA

long.zhao@mavs.uta.edu, matsuoigor@gmail.com, farshid.salehi@mavs.uta.edu, yuhao.zhou@mavs.uta.edu*, wlee@uta.edu

Abstract -- Petrochemical industry not only consumes a large amount of electricity every year but also requires high-quality power supplies. Any unexpected power failure could shut down the entire production line and cause significant financial loss. Meanwhile, due to the large electricity consumption and intensive power demand, in-house cogeneration plants have been equipped for most petrochemical facilities. Thus, any power interruption or disturbance between a petrochemical facility and interconnected power grids could affect both sides of the power systems. Therefore, having high power quality becomes one of the most critical parts for petrochemical facilities. To avoid unexpected power failure and to provide a better understanding of the power system at petrochemical facilities, a fast, precise and reliable power monitoring system is required. A novel Real-Time Web-Based Power Monitoring system on field-programmable gate array (FPGA) platform is developed in this paper for a power substation at the petrochemical facility. Besides the data collecting with event triggering mechanism and measurement data recording functions, Subsynchronous Oscillation (SSO) detection application is also developed in this system. This monitoring system could provide precise data to help engineers with insightful analysis of the electric system to prevent a power failure, and it also could help system operators to have a better understanding of the system operation characteristics.

Index Terms—FPGA, monitoring system, petrochemical, power systems, subsynchronous oscillation (SSO), Subsynchronous control interaction (SSCI), subsynchronous torsional interactions (SSTI).

2.1 INTRODUCTION

30% of industrial energy is consumed by the petrochemical sector, which makes it the largest energy consumer in the industry [1]. More than 225 billion kWh of electricity are consumed by petrochemical industry annually in the U.S, and it is close to 7% of global electricity generation in one year [2, 3]. Since the operation of a petrochemical facility heavily relies on electricity, any short time power interruption could cause an entire plant shutdown and lead to a significant financial loss for petrochemical

businesses [4]. Therefore, it is vitally important to maintain high-power reliability for petrochemical facilities.

Due to the large electricity demand and the special demand characteristics of the petrochemical industry, in-house cogeneration plants have been installed for most petrochemical facilities [5]. Usually, the power demand for these facilities is from both cogeneration plants and interconnected power grids. The excess power generation produced by cogeneration plants could be sold to interconnected power grids [4, 5]. Due to the interconnection between in-house cogeneration and power grids, any unexpected interactions between these two systems could bring serious consequences to both sides. Subsynchronous Oscillation (SSO) could be one of these interactions. With the development of SSO study, subsynchronous torsional interactions (SSTI) and subsynchronous control interaction (SSCI) were also formed based on different scenarios. SSTI is the interaction between the generator and the shaft power control equipment at the subsynchronous frequency [6], and it mainly associate with synchronous machines [7][8]. Another phenomena SSCI is defined as the interaction between wind turbine controller and series compensation system at subsynchronous frequency [6]. In current power systems, capacitor compensation has been applied to improve the quality and efficiency of the transmission network. Meanwhile, due to the energy and environmental concerns, implementation of wind energy has been increased in recent years. However, massive application of series capacitor compensation and wind generation could potentially lead to SSO [8-12]. Due to the special characteristics of SSO, normal protection relays are not able to work properly to prevent serious consequences [13-15]. In Oct 2009, SSCI was caused by a single line to ground fault in South Texas. After the single line to ground fault was cleared, the wind farms were directly connected to series compensated transmission line and 22Hz oscillation was triggered between the wind turbine control system and the fixed series compensation [16]. The system voltage exceeded 2 p.u around 150ms and subsynchronous frequency of all three phase voltages and currents reached to 3 p.u. in 400ms which is shown in Fig. 2.1. This event led to severe damage on wind turbines and series capacitors and caused unstable power and voltage oscillation in the nearby area [6, 16].

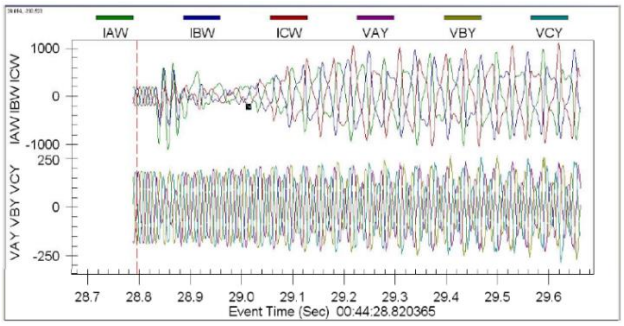

Fig. 2. 1 Oscilloscope record of a subsynchronous event [13]

Therefore, it is necessary to develop an SSO monitoring system for petrochemical facilities with in-plant cogenerations which are interconnected to power grids. This SSO monitoring system with alarm function could provide real-time information for system operators of petrochemical facilities to avoid SSTI on-cogeneration plants, and it can also prevent the impacted of SSCI caused by neighboring facilities.

Currently, various monitoring systems for power substations have been proposed and applied for different purposes [17-23]. In paper [17], a GPRS-based remote online power monitoring system with the multi-information acquisition was proposed. In paper [18], a monitoring system is introduced for energy and power quality analysis so that PQ disturbances and waveform quality could be evaluated. In paper [19], a comprehensive monitoring system based on 10-minute and hourly average measurement data is developed and implemented at a secondary substation for customer power quality monitoring. In paper [20], a combined monitoring system is designed for meter reading and event logging at a substation. In the study [21], the authors used Quality Function Deployment (QFD) tool to develop a substation monitoring system application. In paper [22], a monitoring system research is established based on the virtue of CAN technology for a DC substation. Paper [23] presents a monitoring system for the protection events at the power substation.

In this paper, a real-time web-based power monitoring system is developed with a field-programmable gate arrays (FPGA) platform hardware. FPGAs are reprogrammable silicon chips which were invented in 1985 [24,25]. Due to the special hardware design, FPGAs have better computing power than digital signal processors (DSPs). Therefore, inputs and outputs at the hardware level could be controlled with faster response [24]. In this study, fast response and computing speed provide the precise sampling data so that any analysis that requires high-speed sampling frequency, such as signal frequency domain analysis and transient study analysis, can be realized by using FPGAs. Additionally, since FPGA circuitry is reprogrammable hardware, it is more reliable than software programming environment-based applications [25]. Hence, it can be applied to substations with minimized reliability concerns. In this system, an industrial commercialized device is used in this monitoring system. The hardware resources of this type of FPGA is indicated by the number of slices contained in the FPGA. A slice consists of look-up tables (LUTs) and Flip-Flops. For Kintex-7, a slice contains 4 of LUTs and 8 of Flip Flops [26]. The utilization of the system is shown in Table 2-1.

TABLE 2- 1. FPGA Utilization

Device Utilization	Used	Total	Percent
Total Slices	35044	50950	68.8

Slice LUTs	92916	203800	51.2
Block RAMs	21	445	4.7
DSP48s	317	840	37.7

This paper is organized as follows. Section 2.2 presents the design and functions of the system. Section 2.3 introduces the SSO monitoring application in the system. Section 2.4 presents the in-lab monitoring results of the monitoring system. Section 2.5 is the conclusion.

2.2 STRUCTURE AND FUNCTIONS OF THE MONITORING SYSTEM

This monitoring system on an FPGA platform consists of different data acquisition modules and an embedded controller. The purpose of this system is to collect data at the power substation of petrochemical facilities in real time. Additionally, different event-triggering mechanisms and time-stamped data recording functions are also implemented. The overall structure of the monitoring system is shown in Fig.2.2. As one of the communication options for the controller, TCP/IP is used in this monitoring system.

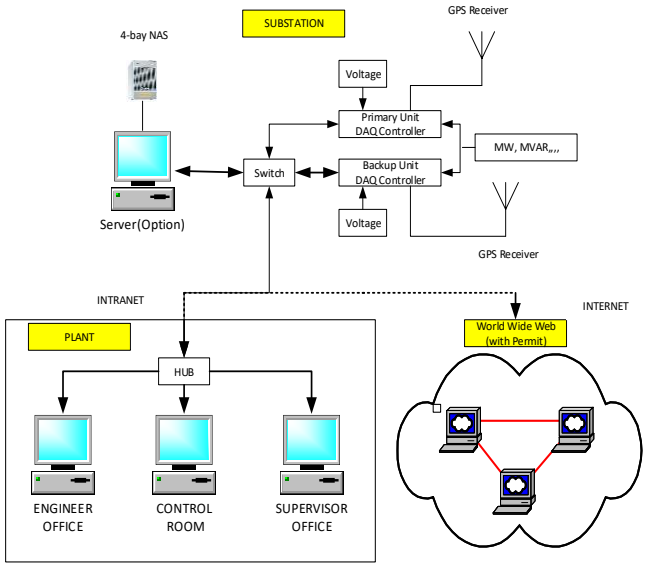

Fig. 2. 2 Real-Time web-based monitoring system

To ensure the reliability of the monitoring system, two sets of IP-addressable data acquisition (DAQ) systems “Primary DAQ” and “Backup DAQ” are designed to equip the power substation at petrochemical facilities. The desired data collected by two DAQ controllers based on the trigger and record mechanisms are streamed to a 4-bay Network-Attached Storage (NAS) whenever it is necessary. As the database of the

system, NAS could help engineers to retrieve the desired historical data for analysis at any time with the username and passwords. Additionally, two Global Positioning System (GPS) modules are applied to provide the universal timestamp for the system without any unnecessary security concern caused by internet time server [27]. This function could help the power system to be synchronized with local power system operators and provide accurate timestamps for the collected data. With this monitoring system, the real-time conditions of the system and historical data could be accessed from multiple authorized locations with an intranet. Besides, because of the IP-addressability of the system, this monitoring system could also be accessed by using internet with permission. Considering the high privacy concern of petrochemical businesses, internet accessibility could be removed at any time by the operators. To meet the cybersecurity standards of North American Electric Reliability Corporation (NREC) and petrochemical facility requirements, different practices for security on the system could be added accordingly [28].

2.2.1 Hardware Configuration

In this monitoring system, a controller with a 4 core Intel procerssor with the frequency 1.91 Ghz is adopted [29]. Because of the modularization of the DAQ controller, different modules could be replaced or expanded based on different monitoring purposes. In this case, the structure of the DAQ controllers are shown in Fig. 2.3. A DAQ controller with 4 different modules is shown in Fig. 2.4. The input data type and data rate of each module are listed in Table 2-2.

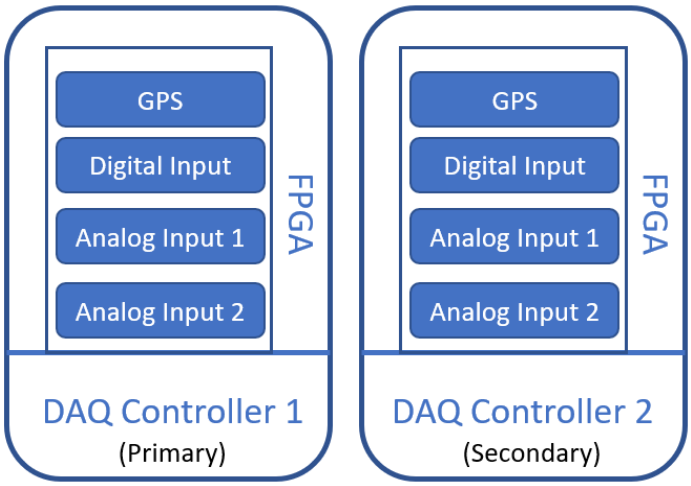

Fig. 2. 3 Structure of DAQ controllers

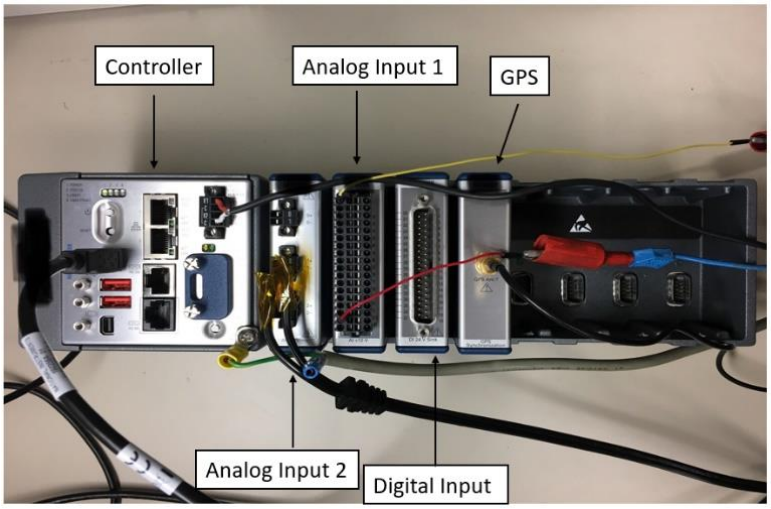

Fig. 2. 4 DAQ controller

The GPS module receives time data from GPS satellites every second to provide accurate timestamping for the monitoring system [30]. The digital input module is a 32-channel, 24 V sinking digital input module which receives circuit breakers signals to provide their statuses [31]. The analog input 1 is a 32-channel, ±200 mV to ±10 V, 16-Bit analog input module that receives DC voltage signal from transducers to monitor the real power and reactive power [32]. The analog input 2 module is a 3-channel, 300 Vrms, 24-Bit analog input module which measures the AC voltage at the secondary side of the Potential Transformer (PT) directly [33]. This requires high sampling frequency to provide sufficient monitoring data.

TABLE 2- 2. Data Type and Data Rate of Each Module on DAQ Controllers

Module	Input Data	Data Rate
GPS	Time	Every Second
Digital Input	Circuit Breaker Status	10 Samples/Second
Analog Input 1	Transducer Voltage/ Real and Reactive Power	10 Samples/Second
Analog Input 2	Voltage	2000 Samples/Second

2.2.2 Event-Triggering Mechanisms and Recording Functions

Different event-triggering mechanisms and recording functions are also included in this monitoring system. These two functions can help system operators to examine the system operation conditions and record events information for future analysis. The triggering thresholds can be decided based on different requirements of petrochemical facilities. In this study, triggering thresholds are chosen

based on the target system.

To optimize and utilize the performance of FPGA and DAQ controllers, different tasks are realized on different targets. Because the detection mechanisms are real-time functions which are extremely time critical, all detection mechanisms are programmed on the FPGA to improve the accuracy and avoid indeterministic issues caused by CPU on DAQ controller. The detection results are Boolean signals that will be transferred through a Direct Memory Access (DMA) First-in-First-Out (FIFO) to the real-time target (DAQ controller) [34, 35]. Once event detection is triggered, DAQ controller will start recording functions with certain recording period buffer to make sure none of the event data is missed.

2.2.2.1 Voltage Detection Mechanism

In this case, the voltage deviation triggering mechanism will be activated based on the following criteria.

- $5\% \leq |V_{dev}| \leq 10\%$ and the situation lasts more than three cycles.
- $|V_{dev}| > 10\%$ and the situation lasts more than one cycle.

If any voltage deviation at the substation exceeds the triggering thresholds, raw voltage sinusoidal data and RMS voltage data will be recorded. To acquire accurate RMS values as fast as possible, voltage RMS is calculated based on the one cycle voltage raw data on FPGA. Meanwhile, the frequency data will also be recorded as a reference for subsequent analyses. The recording period is 2 seconds before and 5 seconds after the event to make sure event data could be recorded completely without missing any data. A dead bus mode is also developed as one special operation mode of the system. If the RMS voltage is less than 0.65 per unit (p.u.) for more than five seconds, the monitoring system switches to the dead bus mode, and only the monitoring function is performed without any triggering and recording functions until the RMS voltage is higher than 0.65 p.u.

2.2.2.2 Frequency Detection Mechanism

As one of the most important parameters in power systems, frequency variations could reflect in the entire operation conditions of the system. In this study, the frequency is calculated based on the single cycle voltage signals' period *T* on FPGA. The period T is measured with "zero-crossing" method [36]. The frequency calculation equation is shown in (1).

$$\text{frequency} = \frac{1}{Period} \qquad (1)$$

The frequency triggering mechanism and recording functions will be activated based on the following criteria.

- $|f| > 0.2$ Hz that lasts more than three (3) cycles, where:

  $|f|$ = |system frequency (Hz)-frequency reference (Hz)|

When the frequency fluctuation is greater than 0.2 Hz, the raw data of the frequency and voltage signals will be recorded. At the same time, one cycle of the RMS voltage data will also be recorded as a reference for a comprehensive analysis. The recording period is 2 seconds before the event and 5 seconds after $|f| \leq 0.05$ Hz.

2.2.2.3 Power Detection Mechanism

The real power and reactive power in the tie line between the power system of the petrochemical facility and the interconnected power grid would be monitored. In this study, the oscillation magnitudes of real and reactive power are chosen to be the monitoring data. The power triggering and recording mechanisms will be activated based on the following situations shown in Table 2-3.

TABLE 2- 3. Power Detection Triggering and Recording Mechanisms

Conditions	Real Power (P)	Reactive Power (Q)
Normal	$P_{osc.\ mag} \leq 5MW$	$Q_{osc.\ mag} \leq 10MVar$
Record	$5MW < P_{osc.\ mag} \leq 10MW$	$10MVar < Q_{osc.\ mag} \leq 20MVar$
Record and Alarm	$10MW < P_{osc.\ mag} \leq 20MW$	$20MVar < Q_{osc.\ mag} \leq 30MVar$
Record and Trip	$P_{osc.\ mag} > 20MW$	$Q_{osc.\ mag} > 30MW$

When the real power, P, oscillation magnitude is greater than 5MW and the reactive power, Q, oscillation magnitude is greater than 10MVar, a triggering signal will be sent from FPGA to the controller through DMA FIFO and the raw data of P and Q will be recorded. The recording period is 2 seconds before and 28 seconds after the event, which is 30 seconds total of recording duration.

2.2.2.4 Circuit Breaker Status Detection

This monitoring system will record the time and location of any circuit breaker operation historical status inside the petrochemical facility. With this function, all operation information of circuit breakers within the facility may be accessed for further analysis.

2.2.2.5 SSO Monitoring Detection

SSO will be monitored and detected based on the high-speed sampling voltage data. The development of the SSO monitoring application is presented in Section III in detail. This monitoring application can help operators and engineers of petrochemical facilities to prevent serious damage in the turbine generators. It can also help interconnected power grid operators to understand the overall grid conditions.

2.3 SUBSYNCHRONOUS OSCILLATION MONITORING

Due to potential risks of SSO, an SSO monitoring function has been included in this monitoring system. The module utilizes both frequency and time domain methods to continuously monitor the signal oscillation and to detect any subsynchronous oscillation at petrochemical facilities caused by internal SSTI on co-generation plants and external SSCI on the interconnected power grid. It calculates a demodulated signal based on the upper and lower envelopes of the original input signal. This demodulated signal will be absent of the natural frequency and any DC component, thus carrying the SSO as the strongest signal. The scheme analyzes the voltage signal and is performed in five steps, which are performed for every sample collected until the SSO is detected. This method is based on [37] and [38], where the interested reader could find more details. The steps descriptions are shown below:

1. Determining parameters: (a) determination of the sampling frequency, Fs, from the discretized signal; and (b) determination of the length of the analog signal to be analyzed. The minimum length, TL, should be equal to the inverse of the lowest detectable frequency. If one wants to detect at least frequencies above 10Hz, then TL=1/10=0.1. This means one should use an analysis window of 0.1 second in the next steps.

2. Finding peaks and filtering the DC component: (a) subtract the mean value (DC component); (b) find all zero-crossings; (c) find all upper and lower peaks.

3. Calculating the demodulated signal: (a) calculate the upper and lower envelopes using the peak values; (b) subtract the lower envelope from the upper envelope. The result is a signal without the natural frequency (without 60Hz in this case). At this point, DC component and the natural frequency are filtered out, only remaining the demodulated signal. It is important to note that, before this whole method is applied, a noise filter should be applied, such as a low-pass filter.

4. First decision about SSO: (a) calculate the RMS value of the demodulated signal; (b) if is it below a certain pre-determined level limit, which depends on the application, there is no SSO; (c) if it is above this limit, there may be an SSO, then proceed to the next step;

5. Spectrum and SSO detection using Fast-Fourier Transform (FFT): (a) calculate the FFT of the demodulated signal. Before that, one may use a Hanning window and zero padding to reduce the side lobes and get a more accurate resolution in the frequency domain; (b) calculate the frequency and RMS value of the highest amplitude found (which should be the SSO signal, if there is one).

In this case, to test the SSO monitoring function, a voltage signal including both a 60Hz signal and sub-synchronous resonance frequency 37.5Hz were generated. The test result is shown in next section of the paper.

2.4 IN-LAB MONITORING SYSTEM TEST

To make sure the developed monitoring system works properly, two DAQ controllers are set up at a laboratory with a 4-Bay NAS to measure the voltage from a 120V AC power socket. A DC power supply is set up as the input voltage from power transducers to measure P and Q. The system setup is shown in Fig.2.5.

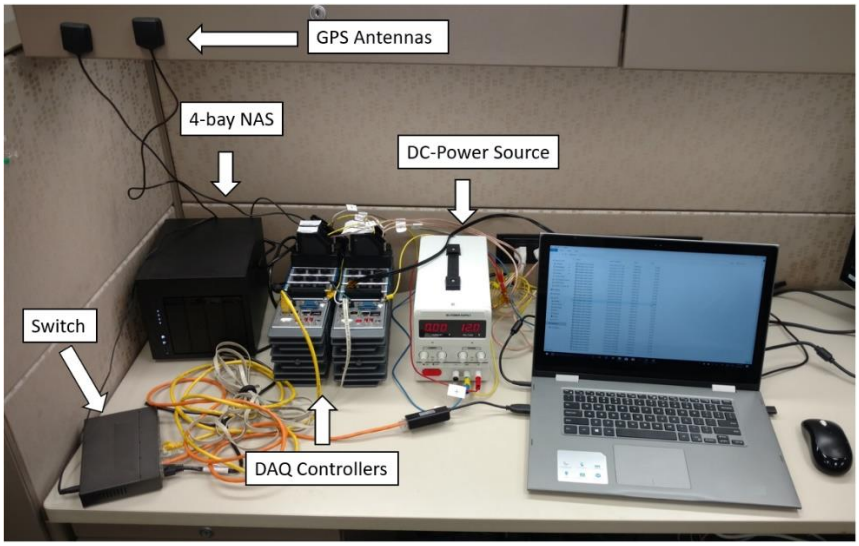

Fig. 2. 5 In-Lab system setup

As mentioned in Section II, voltage and frequency measurements are taken from the AC voltage with a sampling rate of 2000 Samples/second. In this test, the AC voltage input is measured from a 120V (rated value) AC power plug. The raw voltage sinusoidal wave and RMS values are plotted simultaneously, which are shown in Fig. 2.6 and Fig. 2.7, respectively. Frequency measurement based on the single-cycle voltage data is plotted in Fig. 2.8.

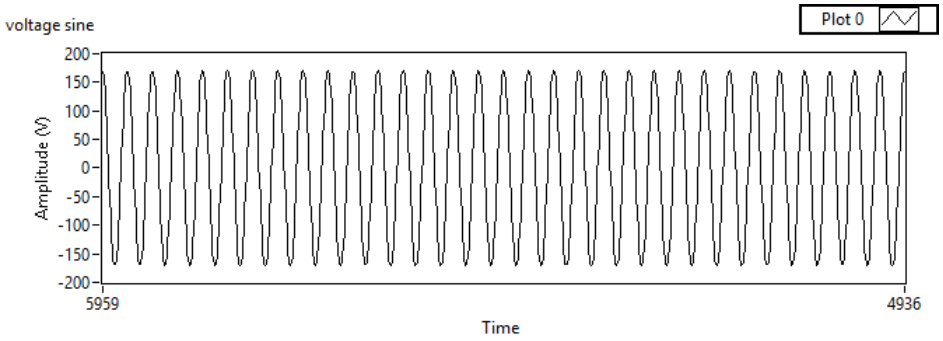

Fig. 2. 6 Raw data of voltage

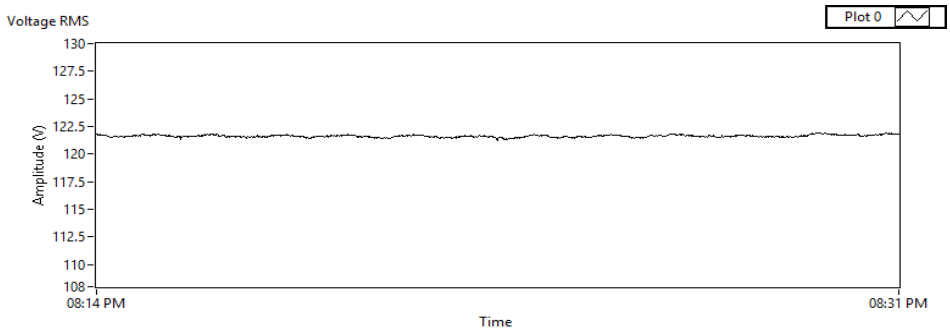

Fig. 2. 7 RMS value of voltage

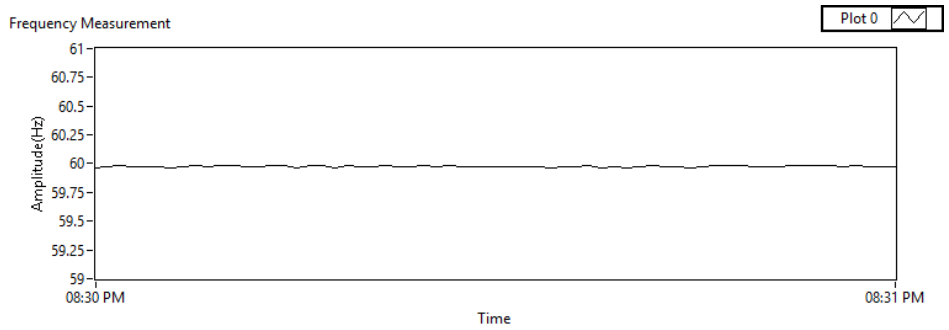

Fig. 2. 8 Frequency of the power system

The front panel of the implemented triggering mechanism and recording functions for voltage, frequency and power is shown in Fig. 2.9. In this test, the voltage reference is 120V and the frequency reference is 60Hz, which could change anytime based on the in-field voltage.

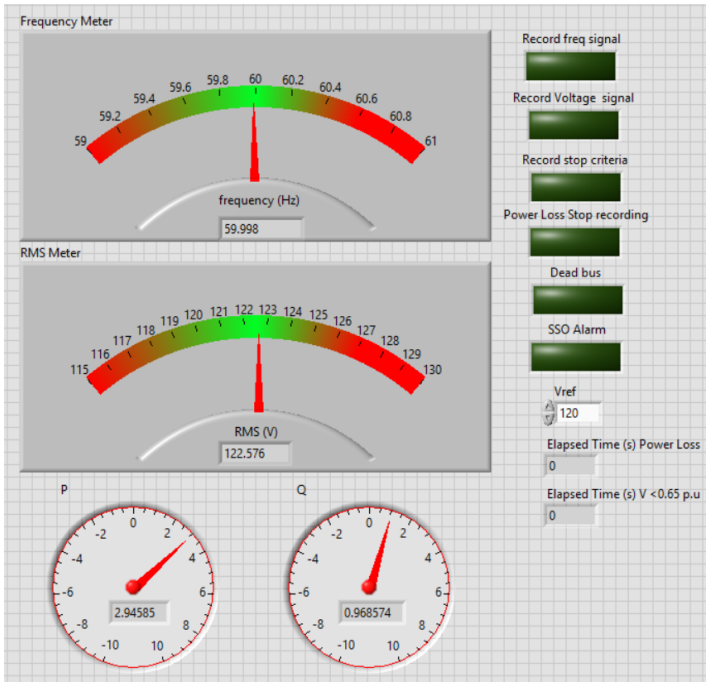

Fig. 2. 9 Voltage, frequency, and power monitoring panel

In Fig. 2.10, different power detection triggering and recording statuses are shown in four pictures based on Table 2-2. In the picture (1), no alarm and recording functions are triggered. In the picture (2), recording function are triggered due to the exceeded power. The picture (3) and (4) show that alarm signals and tripping signals are triggered respectively due to different levels of exceeded power.

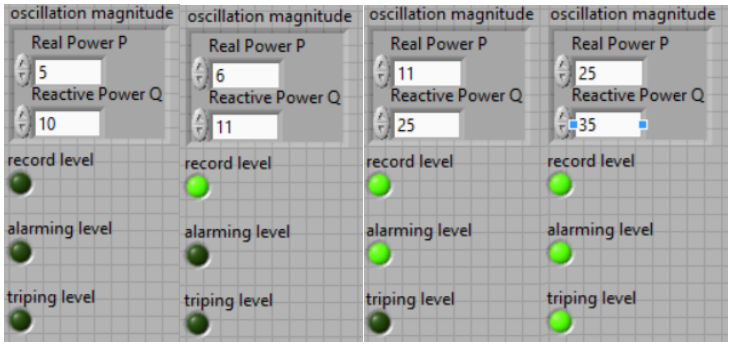

(1) (2) (3) (4)

Fig. 2. 10 Power Osccilation Monitoring Mechanism

In this test, nine circuit breakers input signals are tested with a toggle switch. The circuit breaker status interface is shown in Fig. 2.11. The system recorded the previous switch time and name of circuit breakers for every operation.

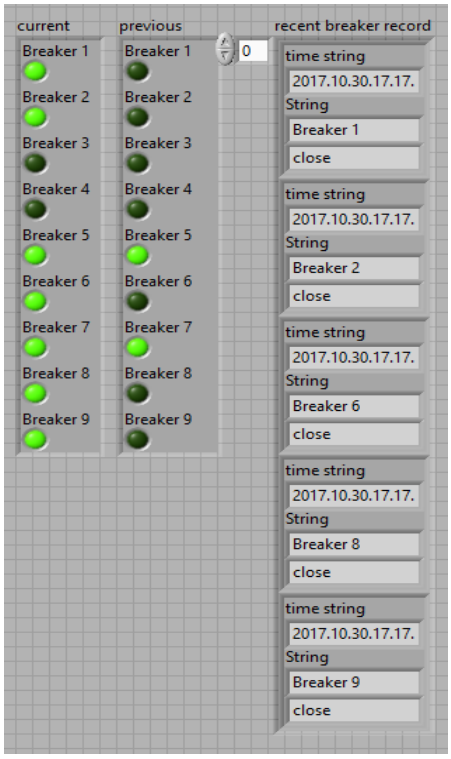

Fig. 2. 11 Circuit Breaker Status

To test SSO monitoring function in the system, a simulated signal including both a 120Vrms 60Hz signal and an SSO signal 12Vrms 37.5Hz were generated which is shown in Fig. 2.12. After the demodulation, FFT is applied to the demodulated signal which is plotted in Fig. 2.13.

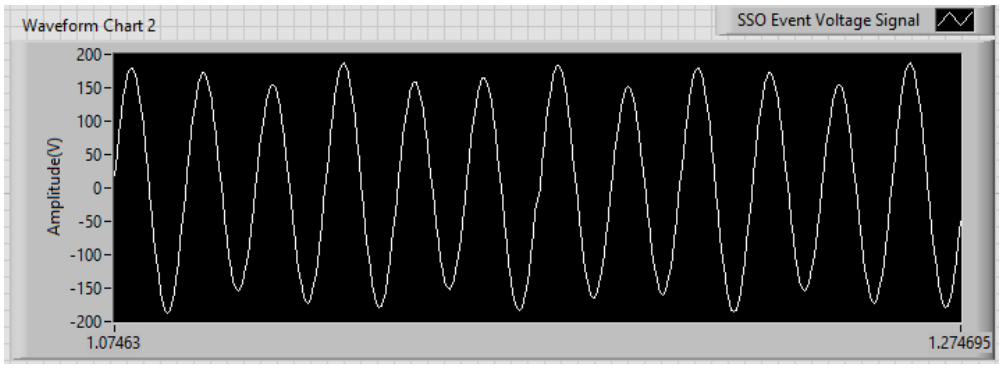

Fig. 2. 12 60Hz 120Vrms signal plus 37.5Hz 12Vrms SSO signal

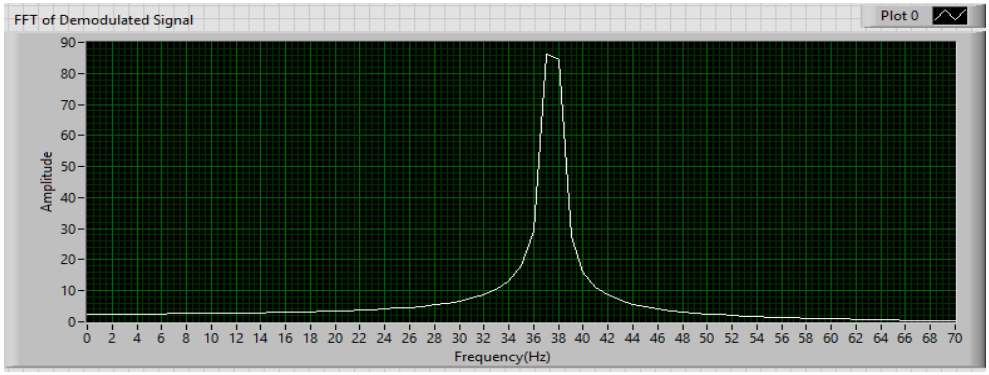

Fig. 2. 13 FFT of the demodulated signal

According to the test result, this method detected a 37.5 Hz signal after 354ms. After processing, the processed signal has 1.3% error in the frequency which depends mostly on the methods of filtering used, as well as how the demodulated signal and FFT are calculated, and the size of the window of the analyzed signal at each step. Considering the time of SSO happened in South Texas [6], the SSO detection time in this test is adequate for a system for monitoring purposes.

In addition, to better test the triggering event under the real-world application situations, a variable voltage transformer [39] and a 1Hz to 999.9 Hz variable frequency power supply [40] are used which are shown in Fig. 2.14. Once the event was triggered, the GPS time-stamped raw voltage data, one cycle RMS, and frequency data are recorded.

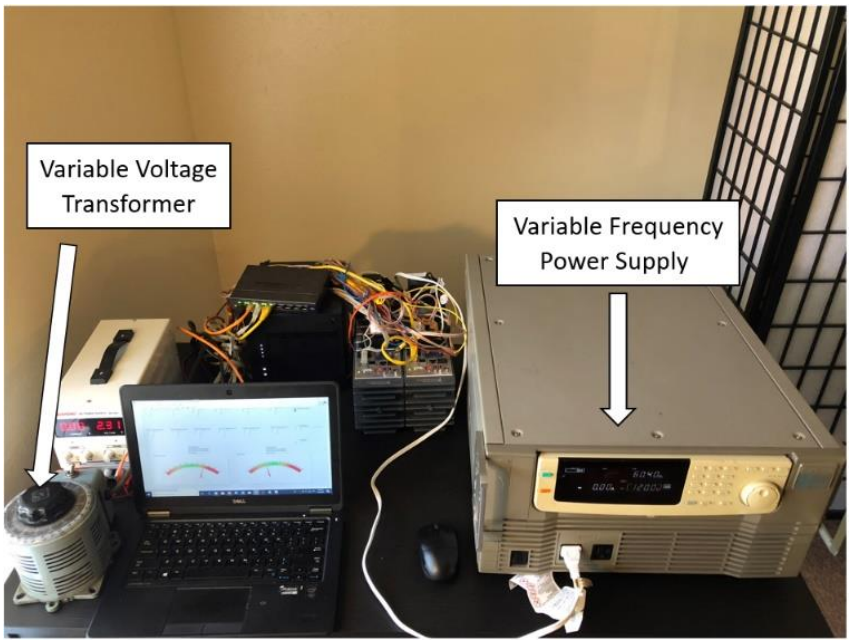

Fig. 2. 14 Variable Autotransformer

As an example, 5 samples of recorded raw voltage data, RMS values, and frequency in the 4 bay-NAS are shown in Table 2-4. Because the 1904 epoch reference time is used in this system, in the recorded data, each timestamp represents an absolute time [41].

TABLE 2- 4. Recorded Raw Voltage Data (2000S/s)

Timestamp (ns)	Raw Voltage (V)	RMS Voltage (V)	Frequency (Hz)
1527543988623270000	97.9920	114.8365	60.00231
1527543988623770000	119.1584	114.8365	60.00231
1527543988624270000	142.5093	114.8365	60.00231
1527543988624770000	149.2547	114.8365	60.00231
1527543988625270000	153.0874	114.8365	60.00231

According to the in-lab test results, the monitoring system with different triggering and recording mechanisms worked properly. Different triggering references of this monitoring system could be changed easily based on in-filed system and monitoring purposes.

2.5 CONCLUSION

In this paper, a real-time web-based power monitoring system with different triggering mechanisms, recording functions and an SSO monitoring application is developed for the power substations at petrochemical facilities. Utilization of the FPGA-based platform controllers enhanced the data acquisition speed and system computing power significantly to provide real-time data precisely. IP-addressability of the system provides flexible system accessibility for system operators so that they can visualize the conditions of power systems without location limitations. By applying this monitoring system, all the necessary data can be recorded based on the triggering mechanisms for further analysis, and engineers and system operators can have a much better understanding of the power system operations inside of petrochemical facilities. Therefore, the reliability of power system of these facilities can be improved by applying this real-time web-based power monitoring system.

2.6 REFERENCES

[1] S. Thorat, G. McQueen, and P. T. Luzunaris, "The role of optimal design and application of heat tracing systems to improve the energy conservation in petrochemical facilities," *IEEE Trans. Industry Application*, vol. 50, pp. 163-173, Jan/Feb. 2014.

[2] L. Zhao, I. Matsuo, F, Salehi, Y, Zhou and W. Lee, “Development of a real-time web-based power monitoring system for the petrochemical facilities,” in *Proc. 2018 IEEE 54th I&CPS. Conf.*

[3] K. Malmedal; P. K. Sen and J. Candelaria, Electrical Energy and the Petro-Chemical Industry: Where are we going?. *IEEE 58th Annual Petroleum and Chemical Industry Conf.*, September 2011, PCIC-2011-01.

[4] T. Wu, S. Shieh, S. Jang, and C. Liu, “Optimal energy management integration for a petrochemical plant under considerations of uncertain power supplies,” *IEEE Trans. Power Syst*., vol. 20, no. 3, pp. 1431–1439, Aug. 2005.

[5] *Industrial cogeneration/CHP applications.* [Online]. Available: http://www.cogeneration.org/chp-primer/industrial-cogeneration-chp-applications.

[6] H. Chen, C. Guo, J. Xu and P. Hou, “Overview of sub-synchronous oscillation in wind power system,” *Energy and Power Engineering*, pp. 454-457, Jul. 2013. doi: 10.4236/epe.2013.54B087

[7] L. Harnefors, “Analysis of subsynchronous torsional interaction with power electronic converters,” *IEEE Trans. Power Syst*., vol. 22, no. 1, pp. 305–313, Feb. 2007.

[8] D. Sun, X. Xie, Y, Liu, K, Wang and M, Ye, "Investigation of SSTI between practical MMC-based VSC-HVDC and adjacent turbogenerators through modal signal injection test," *IEEE Trans. Power Delivery*, vol. 32, pp. 2432-2441, Dec. 2017.

[9] A. E. Leon, "Integration of DFIG-based wind farms into series-compensated transmission systems," *IEEE Trans. Sustainable Energy*, vol. 7, pp. 451-460, Apr. 2016.

[10] Subsynchronous Resonance Working Group of the System Dynamic Performance Subcommittee, "Reader's guide to subsynchronous resonance," *IEEE Trans. Power Syst*., vol. 7, no. 1, pp. 150–157, Feb. 1992.

[11] D. H. Baker, G. E. Boukarim, R. D'Aquila, and R. J. Piwko, "Subsynchronous resonance studies and mitigation methods for series capacitor applications," in *Proc. IEEE Power Eng. Soc. Inaugural Conf. Expo. Africa, 2005*, 2005, pp. 386–392.

[12] H. K. Nia, F. Salehi, M. Sahni, N. Karnik and H. Yin, "Filter-less robust controller for damping SSCI oscillations in wind power plant," in *Proc. 2017 IEEE Power and Energy Society General Meeting.*

[13] S. Rezael, "Impact of sub synchronous resonance on operation of protective relays and prevention method," in *Proc. 2017 IEEE Industrial and Commercial Power Systems Technical Conf,.*

[14] L. C. Gross, "Sub-synchronous grid conditions: new event, new problem, and new solutions," Relay Application Innovation, Inc., Spokane, WA. [Online]. Available: http://relayapplication.com/docs/WPRC_2010_SSF_Detection_Paper.pdf

[15] S, Rezaei, "An adaptive algorithm based on subharmonic and time domain analysis to prevent mal operation of overcurrent relay during sub synchronous resonance," *IEEE Trans. Industry Application*, vol. 54, pp. 2085-2096, May/Jun. 2018.

[16] J. Adams, C. Carter, and S.-H. Huang, "ERCOT experience with subsynchronous control interaction and proposed remediation," in *Proc. 2012 Transmission and Distribution Conf. Expo.,* pp. 1–5.

[17] Z. Donghai, S. Baokui, and F. Hong, "Remote online power system monitoring system based on multi-information acquisition technology," in *Proc. 2004 Power System Technology International Conf.*

[18] R. F. Khelifa, and K. Kelassi, "An energy and power quality monitoring system of a power substation," in *Proc. 2016 Electrical Sciences and Technologies in Maghreb International Conf.*

[19] M. Hyvarinen, S. Pettissalo, P. Trygg, K. Malmberg, J.Holmlud and L. Kumpulainen, "A Comprehensive Secondary Substation Monitoring System", in *Proc 2009 20th International Conference on Electricity Distribution. Prague*.

[20] H. Biyi, Z. Guoping, D. Jianqiang, J. Pengyuan, and X. Su, "Design of combined substation monitoring system based on ATT7022B and RS-485," in *Proc. 2015 Intelligent Transportation, Big Data & Smart City International Conf.*

[21] H. Wang, J. Liu, "Application of substation monitoring system development based on QFD," in *Proc. 2011 Asia-Pacific Power and Energy Engineering Conf.*

[22] Y. Ai-min, W. Li-xia, W. Jun-pin, and X. Qu-li, "Research and design of integrated substation monitoring systems." in *Proc. 2010 Semantics Knowledge and Grid International Conf.*

[23] I. B. M. Matsuo, J. Jardini, L. C. Magrini, F. Crispini and P. Kayano, "Fast system for analysis of protection events," in *Proc. 2015 IEEE PES Innovative Smart Grid Tech Latin America Conf.*

[24] *NI FPGA*. [Online]. Available: http://www.ni.com/fpga/

[25] *Introduction to FPGA Technology: Top 5 Benefits*. [Online]. Available: http://www.ni.com/white-paper/6984/en/

[26] *Slices on an FPGA chip.* [Online]. Available: http://www.ni.com/product-documentation/54503/en/

[27] M. Heidari Kapourchali, M. Sepehry, and V. Aravinthan, "Fault detector and switch placement in cyber-enabled power distribution network," *IEEE Trans. Smart Grid,* to be published, doi: 10.1109/TSG.2016.2573261.

[28] *Overview of best practice for security on RIO system.* [Online]. Available: http://www.ni.com/white-paper/13069/en/

[29] *Specifications NI cRIO-9039 Embedded compactRIO controller with real-time processor and reconfigurable FPGA.* [Online]. Available: http://www.ni.com/pdf/manuals/375697c_02.pdf

[30] *Timing and Synchronization.* [Online]. Available: http://sine.ni.com/nips/cds/view/p/lang/en/nid/210840

[31] *NI-9425 C series digital module.* [Online]. Available: http://www.ni.com/en-us/support/model.ni-9425.html

[32] *NI-9205 C series voltage input module.* [Online]. Available: http://www.ni.com/en-us/support/model.ni-9205.html

[33] *NI-9205 C series voltage input module.* [Online]. Available: http://www.ni.com/en-us/support/model.ni-9225.html

[34] *Transferring data using direct memory access (FPGA module).* [Online]. Available: http://zone.ni.com/reference/en-XX/help/371599M-01/lvfpgaconcepts/fpga_dma_communication/

[35] *How DMA transfers work (FPGA module).* [Online]. Available: http://zone.ni.com/reference/en-XX/help/371599M-01/lvfpgaconcepts/fpga_dma_how_it_works/

[36] *Analog period measurement express VI.* [Online]. Available: http://zone.ni.com/reference/en-XX/help/371599N-01/lvfpga/fpga_period_measurement/

[37] M. Orman, P. Balcerek and M. Orkisz, "A method of subsynchronous resonance detection," EP. Patent 2357483A1, Aug. 17, 2011.

[38] M.Orman, P. Balcerek and M. Orkisz, “Effective Method of subsynchronous resonance detection and its limitations,” *Electrical Power & Energy Systems,* vol. 43, pp. 915-920, Dec. 2012.

[39] *Portable VARIAC 120VAC input, 0-120V/140VAC output.* [Online]. Available: http://www.variac.com/staco_3PN10_20.htm

[40] *Kikusui PCR500L.* [Online]. Available: https://accusrc.com/product-Kikusui-PCR500L-4098?gclid=EAIaIQobChMIh9qbwaer2wIVBIppCh0LZwqFEAQYASABEgIJLvD_BwE

[41] *LabVIEW Timestamp*. [Online]. Available: http://www.ni.com/tutorial/7900/en/

CHAPTER 3.

DESIGN OF AN INDUSTRIAL IOT-BASED MONITORING SYSTEM FOR POWER SUBSTATIONS

DESIGN OF AN INDUSTRIAL IOT-BASED MONITORING SYSTEM FOR POWER SUBSTATIONS[2]

Long Zhao, Igor Matsuo, Yuhao Zhou, Wei-Jen Lee

L. Zhao, I. Matsuo, Y. Zhou. and W. Lee, "Design of an industrial IoT-based monitoring system for power substations," *IEEE Trans. Ind. Appl.,* vol. 55, Nov/Dec. 2019. pp. 5666-5674.

Design of an Industrial IoT-Based Monitoring System for Power Substations

Long Zhao Igor Matsuo Yuhao Zhou* Wei-Jen Lee

Student Member, IEEE Student Member, IEEE Student Member, IEEE Fellow, IEEE

University of Texas at Arlington, 701 S Nedderman Dr, Arlington, TX 76019, USA

long.zhao@mavs.uta.edu, matsuoigor@gmail.com, yuhao.zhou@mavs.uta.edu*, wlee@uta.edu

Abstract -- The Internet of Things (IoT) concept allows objects to share data through wired or wireless connections for communication purposes. The Industrial Internet of Things (IIoT) is an extended concept of IoT that refers to an integration of data acquisition, communication, and processing on a real-time network. Currently, IIoT has been involved with the development of smart grids in many applications. As the operation of power systems is extremely time-critical, low-latency communication needs to be considered for most control and monitoring applications. Real-time capability of IoT is considered as a key feature for monitoring and control applications of power systems. Therefore, system operators can use the real-time monitoring system to provide better decisions for both technical and financial-related matters. In this paper, a high-speed IIoT-based monitoring system with recording functions is developed and implemented for a power system substation. Due to the high reliability and processing speed of FPGAs, an FPGA-embedded controller is adopted in this system. The IoT platform also provides remote visualization for system operators in real time. This paper mainly aims to provide a practical application that was implemented and tested in a real power substation. The system incorporates the features of an IoT platform with the needs of high-speed real-time applications while using a single high-resolution time source as the reference for both steady-state and transient conditions.

Index Terms-- Field-programmable gate arrays, Internet of Things (IoT), Industrial Internet of Things (IIoT), Remote Monitoring, Real-time systems, Smart grids.

3.1 INTRODUCTION

Internet of things (IoT) was first proposed in 1999 by Kevin Ashton, and it has been applied in different areas such as health, agriculture, traffic, and power grids [1-4]. The purpose of IoT is to use networks to build connections among objects while reducing time and location limitations [5]. The Industrial Internet of Things (IIoT) has been applied in various industrial areas. IIoT can be understood as an embedded system using a real-time network to promote the operation of manufacturing processes [6]. In this case, the real-time system is defined as “the system in which the correctness of the system does not depend only on the logical results of computation but also on the time at which the results are produced. It has to perform critical tasks on a priority basis keeping the context switching time minimum. [6]”. Due to the real-time capability of the IoT, many monitoring and control systems have adopted IoT in

various fields. In paper [1], an electrocardiogram (ECG) remote monitoring system has been proposed with the IoT platform. The purpose of this system is to monitor long-term health conditions for patients at the residential level. This IoT-based wearable ECG monitoring system provides accurate ECG signals with lower power consumptions. Paper [2] introduces an IoT solution for online monitoring of anesthetics in human serum. The electrochemical approach and simultaneous detection have been discussed in the paper. By using the IoT platform, the patients' measured parameters could be monitored by the medical doctor in real-time with mobile devices. Paper [3] shows an IoT-based long-term wearable device to monitor the mental wellbeing. Multiple signals are collected and analyzed with the IoT platform. Paper [7] presents a WSN platform for IoT environmental monitoring applications, and the applications requirements and the exploration of possible solutions are discussed. In paper [8], an IIoT-based condition monitoring system is developed for a large-scale and continuous device. In this development, the new technology has been seamlessly integrated with the existing infrastructure to provide data collection and analysis. In paper [9], an IoT-based online monitoring system for steel casting is developed, and four layers of IoT system architecture including sensing, network, service resource, and application layers have been integrated. Paper [4] presents an IoT-based control system for smart precision agriculture and farming in rural areas, and the overall performance can be enhanced from energy and delay perspectives. IoT has also been largely applied to the electric power and energy systems in all levels [10-15]. In paper [12], IoT is applied for a smart grid application to access real-time data for transformers to improve the reliability, performance, efficiency of the substation. In paper [13], a set of sensors are implemented at a power substation with IoT platform to promote the temperature monitoring standard in the industry. Paper [14] introduces a low-cost energy monitoring and control system using IoT devices. Paper [15] presented an IoT-based solution for home power energy monitoring.

Power substations are the interface between important parts of the power grid and are responsible for many critical operations, such as stepping-up and stepping-down the voltage level. Due to the importance of electrical substations, different types of monitoring systems have been developed. In paper [16], a visual monitoring system is developed for remote operation of an electrical substation to provide environmental viewing for system operators. Paper [17] presents an online monitoring system for high voltage equipment at a substation which could help system operators have a better understanding of the related equipment. Paper [18] proposes a new supervisory monitoring system for substations to identify errors in digital switching. Paper [19] proposed a real-time monitoring system for substation grounding potential rise under power system fault conditions. The authors of the paper [20] developed a real-time monitoring system at a substation to detect low-frequency power oscillation on tie-lines. Paper

[21] shows a real-time monitoring system for transformers at a substation using a database application. Paper [22] developed a sensing monitoring system for substation equipment based on IoTs.

The motivation for the proposed development is to better help system operators understanding the system conditions using IoT platform and an integrated real-time monitoring system. In this manner, we can use a single device to efficiently capture both steady-state conditions and transient phenomena of the power system.

A high-sampling rate IIoT-based monitoring system with data logging functions is developed and implemented to monitor various critical parameters, including voltage, frequency, real power, reactive power, circuit breaker status, and transformer temperatures in power substations. Meanwhile, as an IoT application in power and energy systems, cybersecurity methods are introduced and implemented in this paper. The developed system has been implemented and installed at a power substation recently, and it has successfully detected and recorded the first fault event. The system operators have utilized the recorded data for further analysis so as to take the necessary actions.

This paper aims to show a practical development of an IIoT-based real-time monitoring system with high sampling rate for monitoring and control of substations. With this developed system, system operators can remotely monitor the overall conditions in both steady-state and transient conditions of the power substation. High-speed sampling and lossless data logging provide more detailed data for both online and offline analysis. In section 3.2, the framework of the monitoring system is introduced. Section 3.3 presents the communication and data processing of this monitoring system. Section 3.4 presents the cybersecurity setup, section 3.5 shows the field testing and application, and section 3.6 discussed the novelty of the developed monitoring system. The conclusion of this paper is shown in section 3.7.

3.2 FRAMEWORK OF THE IIOT-BASED MONITORING SYSTEM

As one of the unique characteristics, IoT should have the capability to process and analyze data in real-time with very low latency [11]. A real-time monitoring system in power substations can provide system operators with the overall conditions of the monitoring objects so that the reliability of the system and efficiency of the operation can be enhanced. In this paper, an industrial-standard Field-Programmable Gate Array (FPGA) embedded controller with Linux operating system (OS) is programmed to collect voltage, real power, reactive power, circuit breaker status, and transformer temperature data with different sampling speeds in real-time. The FPGA is made of reprogrammable silicon chips which have more powerful computing ability and faster response speed comparing with digital signal processors (DSPs) [23], [24]. Currently, many studies have shown different implementations with FPGA technology. In paper [25], the authors designed an FPGA-based waveform character searching technology. A Kintex-7 chip of

Xilinx with 34Mb internal RAM is adopted in their research. In paper [26], the authors discussed the FPGA technology for high-performance computing platforms. Communication-oriented and computation-oriented FPGA technologies are presented in the paper. In paper [27], a 3D FFTs and implications for molecular dynamics are developed on FPGA clouds to improve the performance. Also, a hardware generator is developed on FPGA to be applied for high-performance designs in paper [28].

In the power system, many analyses and studies require high-speed sampling frequency, such as signal frequency domain analysis and transient study analysis. Because the processing operations on FPGAs are entirely parallel without competing for the same resources, FPGAs have huge advantages for high-speed multiple-input-and-output (MIMO) applications. Meanwhile, the hardware execution has better determinism than most processor-based software solutions, and jitter issues of software execution can be eliminated, which is extremely helpful for a real-time system with high-sampling speed. Therefore, data acquisition and detection mechanisms are programmed on the FPGA target in this system to have a reliable and high-speed performance.

However, due to some technical limitations, some complex functions and communication functions such as sorting and searching methods or floating-point arithmetic cannot be solely realized on FPGAs. Therefore, processor-based devices are still needed. As a result, an FPGA target and a processor-based target combined could compensate each other and provide the most optimal performance for high-speed real-time monitoring systems with multiple I/Os. In this system, an industrial-standard controller with 1.91 GHz Quad-Core CPU, 2 GB DRAM, 16 GB Storage, Kintex-7 325T FPGA, and an RJ-45 Gigabit Ethernet port is used which is shown in the Fig. 3.1 [29]. As it is shown in Fig. 3.1, three different input modules are applied with the controller. The analog input 1 is a DC + 10V 16-bit analog input module which has absolute accuracy 6230 µV at full scale [30]. The analog input 2 is an AC 300Vrms, 24-bit simultaneous analog input module with 2mVrms input noise, 50kS/s maximum data rate range using internal master time-based [31]. The digital input is a 24V sinking digital input module [32].

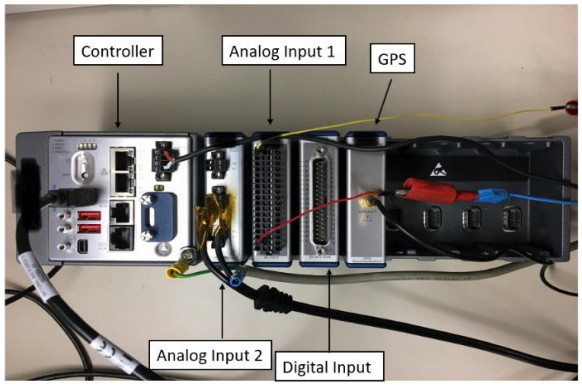

Fig. 3. 1 FPGA Embedded Controller

In this IIoT-based monitoring system, a Network-Attached Storage (NAS) is adopted as the repository to store data and to enable remote access. Comparing with the direct-attached storage (DAS) and storage area network (SAN), NAS is file storage that can be accessed by multiple authorized users and heterogeneous client devices to retrieve the data in different categories from a centralized location in the network [33]. In this way, the system operator can retrieve the desired data based on the time and necessities using the network with a username and password.

As it is shown in Fig. 3.2, inside of the substation, the FPGA-embedded controller, a host computer and the NAS are connected to a hardware firewall through ethernet cables. A computer in the control room receives the data in real-time. In this section, the structure of the system is introduced in sequential order of the data flow in the system.

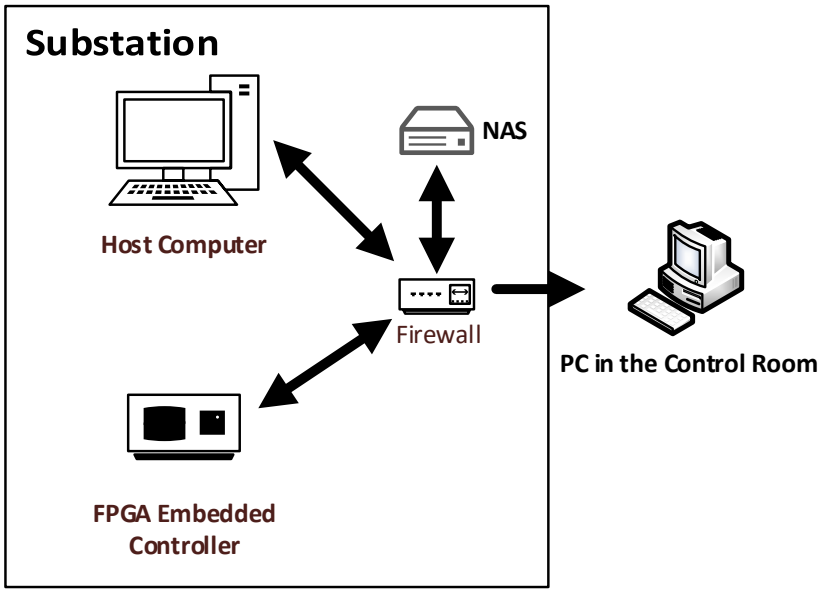

Fig. 3. 2 Framework of IoT-Based Real-time Monitoring system

3.2.1 Data Acquisition

To acquire different types of input data with different sampling rates, three types of input modules are adopted in this system as shown in Table 3-1. All data will be collected and processed on the FPGA. To have the high-resolution data of voltage and frequency signals for detailed analysis, AC analog voltage signals are sampled with 2000 samples/second. Real power, reactive power and transformer temperatures signals are converted by transducers. Power, temperature, and circuit breaker status signals are acquired with sampling speed 10 samples/second.

TABLE 3 - 1. Data Acquisition Modules and Sampling Rates

Module Type	Measurement Objects	Sampling Rate
AC Analog Voltage Input Module (- 300 to 300Vrms)	Voltage and Frequency	2000 S/s
Analog Voltage Input Module (-10 to 10V)	Real Power, Reactive Power and Transformer Temperatures (Transducers)	10 S/s
Digital Input Module	Circuit Breaker Status	10 S/s

To acquire the system frequency f (Hz), the zero-crossing method [34] is used to find the period T(s) of the input voltage and to calculate the system frequency based on (1).

$$f\ (Hz) = \frac{1}{T} \qquad (1)$$

Once the predefined events such as over-voltage, under-voltage, over-frequency, under-frequency, and transformer overheating are triggered, the sampled data will be recorded by the controller and sent to a NAS which can be accessed by the system operator anytime from the Local Area Network (LAN).

3.2.2 Timestamps and Synchronization

As a real-time monitoring system with high sampling speed, both high resolution and accurate time sources are also required. As an IoT-based monitoring system for power substations, cybersecurity is a critical factor which needs to be considered. One of the most applied networking protocols for clock synchronization Network Time Protocol (NTP) is not adopted in the system considering the cybersecurity concern. Instead, an industrial standard GPS synchronization module with $\pm$100ns of accuracy is applied, providing timestamps for the sampled data. As a simplified illustration, the synchronization process is shown in Fig. 3.3. To synchronize and timestamp the collected data on the FPGA, the absolute time provided by a 40MHz FPGA internal clock is synchronized to the GPS time. Once the data are timestamped, they are sent to the processor-based on the device for the next step.

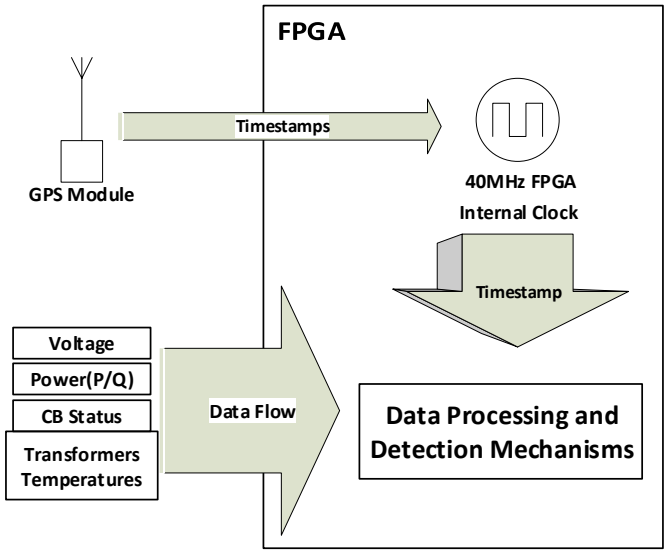

Fig. 3. 3 Synchronization and Timestamping Process

All data are timestamped as they are processed for data display and logging. When the predefined detection mechanisms are triggered, all timestamps and sampled data are recorded to the NAS, which is shown in Fig. 3.4. In this case, epoch time is used as the GPS time reference, and the time refence starts from 01/01/1904 00:00:00.000 UTC [35].

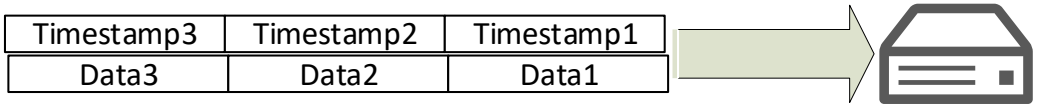

Fig. 3. 4 Data Synchronization and Logging

3.2.3 Data Display

As mentioned in the previous sections, because of the computing capabilities and determinism, all the data acquisition and predefined detection mechanisms are programmed on the FPGA target. To display the data in real time on the computers at the substation and at the control room, data are continuously transferred through the network. Human-Machine Interface (HMI) on both computers are shown in Fig. 3.5. Due to security and confidentiality concerns, all power indicators and time are censored in this paper. Considering the scalability of the system and facilitating other authorized computers to access the HMI of the monitoring system, tag communication method which is introduced the following section is adopted in the system.

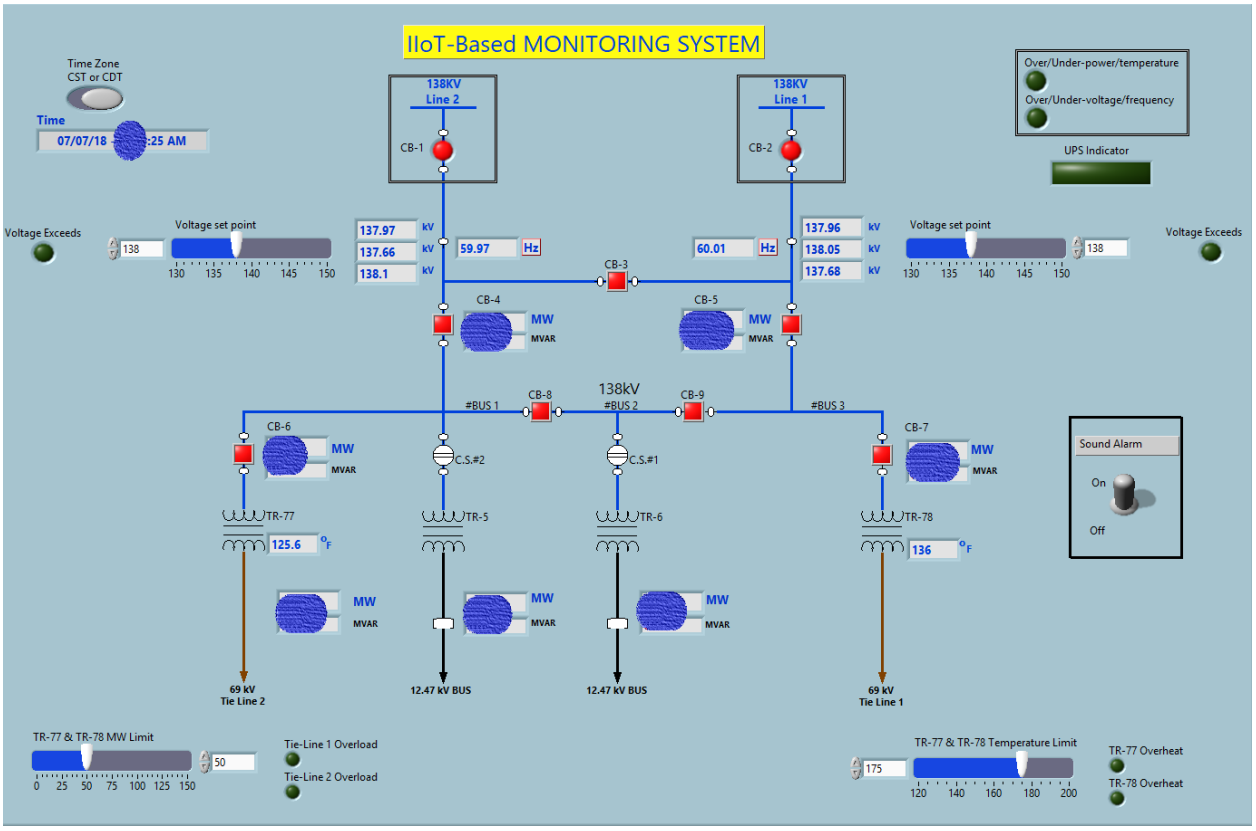

Fig. 3. 5 HMI of the Monitoring System

3.2.4 Data Logging

As one of the most important features of this monitoring system, data logging is processed on the CPU-based target. Once the predefined event mechanisms are triggered, the data is sent from the FPGA to the memory on the CPU-based target, and then saved to files in binary format in the local storage. File Transfer Protocol (FTP) is used to transfer these files from the local storage to the NAS. As an example of the recorded data, one phase of voltage recorded data file is shown in Table 3-2. In this system, RMS and frequency data are calculated based on one cycle of raw voltage data.

TABLE 3 - 2. One Phase of Voltage Data Logging File

Timestamp (μs)	**Raw (kV)**
1533116616359500	-71.96577761
1533116616360000	-34.92403722
1533116616360500	3.456600666
1533116616361000	40.08871722
1533116616361500	76.97151464
1533116616362000	110.4259613
RMS (kV)	**Frequency (Hz)**
137.6861599	60.0234375

3.3 DATA COMMUNICATION AND PROCESSING

Similar to most of the IoT applications, this monitoring system produces a large amount of data during operation. Three phases of voltages on two 138kV lines are measured simultaneously with a sampling rate of 2000 samples per second for each phase, which produces 12000 input data every second. Fourteen real/reactive power inputs signals, nine circuit breaker status and two transformer temperatures are measured simultaneously with a sampling rate of 10 samples per second, producing an additional 250 input data every second. Moreover, every datum will carry a corresponding timestamp. To overcome the data computing challenges and satisfy real-time communication (RTC) requirements, different types of communication methods are adopted. Meanwhile, it is worth noting that limited resources on the CPU and Dynamic RAM of the controller also need to be considered to maintain the reliability of the system according to the application specifications. In this section, the communication methods and protocols used in this monitoring system are introduced.

The IoT platform provides IP (Internet Protocol) addressability for the FPGA-embedded controller, NAS, and both computers. To build a network for this monitoring system, static IP addresses are provided for each device. TCP/IPv4 (Transmission Control Protocol/Internet Protocol version 4) is applied as the base communication protocol of the system.

As an IoT-based real-time monitoring system with data logging functions, different communication methods and protocols need to be considered to achieve an optimal and secure performance of the system.

3.3.1 Tag Communication method

To display all the most updated data in real-time on the HMI, tag communication (latest value communication) is implemented. Tag communication is defined as "transfer only the current (most recent) data value between two process loops or between two targets" [36]. For the display purpose, tag communication provides the most updated information with low latency and high-channel-count for system operators without using too much CPU and RAM resources of the controller [37]. In this system, the data update frequency on the HMI is set to one sample per second to reduce the CPU usage on the controller. However, tag communication is a lossy communication that might lose some of the data during the communication. Therefore, the tag communication method is only applied to the data display in this system.

3.3.2 Stream Communication method

As an embedded controller, communication between the FPGA-based target and the CPU-based target of the controller is extremely critical. Once the data acquisition and the detection mechanisms are complete on the FPGA target, all the data need to be transferred to the CPU-based target for further communication and processes.

To make sure all the high-speed-sampled data are recorded once the predefined events are detected, a lossless communication called stream communication method is adopted. Stream communication uses buffering to transfer each data point. Comparing with the tag communication method, stream communication provides better throughput but higher latency. Fig. 3.6 shows the stream communication on the controller.

As one of the stream communications options, Direct Memory Access (DMA) First-In-First-Out (FIFO) queues are applied between the FPGA and CPU targets. A DMA channel has two buffers on both the FPGA-based target and CPU-based target respectively. Every data point available is then transferred from the FPGA target buffer to the CPU target buffer. Computational overhead of the CPU is drastically reduced since data transfer and data processing can take place at the same time. Hence, more computing and processing power can be used for other tasks on the CPU-based target [38-40].

Once the data are transferred from the FPGA target to the CPU target by using DMA FIFO in the controller, the data are stored on the CPU-based target before being transferred to the NAS in the network.

In order to do this, a fixed-size queue called Real-Time FIFO (RT FIFO) is applied to achieve a deterministic process within the CPU and pre-allocate memory for the data in the controller [41]. The data can then be stored to binary files in the local storage without data loss. To optimize the memory in the controller and avoid overflow in the buffer, appropriate buffer sizes need to be considered for the RT FIFO according to the application.

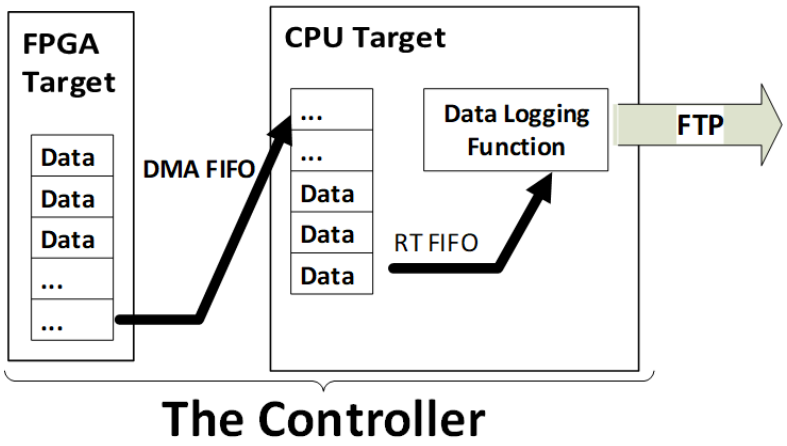

Fig. 3. 6 Stream Communication on the Controller

3.3.3 File Transfer Protocol (FTP)

To transfer the binary files from the local storage of the CPU-based target to the NAS over the network, a connection-oriented protocol called File Transfer Protocol (FTP) is applied in this system considering the low latency requirements. Comparing with connectionless protocols such as WebDAV, FTP has a higher one-time overhead because a session between the NAS and the controller needs to be built before the data are sent. However, WebDAV usually carries artificial session information that increases the latency. As a result, successive requests of FTP sessions have a lower latency, which is critical for this IoT-based real-time system [42].

3.3.4 Publish-Subscribe Pattern (PSP)

To send the data from the substation to the control room, PSP is used between the controller at the substation and the computer in the control room. PSP provides publishers and subscribers in the communication between the data senders and receivers. Subscribers only receive the data that they subscribed to receive [43], without knowledge of who the publisher is. Publishers also do not know who the subscribers are. This messaging pattern allows for easy communication and increases scalability, facilitating other authorized computers to be added at any time to the system and act as subscribers without having to configure the messages and publishers again. In this system, the computer in the control room subscribes to receive the information published by the controller in the network for displaying

purposes. Due to security concerns, this computer can only read the data from the controller without writing access capabilities.

3.4 CYBERSECURITY OF THE SYSTEM

As an IoT-based real-time monitoring system, cybersecurity is a vital factor which needs to be considered in the application. As mentioned in previous items, the first main cybersecurity concern led to the use of the GPS synchronization method instead of NTP. The second concern led to denying writing access to the controllers from the computers with displaying purposes.

Additionally, to improve the cybersecurity of the IoT application, adding hardware security features and more layers of security may be considered as possible solutions [11]. For this developed system, a hardware firewall is installed at the substation. The FPGA-embedded controller and NAS which have the highest security level are protected by the hardware firewall, while the host computers and computer in the control room are in a demilitarized zone (DMZ), as shown in Fig. 3.7. DMZ is defined as a subnetwork that is between a trusted network and an untrusted network [44]. The DMZ provides an additional layer of security to prevent unwanted access to the controller and allow time to take necessary actions to detect and block breaches. Meanwhile, the source code in the host computer and the computer in the control room can be removed. In this way, even if the attacker/unauthorized person accesses the either computer, they would not be able to modify or disrupt the monitoring system easily.

To easily distribute the application and to facilitate authorized computers to have HMI of the monitoring system without having access to the internal code, an executable file of the monitoring system is generated. The authorized computers could easily install the file to observe the condition of the system in real-time through HMI. In this way, scalability and security of the system can be satisfied at the same time. To access the NAS, a username and password are also required every time.

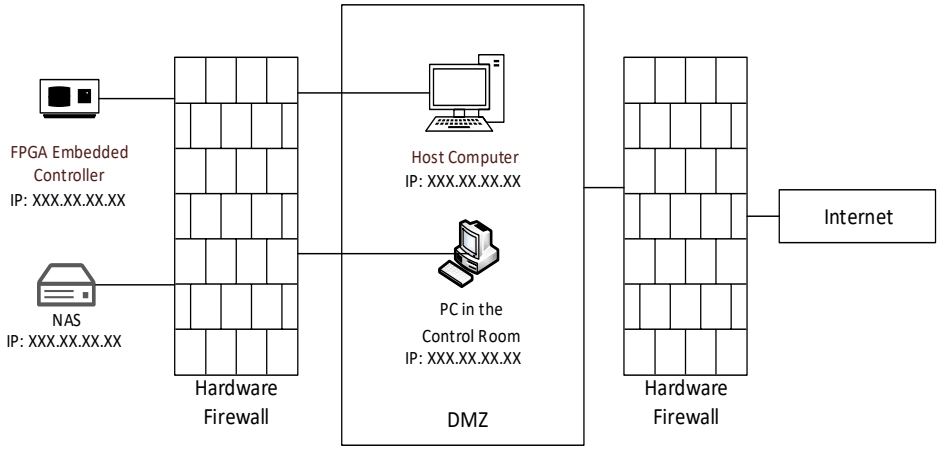

Fig. 3. 7 Cybersecurity Setup of the System

3.5 IN-FIELD TEST AND APPLICATION

The developed monitoring system has been installed in a local power substation of a petrochemical facility recently in Texas, USA, as shown in Fig. 3.8. Considering the redundancy scheme requirements [45], two sets of FPGA-embedded controllers which have the same inputs and functionalities are installed.

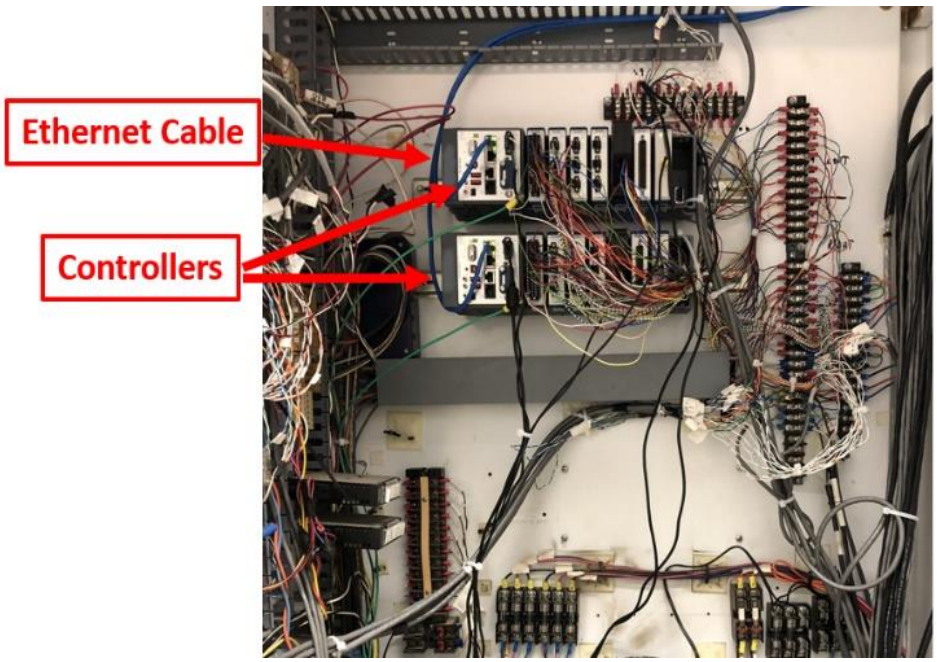

Fig. 3. 8 Installation at the Substation.

On Aug 1st, 2018, all circuit breakers in the feeders at the substation opened at 4:43:39 AM due to an under-voltage event on phase B of the 138kV lines. During the fault, both voltage RMS values dropped from 138kV to around 35kV for three cycles. With the newly developed IoT platform, the operators in the control room received the alarm immediately and retrieved the recorded data on the network from the NAS. The monitoring system was triggered and successfully recorded the circuit breaker statuses, raw voltage data, RMS values and frequency on both 138kV lines. As an example, the recorded raw voltage data during the event on both Line 1 and Line 2 are plotted in Fig. 3.9. As it is shown, three cycles of fault voltage data on both 138kV lines are recorded with the high sampling rate. High-resolution GPS provides the accurate timestamps for the recorded data with the 1904 epoch time reference in ns [46]. The Digital Fault Recorder (DFR) that was previously installed at the substation did not provide all this detailed information. The implemented IoT-based monitoring system provides accurate and detailed information for system operators to do the post-fault analysis.

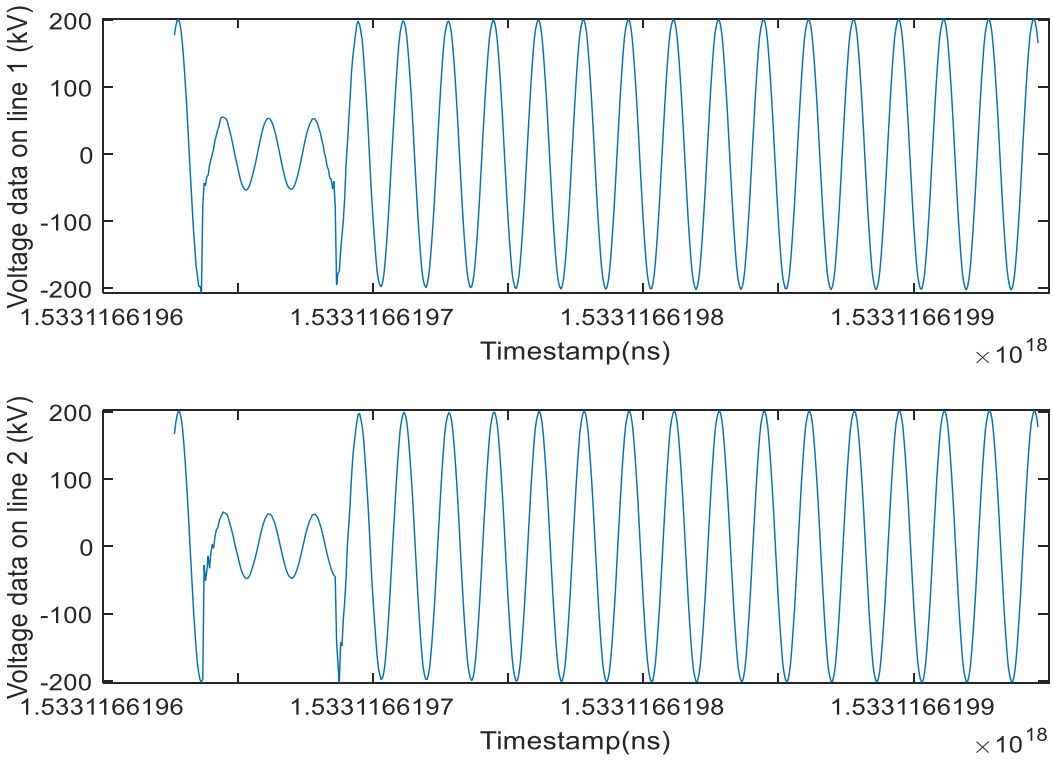

Fig. 3. 9 Recorded Voltage Fault Event Data

3.6 NOVELTY OF THE DEVELOPED MONITORING SYSTEM

Currently, there are various devices and platforms which can be applied for the power substations monitoring. Among different monitoring devices, IEC 61850 standard application is one of the most commonly used monitoring platforms for power systems [47]. Comparing with IEC 61850, the developed monitoring system has better flexibility to be applied with different functionalities. Due to the programmability of the FPGA, the features of the monitoring system can be modified or added based on the operator's needs without extra costs. Meanwhile, the developed monitoring system is designed with energy monitoring and recording functions, which enables the power generation units to participate in the demand response programs in deregulated electricity markets. In this way, the developed system could benefit both the generation unit and system operator financially and technically. As a real-world application system, this developed monitoring system has been applied for Demand Response (DR) program in electric reliability council of Texas (ERCOT) market to improve the operation of the system and brought significant financial benefits to the DR participant. Thus, comparing with most of the monitoring platforms in the market, this system can be applied as a reprogrammable multipurpose monitoring platform at the power substations.

3.7 CONCLUSION

In this paper, an Industrial IoT-based monitoring system for a power substation was developed in the FPGA-embedded controller. All the critical parameters at the substation, including voltage, frequency, power, circuit breaker status, and transformer temperatures are monitored in real-time. The predefined event triggering mechanisms are also programmed on the controller with the recording functions. Once these events are triggered, the data is recorded by the controller and transferred to a NAS in the network. Industrial-Standard GPS is applied to provide high-resolution timestamps and synchronization functions. The FPGA-embedded controller provides high-speed and reliable data acquisition and processing functionalities. Due to the high sampling rate of the system, both steady-state and transient conditions of the power systems are monitored using a single time source. With the IoT platform, the data are transferred and stored through the LAN. System operators can remotely access the data in real-time and retrieve the data from the NAS on the network. The communication methods and protocols, along with the cybersecurity measures demonstrated, were implemented in this IoT-based monitoring system, which at last enables the system operator to visualize the overall operations of the substation in real-time. Recorded high-speed sampled data in the NAS provides detailed information for the system analysis to avoid similar fault incidents in the future. This IoT-based monitoring system has been installed at a local power substation of a petrochemical facility in Texas, USA. It has successfully captured the first fault event and provided valuable information to the system operators for post-event analysis.

3.8 REFERENCE

[1] E. Spano, S. D. Pascoli and G. Iannaccone, “Low-power wearable ECG monitoring system for multiple-patient remote monitoring,” *IEEE Sensors Journal*, vol. 16, no. 13, pp. 5452–5462, Jul. 2016, 10.1109/JSEN.2016.2564995

[2] F. Stradolini, A. Tuoheti, T. Kilic, S. L. Ntella, N. Tamburrano, Z. Huang, G. D. Micheli, D. Demarchi and S. Carrara, “An IoT solution for online monitoring of anesthetics in human serum based on an integrated fluidic bioelectronic system,” *IEEE Trans. Biomedical Circuits and System*, vol. 12, no. 5, pp. 1056–1064, Oct. 2018, 10.1109/TBCAS.2018.2855048

[3] S. Yang, B. Gao, L. Jiang, J. Jin, Z. Gao, X. Ma and W. L. Woo, “IoT structured Long-Term wearable social sensing for mental wellbeing” *IEEE Internet of Things Journal*, vol. 6, no. 2, pp. 3652-3662, Apr. 2019, 10.1109/JIOT.2018.2889966

[4] N. Ahmed, D. De and M. I. Hussain, "Internet of things (IoT) for smart precision agriculture and farming in rural areas," *IEEE Internet of Things Journal*, vol. 5, no. 6, pp. 4890-4899, Dec. 2018, 10.1109/JIOT.2018.2879579

[5] P. Hambarde, R. Varma, and S. Jha, "The survey of real time operating system: RTOS," in *Proc*. *ICESC*, Nagpur, India, 2014, pp. 34-39.

[6] S. Du, B. Liu, H. Ma, G. Wu, and P. Wu, "IIoT-Based intelligent control and management system for motorcycle endurance test," *IEEE Access*, vol. 6, issue. 2, pp. 30567–30576, Dec. 2016, 10.1109/ACCESS.2018.2841185.

[7] M. T. Lazarescu, "Design of a WSN platform for long-term environmental monitoring for IoT applications," *IEEE Journal on Emerging and Selected Topics in Circuits and Systems*, vol. 3, no. 1, pp. 45-54, Mar. 2013, 10.1109/JETCAS.2013.2243032

[8] G. Wang, M. Nixon and M. Boudreaux, "Toward cloud-assisted industrial IoT platform for large-scale continuous condition monitoring," *Proceedings of IEEE*, vol. 107, issue 6, pp. 1193-1205, Jun. 2019, 10.1109/JPROC.2019.2914021

[9] F. Zhang, M. Liu. Z. Zhou and W. Shen, "An IoT-based online monitoring system for continuous steel casting" *IEEE Internet of Things Journal*, vol. 3, no. 6, pp. 1355-1363, Dec. 2016, 10.1109/JIOT.2016.2600630

[10] S. E. Collier, "The emerging enernet: convergence of the smart grid with the internet of things," *IEEE Mag. Industry Application*, vol. 23, issue. 2, pp. 12–16, Dec. 2016, 10.1109/MIAS.2016.2600737.

[11] G. Bedi, G. K. Venayagamoorthy, R. Sigh, R. R. Brooks, and K. C. Wang, "Review of internet of things (IoT) in electric power and energy systems," *IEEE IoT J*, vol. 5, issue. 2, pp. 847–870, Feb. 2018, 10.1109/JIOT.2018.2802704.

[12] R. V. Jadhav, S. S. Lokhande, and V. N. Gohokar, "Monitoring of transformer parameters using internet of things in smart grid," in *Proc. ICCUBEA*, Pune, India, 2016, pp. 1-4.

[13] Y. Tian, Z. Pang, W. Wang, L. Liu, D. Wang, "Substation sensing monitoring system based on power internet of things," in *Proc. IEEE ITNEC*, Chengdu, China, 2017, pp. 1613-1617.

[14] W. T. Hartman, A. Hansen, E. Vasquez, S. EI-Tawab, and K. Altaii, "Energy monitoring and control using internet of things (IoT) system," in *Proc. SIEDS*, VA, USA, 2018, pp. 13–18.

[15] L. M. L. Oliveira, J. Reis, J. J. P. C. Rodrigues, and A. F. de Sousa, "IoT based solution for home power energy monitoring and actuating," in *Proc. INDIN*, Cambridge, UK, 2015, pp. 988-992.

[16] M. R. Bastos, and S. S. L. Machado, "Visual, real-time monitoring system for remote operation of electrical substation," in *Proc. IEEE/PES T&D-LA*, Sao Paulo, Brazil, 2011, pp. 417-421.

[17] Q. Gao, W. Ge, C. Wang, J. Zhang, B. Geng, and X. Jiang, "High voltage equipment online monitoring system of smart substation," in *Proc. IEEE PES ISGA*, Tianjin, China, 2012, pp. 1-5.

[18] S. Park, E. Lee, W. Y, H. Lee, and J. Shin, "State estimation for supervisory monitoring of substations," *IEEE Trans. Smart Grid*, vol. 4, no. 1, pp. 406–410, Feb. 2013, 10.1109/TSG.2013.2240322.

[19] M. B. Bastian, W. D. Carman, and D. J. Woodhouse, "Real-time monitoring of substation ground potential rise and grounding system impedance using power system faults," *IEEE Trans. Industry Application*, vol. 51, no. 6, pp. 5298–5304, Apr. 2015, 10.1109/TIA.2015.2425361.

[20] W. Lee, J. Gim, M. Chen, S. Wang, and R. L, "Development of a real-time power system dynamic performance monitoring system," *IEEE Trans. Industry Application*, vol. 33, no. 4, pp. 1055–1060, Jul/Aug. 1997, 10.1109/28.605748.

[21] F. Zhao, Q. Sun, J. Zhan, L. Nie, and Z. Xu, "The real-time database application in transformer substation hotspot monitoring system," in *Proc. ICACT*, PyeongChang, South Korea, 2014, pp. 941-944.

[22] Y. Tian, Z. Pang, W. Wang, L. Liu, and D. Wang, "Substation sensing monitoring system based on power internet of things," in *Proc. ITNEC*, Chengdu, China, 2018, pp. 1613-1617.

[23] *NI FPGA*. [Online]. Available: http://www.ni.com/fpga/

[24] *Introduction to FPGA Technology: Top 5 Benefits*. [Online]. Available: http://www.ni.com/white-paper/6984/en/

[25] Z. Hao, G. Lianping, M. Jie and Y. Peng, "Research on the hardware co=processing technology for waveform character searching with a digital oscilloscope," in *Proc. IEEE ICEMI*, Yangzhou, China, 2017.

[26] F. A. Escobar, X. Chang and C. Valderrama, "Suitability analysis of FPGAs for heterogeneous platforms in HPC," *IEEE Trans. Parallel and Distributed System*, vol. 27, no. 2, pp. 600–612, Feb. 2016, 10.1109/TPDS.2015.2407896

[27] J. Sheng, C. Yang, A. Sanaullah, M. Papamichael, A. Caulfield and M. C. Herbordt, "HPC on FPGA clouds: 3D FFTs and implications for molecular dynamics," in *Proc. 2017 27th International Conference on Field Programmable Logic and Applications (FPL), Ghent, Belgium.*

[28] R. Chen and V. K. Prasanna, "Computer generation of high throughput and memory efficient sorting designs on FPGA," *IEEE Trans. Parallel and Distributed System*, vol. 28, no. 11, pp. 3100–3113, Nov. 2017, 10.1109/TPDS.2017.2705128

[29] *cRIO-9039 CompactRIO Controller.* [Online]. Available: http://www.ni.com/en-us/support/model.crio-9039.html

[30] *NI-9205.* [Online]. Available: http://www.ni.com/pdf/manuals/374188f.pdf

[31] *NI-9225*. [Online]. Available: http://www.ni.com/pdf/manuals/374707e.pdf

[32] *NI-9425*. [Online]. Available: http://www.ni.com/pdf/manuals/373782j.pdf

[33] *Data Center Storage Evolution.* [Online]. Available: https://www.siemon.com/us/white_papers/14-07-29-data-center-storage-evolution.asp

[34] *Analog period measurement expresses VI.* [Online]. Available: http://zone.ni.com/reference/en-XX/help/371599N-01/lvfpga/fpga_period_measurement/

[35] *LabVIEW Timestamp.* [Online]. Available: http://www.ni.com/tutorial/7900/en/

[36] *RIO Developer Essentials Guide for Academia Glossary.* [Online]. Available: https://learn-cf.ni.com/teach/riodevguide/glossary.html#tag

[37] *Understanding Communication Options Between the Windows HMI, RT Processor, and FPGA.* [Online]. Available: http://www.ni.com/white-paper/53345/en/#RTHMICommunication

[38] A. Rubni and J. Corbel, "Direct memory access and bus mastering," in *LINUX Device Drivers, 2nd* ed. Boston, MA, USA: O'Reilly & Associates, 2001, ch. *13*, pp. *401-403.*

[39] *Host memory buffer overview.* [Online]. Available: http://www.ni.com/white-paper/53881/en/

[40] L. Zhao, I. Matsuo, Y, Zhou and W. Lee, "Design of an industrial IoT-based monitoring system for power substations," presented at the IEEE 55th I&CPS. Conf, Calgary, Canada, 2019.

[41] *Getting stared with the LabVIEW real-time module.* [Online]. Available: http://www.ni.com/pdf/manuals/371375d.pdf

[42] P. C. Heckel, "Minimizing remote storage usage and synchronization time using deduplication and multichunking: syncany as an example," M.S. thesis, Dept. Bus Infor Math., Mannheim Univ., Mannheim, Germany, 2012.

[43] C. Esposito, A. Castiglione, F. Palmieri, M. Ficco, K. R. Choo, "A published/subscribe protocol for event-driven communications in the internet of things," in *Proc. IEEE DASC/PiCom/DataCom/CyberSciTech*, Auckland, New Zealand, 2016, pp. 376-383.

[44] D. C. Mazur, R. A. Entzminger, P. A. Morell, J. A. Kay, and E. Syme, "Defining the industrial demilitarized zone and its benefits for mining applications," *IEEE Trans. Industry Application*, vol. 52, no. 3, pp. 2731–2736, Feb. 2016, 10.1109/TIA.2016.2530045.

[45] I. B. M. Matsuo, L. Zhao, and W. Lee, "A dual modular redundancy scheme for CPU-FPGA platform-based systems," *IEEE Trans. Industry Application*, early access, Jul. 2018, 10.1109/TIA.2018.2859386.

[46] *LabVIEW Timestamp*. [Online]. Available: http://www.ni.com/tutorial/7900/en/

[47] S. Matsuda, Y. Watabe, I. I. Asrizal, S. Katayama, K. Okuno, and K. Kasuga, “Issues overcome in the design and application of iec 61850– compliant substation automation systems,” in Advanced Power System Automation and Protection (APAP), 2011 International Conference on, Oct. 2011, pp. 198–202

CHAPTER 4.

THE DESIGN OF A REMOTE ONLINE HOLISTIC MONITORING SYSTEM FOR A WIND TURBINE

THE DESIGN OF A REMOTE ONLINE HOLISTIC MONITORING SYSTEM FOR A WIND TURBINE[3]

Long Zhao, Igor Matsuo, Yuhao Zhou, Wei-Jen Lee

L. Zhao, Y. Zhou, I. Matsuo, S K. Korkua, and W. Lee, "Design of a remote online holistic monitoring system for a wind turbine," *IEEE Trans. Ind. Appl.,* vol. 56, Jan/Feb. 2020. pp. 14-21.

The Design of a Remote Online Holistic Monitoring System for a Wind Turbine

Long Zhao[1] Yuhao Zhou[1] Igor Matsuo[1]

Student Member, IEEE

S K. Korkua[2]

Wei-Jen Lee[1]

Fellow, IEEE

long.zhao@mavs.uta.edu; yuhao.zhou@mavs.uta.edu; matsuoigor@gmail.com; ksuratsa@wu.ac.th; wlee@uta.edu

[1]University of Texas at Arlington, 701 S Nedderman Dr, Arlington, TX 76019, USA

[2]Walailak University, Nakhon Si Thammarat, 80161, Thailand

Abstract -- As one of the most promising renewable energy resources, a large amount of wind energy has been implemented all around the world since 1990s. Increasing the size of the wind turbines and the harsh operating environment lead to higher failure rates on the wind turbines compared with other renewable resources. As the result, not only unplanned maintenance and repairments but also downtime of the wind turbine increases the operation cost significantly. In addition, the long-distance transmission lines are required to transfer the wind generation power to the load centers due to the remote operation location of the wind farms. To improve the power transfer capability, series compensated lines are adopted in many cases. However, subsynchronous control interactions (SSCI) could happen between series compensated transmission lines and wind turbines. This may damage wind turbine components severely and cause stability issues in the power grids. Currently, various condition monitoring systems have been developed and applied for wind turbines. Different SSCI detection mechanisms are also proposed in many studies. This paper proposes an FPGA-CPU based holistic monitoring system which not only provides both condition and SSCI monitoring functions simultaneously in real-time but also records necessary data for post-event analysis.

Index Terms-- Condition monitoring, Internet of Things, Real-time systems, Renewable energy sources, Smart grids, SSCI, SSO, SSR, Wind farms.

4.1 INTRODUCTION

As one of the most promising renewable energy resources, the wind energy has been expended remarkably since 1990s. By 2017, more than 51.2 GW of capacity has been installed globally [1]. However, large implementation of wind energy also brought enormous potential challenges and issues for the system operations and maintenance. Increasing size of the wind turbines and harsh operation

environment leads relatively high failure rates for wind turbines, and more than 30% of wind energy cost is from unplanned operation and maintenance (O&M) [1-4]. To reduce the unplanned downtime and maintenance costs, the condition monitoring has been developed to provide the necessary information for system operators. The condition monitoring is defined as a system using collected data with an automation system to evaluate the condition of the monitoring object to prevent failures [5]. Many studies have discussed different condition monitoring systems for wind turbines. In the paper [6], a data acquisition platform is developed for a wind turbine condition monitoring system. In this case, different parameters data are acquired with different sampling frequencies to predict the faults of the wind turbine. In the paper [7], the authors use wavelets to analyze the output power of wind turbines for the off-line condition monitoring system. By analyzing the frequency components, characteristics of mechanical and electrical conditions of wind turbines are established. In the paper [8], a real-time condition monitoring system is developed with a high-resolution diagnostic method for wind turbine blades. In the paper [9], the authors developed a real-time conditioning monitoring and fault diagnosis system in China. The paper [10] introduces a wind turbine gearbox failure identification method using deep neural networks for condition monitoring purpose. Regardless the monitoring system design, transfer necessary real time data to the control center is another challenge for the applicability of the system.

Furthermore, due to the remote locations of wind farms, series compensated lines are used to transfer power to the load centers. However, some unexpected interactions may be generated between compensated generation lines and wind turbines. One of the interactions is subsynchronous oscillation (SSO). Currently, different types of SSO is defined under different scenarios. For wind generation, subsynchronous control interaction (SSCI) is considered as the interaction between wind turbine controller and series compensation system at subsynchronous frequencies [11]. SSCI could damage the wind turbine severely and affect the stability of the power grids. In October 2009, an SSCI was observed in South Texas, USA. During the event, crowbar systems of wind turbines were damaged, and system voltage increased to more than 200% in 150ms [12]. This SSCI event brought serious concern to the Electric Reliability Council of Texas (ERCOT). Similar SSCI events have also happened at the wind farms in China [13,14]. To mitigate the impacts of SSCI on the system, many researches have been performed and different SSCI detection mechanisms for different situations have been proposed. In the paper [15], SSCI studies between full-converter wind turbines and series-compensated AC transmission lines were presented. In the paper [16], SSCI detection and protection for a doubly-fed generator is developed based on discrete-time Fourier transform (DTFT). The paper [17] developed an SSCI detection mechanism using modal identification analysis. In the paper [18], the authors used reactance crossover techniques to

evaluate the SSCI for wind turbines. In the paper [19], a supplementary damping control using multiple-input and multiple-output (MIMO) state-space approach to mitigate SSCI in wind farms is proposed. The paper [20] analyzed SSCI using eigenvalue analysis technique for a part of ERCOT network. The authors in the paper [13] proposed an SSCI stability analysis method based on the impedance network model, which can accurately and quantitatively evaluate the SSCI for a large-scale wind power system.

However, most monitoring systems for the wind turbine are developed either only for wind turbine condition monitoring or SSCI detection. Very limited monitoring systems have been developed with both functions at the same time to provide a holistic monitoring with lossless data logging for system operators. To reduce the unnecessary complexities and redundant coordination between two independent monitoring systems for the same wind turbine, a holistic Internet of Things (IoT)-based monitoring system is developed for the wind turbines. The Field Programmable Gate Array (FPGA)-CPU hybrid controller is adopted in the system to enhance the system performance. Additionally, to provide more detailed information for system operators to perform the post-event analysis, Network Attached Storage (NAS) with data redundancy scheme is applied to record the event data.

For the rest of the paper, the structure of the monitoring system is introduced in Section 4.2. Operation of the developed monitoring system is shown in Section 4.3. Section 4.4 shows the SSCI detection and condition monitoring of wind turbine. Section 4.5 shows the in-lab test of the developed monitoring system. The conclusion is of this paper is presented in Section 4.6.

4.2 STRUCTURE OF THE MONITORING SYSTEM

This IoT-based monitoring system is consisted of a FPGA-CPU hybrid controller, a host computer, an uninterruptable power supply (UPS), a Network-Attached-Storage (NAS), and a hardware firewall. As reprogrammable silicon chips, FPGA is a reprogrammable hardware which has better reliability than most processor-based systems. Parallel processing of FPGAs provides equal resources for different tasks without processing resources competition [21]. This parallel processing nature enables the deterministic processing for the FPGAs which is extremely critical for a real-time system with multiple inputs processing. However, due to the technical limitations of the FPGAs, CPU is also required for the data logging and network communications in this application. An industrial standard controller with 1.91 GHz Quad-Core CPU, 2GB DRAM, 16GB storage, Kintex-7 325T FPGA, and an RJ-45 Gigabit Ethernet port is adopted. The controller is powered by an UPS to prevent monitoring system fail caused by power loss or interruption. A 4-Bay 8 TB NAS is applied as the data storage to record all detailed event data which can be accessed remotely through the Local Area Network (LAN) with the authorization. As an IoT-based application, cybersecurity is a critical factor that needs to be considered in the design. Thus, a hardware firewall is

considered over software firewall in this application due to the faster speed and higher security levels. As a simplified illustration, the structure of a holistic IoT-based monitoring system for wind turbines is shown in Fig. 4.1.

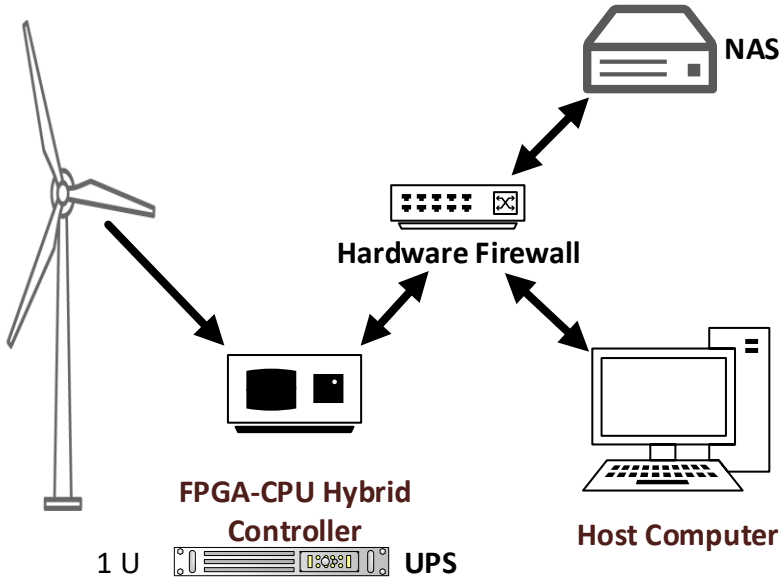

Fig. 4.1 Structure of a Holistic IoT-Based health monitoring system

In this system, IoT provides real-time and remote communication in this monitoring system. The data communication is realized through a LAN, and the monitoring objects can be visualized in real-time by the system operators in the control room with the authorized computer in the network.

4.3 OPERATION OF THE MONITORING SYSTEM

In this monitoring system, operation of the system can be considered as 3 sequential parts which are data acquisition, data processing and data logging. Different tasks are processed with the different targets on the FPGA-CPU hybrid controller.

4.3.1 Data Acquisition

In this monitoring system, different types of data are collected with three different input modules on the controller. An industrial standard GPS is also equipped to provide accurate timing with ± 100ns and geographic location information [22]. The inputs and data rate of each module are shown in Table 4-1. To have sufficient data meanwhile and to avoid high CPU usage, different sampling rates are chosen based on the type of the signals and different purposes. Thus, the sample rates have chosen based on the multiple long-term system in-lab tests considering the overall performance of the system. The standard update rate for most GPS devices is 1Hz. In our system, the module we are using has factory default sample rate which is also 1Hz (updates once a second). Uninterruptable power supply (UPS) does not require the

high sample rate. Therefore, 1 sample/second is enough for the UPS monitoring. To capture transient phenomena for the voltage signals without affect the CPU usage and to have enough data for post-event analysis, the sample rate for the voltage signal is set to 2000 samples per second. 1000 samples/second sample rate is set for the vibration signals monitoring which is enough for the vibration data analysis without affecting the CPU performance.

TABLE 4 - 1. Input Data Type and Rates of Input Modules

Module	Input Data	Data Rate
GPS	Time	Every Second
Digital Input	UPS Status	1 Samples/Second
Analog Input 1	Vibration Signal	1000 Samples/Second
Analog Input 2	Induction Generator Voltage	2000 Samples/Second

Digital input module monitors the condition of the power source to ensure that system operator can take necessary actions during power failure before UPS runs out of power. Analog input 1 is a ±10 V voltage input module that receives the vibration signal measured by accelerometers for the wind turbine condition. Analog input 2 is a 300Vrms voltage input module that collects the wind turbine voltage output data with 2000 Samples/Second sampling speed. The actual FPGA-CPU hybrid controller with all input modules is shown in Fig. 4.2

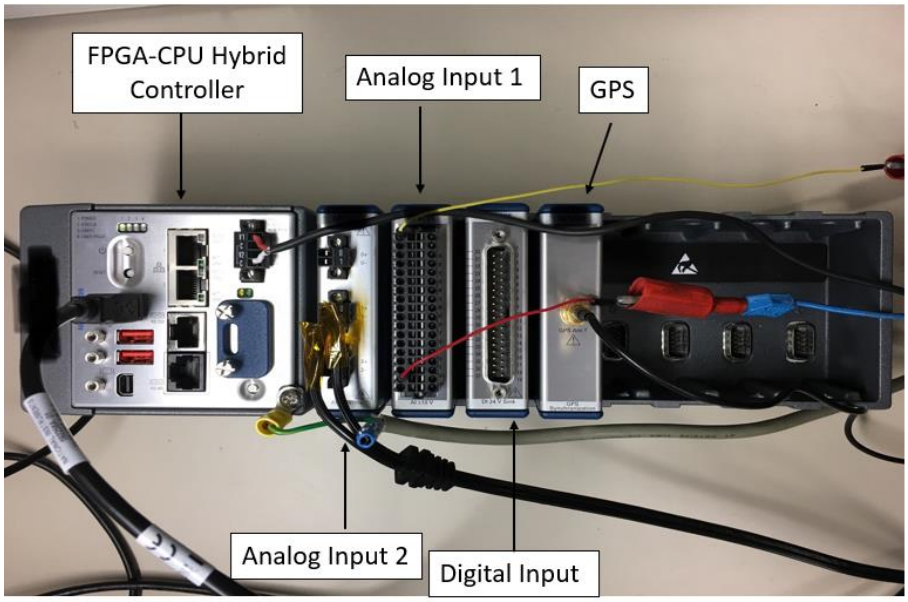

Fig. 4.2 The FPGA-CPU hybrid controller with input modules

4.3.2 Data Processing

Due to the hardware-timed speed and reliability, FPGAs are applied for data processing once the data are collected. As mentioned before, parallel and deterministic processing are considered as the biggest advantages of the FPGA over traditional CPU. Thus, SSCI detection and wind turbine condition analysis are performed on the FPGA in this monitoring system. Once the pre-defined detection mechanisms are triggered on the FPGA, the signals are sent to the processor-based target for the recording tasks. Considering the synchronization is extremely critical for a real-time monitoring application, all the collected input data is timestamped with the GPS signal on the FPGA as well.

4.3.3 Data Logging

A 4 Bay 8 TB NAS is equipped in the system for data logging purpose. In this monitoring system, the vibration and voltage signals are recorded whenever the predefined detection mechanisms are triggered on the FPGA target. Due to the technical limitations of the FPGAs, data logging is realized on the CPU target. The recorded data will be sent from FPGA target to CPU target and stored to the NAS. Data in the NAS can be accessed through LAN anytime for qualified personnel.

Lossless data logging with accurate timestamps enable better event analysis and improve system operators. To provide a better illustration of FPGA-CPU hybrid controller operation, a simplified controller operation processing is shown in Fig. 4.3.

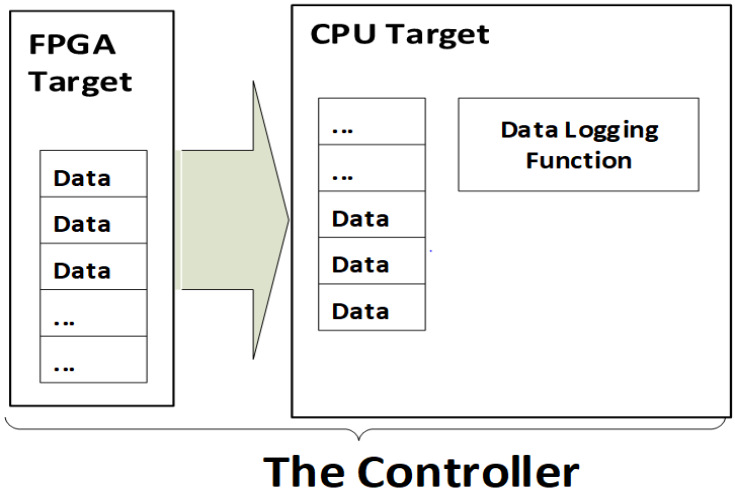

Fig. 4.3 FPGA-CPU hybrid controller operation

4.4 SSCI DETECTION AND CONDITION MONITORING OF THE WIND TURBINES

As a holistic monitoring system for the wind turbines, condition monitoring and SSCI detection are developed under the same platform.

4.4.1 SSCI Detection

To take advantage of the parallel processing capability of the FPGAs and to improve the SSCI detection speed, an SSCI detection using modal identification analysis and Fast Fourier transform (FFT) is adopted in this multipurpose monitoring system [17]. With the SSCI detection method proposed in the paper [17], the frequency, magnitude and derivative of the magnitude of the voltage signal can be monitored simultaneously to detect SSCI event within a short time period while improving the detection accuracy. In this way, the voltage input signals are processed with three algorithms which are Eigensystem Realization Algorithm (ERA), Prony and Moving Window FFT simultaneously in parallel. ERA and Prony are used as modal analysis techniques to calculate the frequency and magnitude of the voltage signal modes. Moving Window FFT calculates the frequency and magnitude of voltage input signals. The simplified detection process on the controller is shown in Fig. 4.4.

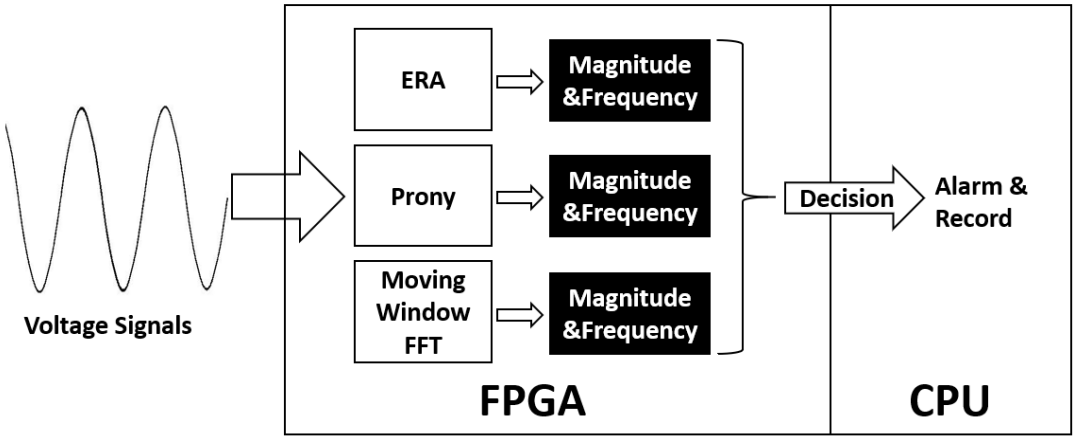

Fig. 4.4 SSCI detection process on the hybrid controller

As it is shown in Fig. 4.4, three different detection algorithms are applied to monitor the magnitude and frequency of the input voltage signals simultaneously on the FPGA. Alarm and recording are triggered on the CPU target based on the decision signal sent from the FPGA target. In this system, only if two of the algorithms detect the SSCI at the same time, the alarm and recording function will be triggered. With this SSCI detection method, SSCI event can be detected within 150ms [17].

4.4.2 Condition Monitoring of Wind Turbines

Among all failures, the gearbox failures caused the longest downtime and the highest maintenance cost which increases the energy costs remarkably [1, 7, 23]. To better utilize the condition

monitoring systems for wind turbines, the vibration sensor is mainly used in condition monitoring system to detect the abnormal operations on the gearbox because abnormal operation vibration pattern can be easily distinguished from normal operating conditions. [1, 24-26].

For wind turbine condition monitoring, different components of the wind turbines can be used. However, to provide the key and overall information of the wind turbines, only major electrical and mechanical components are monitored in this system. In this monitoring system, vibrations are measured to monitor the wind turbine conditions and predict the fault [27]. To measure vibration on the wind turbine, vibration transducers are used. Both time domain and frequency domain analysis are applied to process the vibration signals. By characterizing the correlation between corresponding signals and fault conditions, the healthy components of the wind turbine can be identified, and the lifespan of the wind turbine components can be estimated [27]. The vibration analysis scheme is shown in Fig. 4.5.

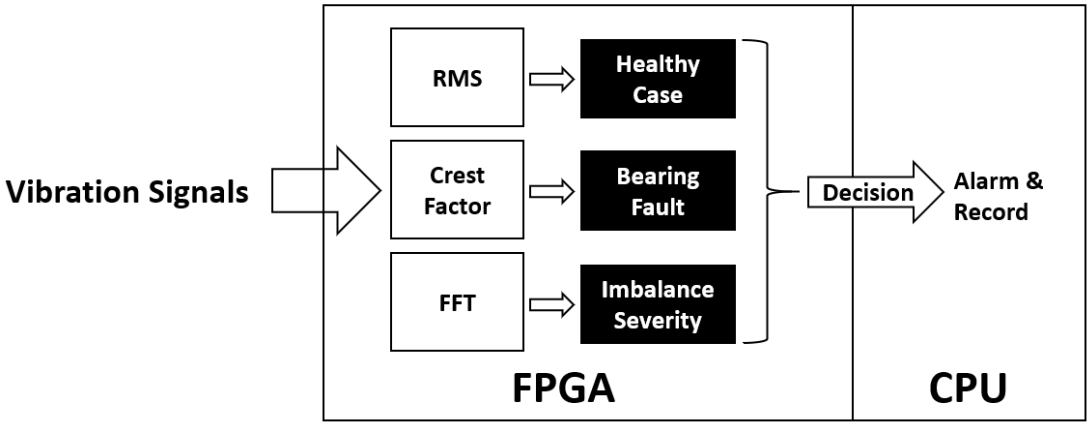

Fig. 4.5 Process of the wind turbine vibration analysis scheme

In this system, the root mean square (RMS) value and crest factor of vibration signal are calculated in the equation (1) and (2).

$$RMS = \sqrt{\frac{X_1^2 + X_2^2 + \ldots + X_{n-1}^2 + X_n^2}{n}} \qquad (1)$$

$$\text{Crest Factor} = \frac{\text{Peak Value of Vibration Signal}}{\text{RMS Value of Vibration Signal}} \qquad (2)$$

Where X is vibration signal, and n is number of samples.

To provide the condition monitoring for the wind turbine, three parameters are used to indicate health conditions of the wind turbines. RMS values of normal operation vibration signals are considered as RMS baseline to decide the overall wind turbine health status. The crest factor has been applied to indicate the wear of the rolling elements such as bearing wear and gear tooth wear in mechanical

engineering [28, 29]. Using the crest factor of the normal operating condition as the baseline, the fault on the bearing system can be identified in real-time. FFT is also applied for the rotor imbalance analysis, and it provides the severity levels of the rotor imbalance. With this vibration analysis mechanism, the faulty components of the wind turbine can be identified, and the wind turbine health condition can be estimated.

4.5 IN-LAB MONITORING SYSTEM TEST

To ensure the developed monitoring system works properly, the SSCI detection mechanism and condition monitoring are tested in the lab.

4.5.1 SSCI Detection

To validate the SSCI detection mechanism in the monitoring system, the SSCI event is simulated from the following grid, which consists of a wind farm with 60 units of GE 1.5MW wind turbines connected to a series-compensated line. The wind turbines are based on the model presented on reference [30]. The grid parameters, including the equivalent system, transmission line, gen-tie line, and collection system of the wind farm, are taken from reference [17]. A compensation level of 70% is used. The 345kV bus voltage output data with subsynchronous frequency is shown in Fig. 4.6 (a). Three detection mechanisms are applied simultaneously on the FPGA target, SSCI frequency and magnitude are shown in Fig. 4.6 (b) and (c) respectively. In this test, the pre-defined triggering criteria are considered as 7kV. However, the system operator may adjust it based on practical situations. Based on the simulation result, the SSCI event was successfully detected after 130ms.

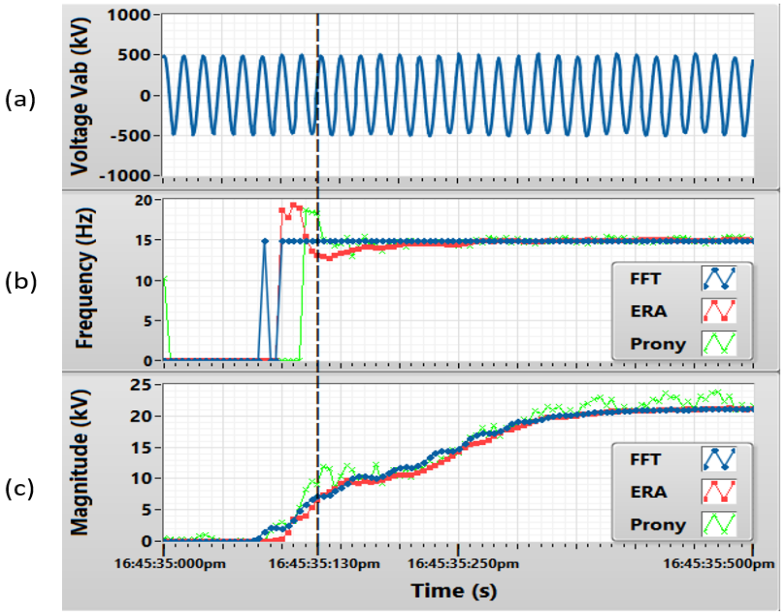

Fig. 4.6 SSCI Testing Simulation

4.5.2 Fault Detection of Induction Machine

To validate the vibration detection scheme for the wind turbine, an induction motor under rotor imbalance conditions is used to create the vibration signals. As one of the most common mechanical faults, the vibration caused by rotor imbalance can be observed from different load torques. In this case, A 3-phase, 2-pole, 1 h. p. squirrel cage induction motor is adopted with a modified flywheel. A variable speed drive is used to feed the induction motor at 50Hz. The modified flywheel is made with drilled holes to create the motor imbalance condition as shown in Fig. 4.7.

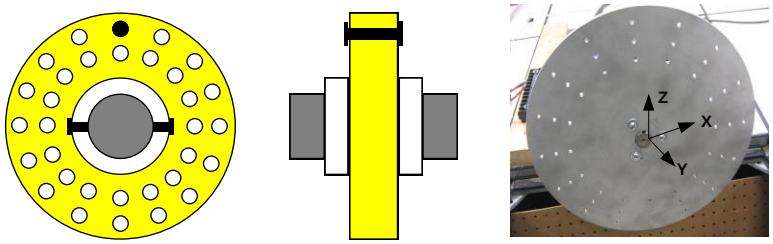

Fig. 4. 7 Flywheel Design for Rotor Imbalance

In this test, an ADXL330 Tri-axial accelerometer is installed to collect the vibration signal on the motor housing which is shown in Fig. 4.8.

Fig. 4. 8 Tri-axial Accelerometer Measurement on the Motor Housing

To better present the test configuration of the rotor imbalance condition, a simplified diagram of a rotor imbalance test setup is shown in Fig. 4.9. The vibration signals are measured by the accelerometer and sent to the FPGA-CPU hybrid controller for the vibration signal analysis. To create an imbalance on

the rotor, load with different masses are added to the flywheel. The fault severity level is estimated based on the different load masses.

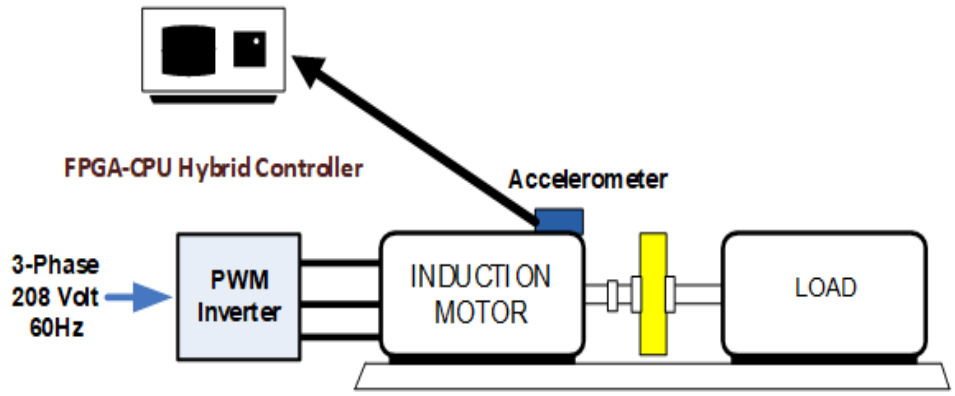

Fig. 4. 9 The System Setup for Rotor Imbalance Test

In this test, 5g, 10g, 15g and 20g of load are added to the modified flywheel for the tests. The RMS value of vibration signals for each load mass on three axes are measured and shown in Table4-2. Comparing with the RMS based line, the vibration RMS increases along with the load mass.

TABLE 4 - 2. RMS VALUES OF THE VIBRATION SIGNAL

MASS	X-axis	Y-axis	Z-axis
0g	0.71	0.25	0.11
5g	1.74	0.49	0.31
10g	2.48	0.8	0.7
15g	2.62	2	0.91
20g	2.71	2.42	1.22

To further analyze the vibration signals, crest factor for each load is measured and calculated and it is plotted in Fig. 4.10.

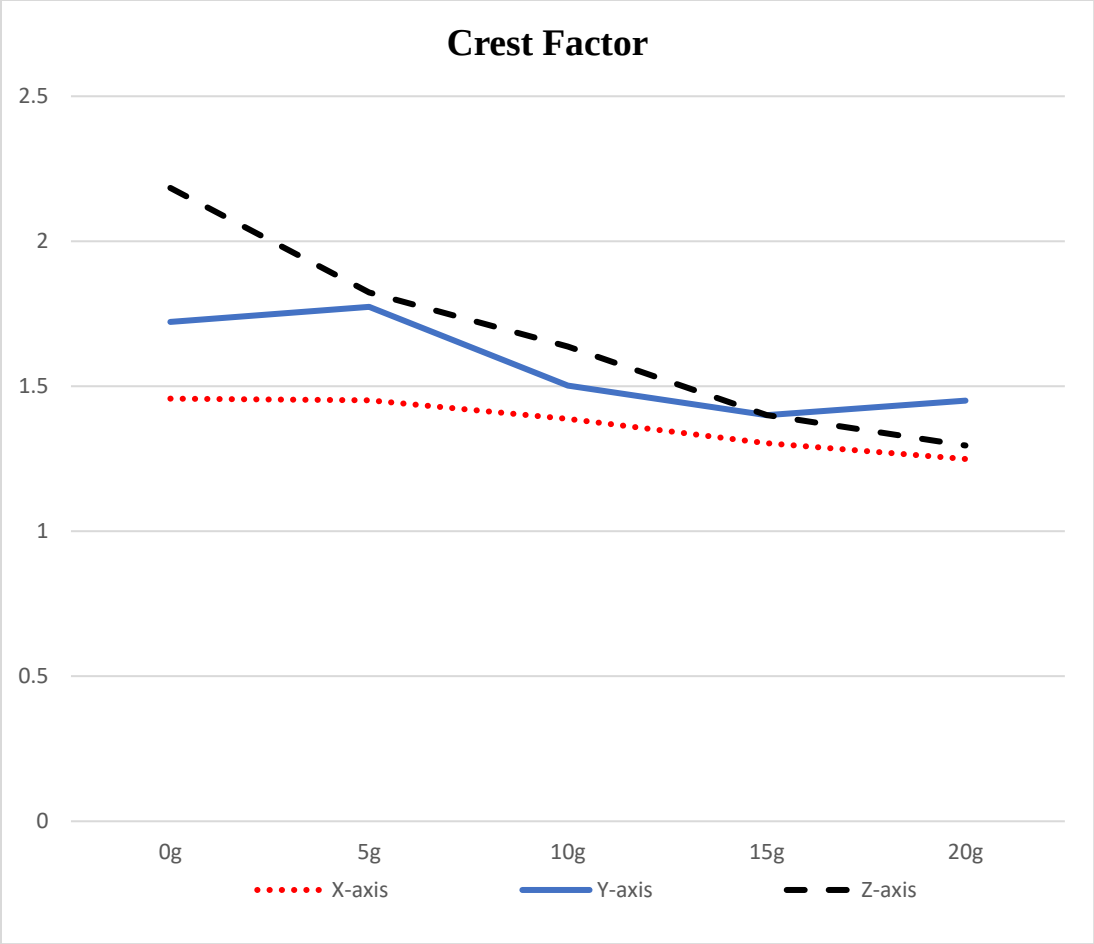

Fig. 4. 10 Crest Factor for Different Load Masses

As it is shown in Fig. 4.10, values of crest factor did not deviate significantly when the mass increased. As mentioned in the previous section, crest factor has been applied to indicate the bearing system conditions. Thus, in this test, the fault is not mainly contributed by the bearing element.

In Fig. 4.11, the FFTs of vibration signal are plotted for X-axis, Y-axis and Z-axis respectively. According the detection scheme in the Fig. 4.5, FFT is applied to analyze the vibration signal in the frequency domain for rotor imbalance severity. As it is shown in Fig. 4.11, the magnitude of the FFT on each axis increases when the load mass increases. Therefore, rotor imbalance severity can be indicated with FFT analysis on the vibration signals.

The front panel of the monitoring system is shown in Fig. 4.12. Based on the front panel, the system operator could visualize the major wind turbine components' conditions and estimate the maintenance time based on the health indication parameters. SSCI can also be monitored and detected in real-time with the visual and sound alarm function. Once the pre-defined detection mechanisms are triggered, related data will be recorded and stored to the NAS.

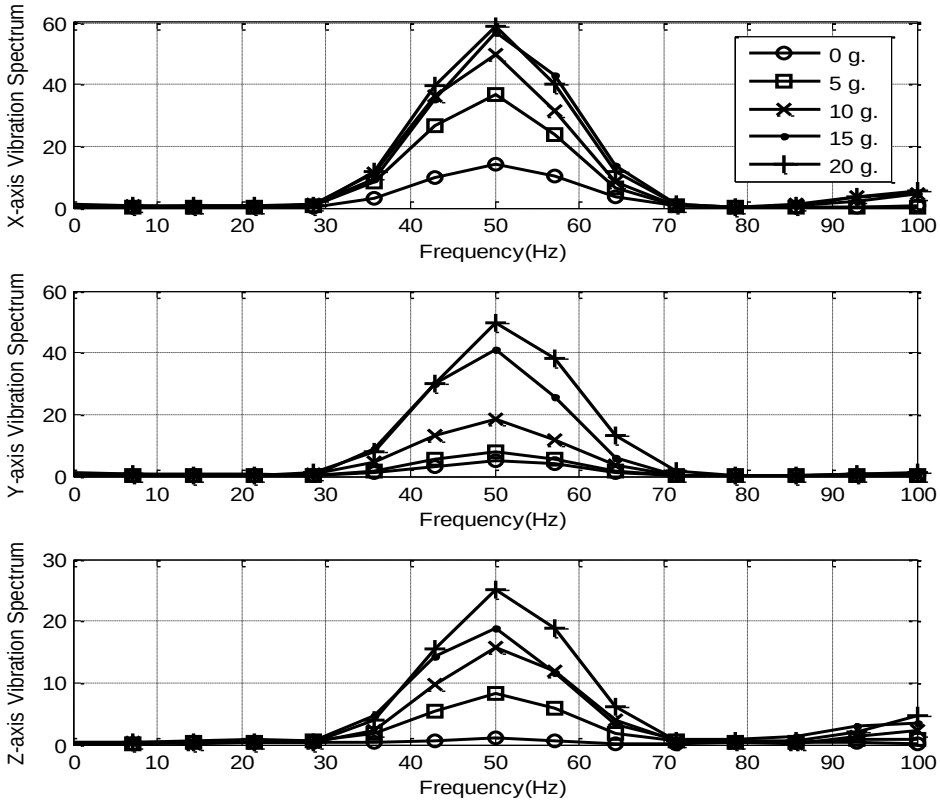

Fig. 4. 11 The FFT of the Vibration Signal with Different Masses for Each Axis

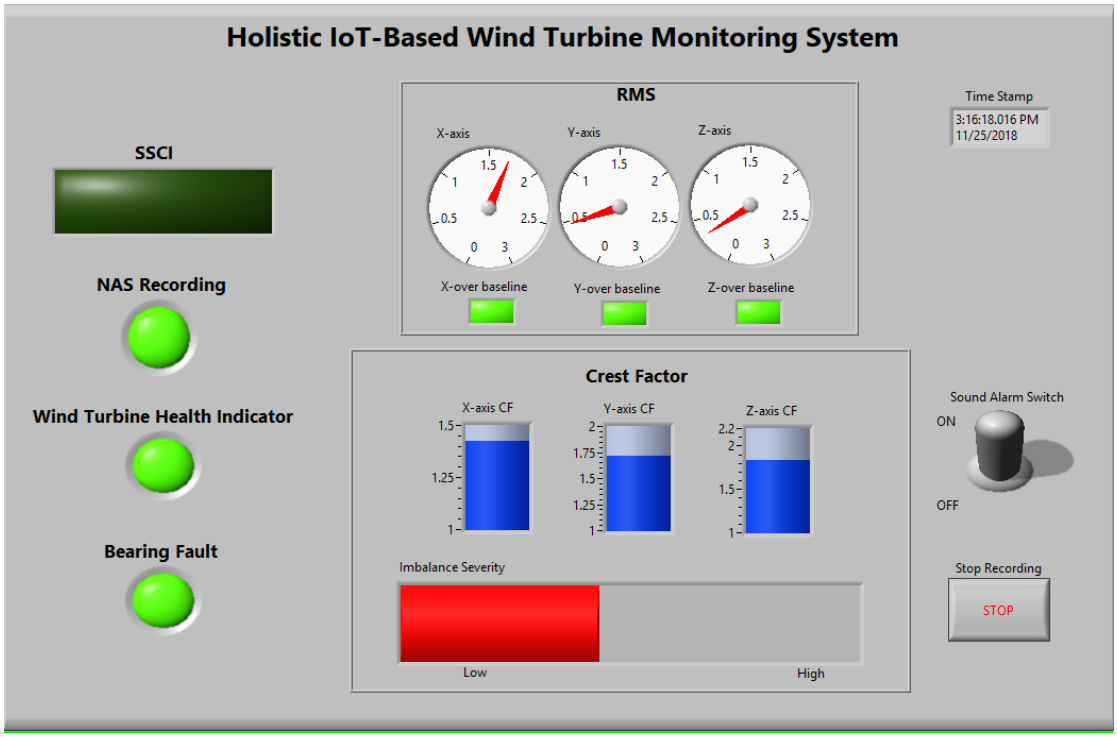

Fig. 4. 12 Front Panel of the IoT-Based Multipurpose Monitoring System

4.6 CONCLUSION

In this paper, an IoT-based holistic monitoring system is developed for the wind turbine. The monitoring system for both SSCI events and wind turbine condition are developed on an FPGA-CPU hybrid controller with the IoT platform. Additionally, lossless data logging enables the post-event analysis with detailed information for system operators/engineers. With this developed holistic monitoring system, both condition monitoring and SSCI detection can be realized simultaneously in real-time, which could help system operators to avoid unnecessary coordination caused by two independent monitoring systems.

4.7 REFERENCES

[1] Y. Li, C. Zhu, C. Song, and J. Tan, "Research and development of the wind turbine reliability," *International Journal of Mechanical Engineering and Applications*, Vol. 6, PP. 35-45, Apr. 2018.

[2] C. C. Ciang, J-R. Lee, and H-J Bang, "Structural health monitoring for a wind turbine system: a review of damage detection methods, " *Measurement Science and Technology*, PP. 1-20, Oct. 2008.

[3] W. Qiao, and D. Lu, "A survey on wind turbine condition monitoring and fault diagnosis-part I: components and subsystems," *IEEE Trans. Ind. Electron*. Vol. PP. 6536-6545. Oct. 2015.

[4] L. Zhao, Y. Zhou, I. Matsuo, S K. Korkua and W-J. Lee, "The design of a holistic IoT-Based monitoring system for a wind turbine," in *Proc. IEEE/IAS 55th Ind. Commercial Power Syst. Tech. Conf.*, Calgary, AB, Canada, 2019, pp. 1-7.

[5] D. C. Mazur, J. A. Kay, and K. D. Mazur, "Advancements in vibration monitoring for the mining industry," *IEEE Trans. Ind. Appl,* vol. 51, pp. 4321-4328, Sep/Oct. 2015.

[6] G. Swiszcz, A. Cruden, C. Booth, and W. Leithead, "A data acquisition platform for the development of a wind turbine condiiton, " in *Proc. 2008 Condition Monitoring and Diagnosis Conf.*, pp. 1358-1361.

[7] S. J. Watson, B. J. Xiang, W. Yang, P. J. Tavner, and C. J Crabtree "Condition monitoring of the power output of wind turbine generators using wavelets," *IEEE Trans. Energy Convers*, vol. 25, pp. 715-721, Sep. 2010.

[8] K-Y. Oh, J-Y. Park, J-S. Lee, B. I. Epureanu, and J-K. Lee "A novel method and its field tests for monitoring and diagnosing blade health for wind turbines," *IEEE Trans. Instrumentation and Measurement*, vol. 64, pp. 1726-1733, Jun. 2015.

[9] X. Chen, R. Yan and Y. Liu "Wind turbine condition monitoring and fault diagnosis in China, " *IEEE Instrum. Meas. Mag*, vol. 64, pp. 22-28, Apr. 2016.

[10] L. Wang, Z. Zhang, H. Long, J. Xu, and R. Liu "Wind turbine gearbox failure identification with deep neural networks," *IEEE Trans Ind. Informat*, vol. 13, pp. 1360-1368, Jun. 2017.

[11] L. Zhao, I. Matsuo, F. Salehi, Y. Zhou and W-J. Lee, "Development of a real-time web-based power monitoring system for the substation of petrochemical facilities," *IEEE Trans. Ind. Appl.,* vol. 55, pp. 1360-1368, Jan/Feb. 2019.

[12] J. Adams, C. Carter, and S.-H. Huang, "ERCOT experience with subsynchronous control interaction and proposed remediation," in *Proc. 2012 Transmission and Distribution Conf. Expo.,* pp. 1–5.

[13] H. Liu, X. Xie, X. Gao, H. Liu, and Y. Li "Stability analysis of SSR in multiple wind farms connected to series-compensated systems using impedance network model," *IEEE Trans. Power Syst*, vol. 33, pp. 3118-3128, May. 2018.

[14] L. Wang, Z. Lu, J. Peng, and X. Sun, "Influence on subsynchronous control interaction from different wind turbine generators," in *Proc. 43rd Annual Conf of the IEEE Industrial Electronics Society., pp. 4944-4948.*

[15] H. T. Ma, P. B. Brogan, K. H. Jensen, and R. J. Nelson, "Sub-synchronous control interaction studies between full-converter wind turbines and series-compensated AC transmission lines," in *Proc*. *2012 IEEE Power and Energy Society General Meeting.,* pp. 1-5.

[16] Z. Zhang, S. Liu, G. Zhu, and Z. Lu, "SSCI detection and protection in doubly fed generator based on DTFT," in *Proc*. *The 6th international conference on renewable power generation.,* pp. 2104-2107.

[17] F. Salehi, I. B. M. Matsuo, and W-J Lee, "Detection of sub-synchronous control interaction (SSCI) using modal identification analysis and FFT," presented at the North American Power Symposium (NAPS), Fargo, ND, USA, 2018.

[18] Y. Cheng, M. Sahni, D. Muthumuni, and B. Badrzadeh, "Reactance scan crossover-based approach for investigating SSCI concerns for DFIG-based wind turbines," *IEEE Trans. Power Del*, vol. 28, pp. 742-751, Apr. 2013.

A. E. Leon and J. A. Solsona, "Sub-synchronous interaction damping control for DFIG wind turbines," *IEEE Trans. Power Syst*, vol. 30, pp. 419-428, Jan. 2015.

[19] H. A. Mohammadpour and E. Santi, "Analysis of subsynchronous control interaction in DFIG-based wind farms: ERCOT case study," in *Proc*. *2015 IEEE Energy Conversion Congress and Exposition (ECCE).,* pp. 500-505.

[20] *Introduction to FPGA Technology: Top 5 Benefits*. [Online]. Available: http://www.ni.com/white-paper/6984/en/

[21] *Getting Started Guide NI 9467.* [Online]. Available: http://www.ni.com/pdf/manuals/373230c.pdf

[22] *Statistics Show Bearing Problems Cause the Majority of Wind Turbine Gearbox Failures.* [Online]. Available: https://www.energy.gov/eere/wind/articles/statistics-show-bearing-problems-cause-majority-wind-turbine-gearbox-failures

[23] Z. Zhang, A. Verma and A. Kusiak "Fault analysis and condition monitoring of the wind turbine gearbox," *IEEE Trans. Energy Convers*, vol. 27, pp. 526-535, Jun. 2012.

[24] D. Zappala, P. J. Tavner, C. J. Crabtree, and S. Sheng, "Side-band algorithm for automatic wind turbine gearbox fault detection and diagnosis," *IET Renewable Power Generation,* vol. 8, pp. 380-389, Nov. 2013.

[25] K. Alewine and W. Chen, "A review of electrical winding failures in wind turbine generators," *IEEE Trans. Insul. Mag*, vol. 28, pp. 8-13, Jul/Aug. 2012.

[26] S. K. Korkua, "Wireless health monitoring and improvement system for wind turbines," Ph.D. dissertation, Dept. Elec. Eng., Univ. Texas at Arlington, Arlington, 2011.

[27] *What is the "Crest Factor" and why is it used-Azima DLI.* [Online]. Available: http://azimadli.com/wp-content/uploads/TECH-CrestFactor.pdf

[28] D. Kutalek and M. Hammer, "Vibration diagnostics of rolling bearings using the time series analysis," *MM Science Journal,* Dec. 2015. [Online serial]. Available: http://www.mmscience.eu/content/file/MM_Science_201548.pdf. [Accessed Nov. 29, 2018].

[29] N. W. Miller, J. J. Sanchez-Gasca, W. W. Price, and R. W. Delmerico, "Dynamic modeling of GE 1.5 and 3.6 MW wind turbine generators for stability simulations," in *Proc. 2003 IEEE Power Engineering Society General Meeting.*, pp. 1977-1983.

CHAPTER 5

THE IMPACT OF TIME OF USE RATE STRUCTURE ON CONSUMPTION PATTERNS OF THE RESIDENTIAL CUSTOMERS

THE IMPACT OF TIME OF USE RATE STRUCTURE ON CONSUMPTION PATTERNS OF THE RESIDENTIAL CUSTOMERS[4]

Long Zhao, Zhiyong Yang, Wei-Jen Lee

L. Zhao, Z. Yang, and W. Lee, "The impact of Time of Use (TOU) rate structure on consumption patterns of the residential customers," *IEEE Trans. Ind. Appl.,* vol. 53, Nov/Dec. 2017. pp. 5130-5138.

The Impact of Time of Use (TOU) Rate Structure on Consumption Patterns of The Residential Customers

Long Zhao Zhiyong Yang Wei-Jen Lee

Student Member, IEEE Fellow, IEEE

University of Texas at Arlington, 701 S Nedderman Dr, Arlington, TX 76019, USA

long.zhao@mavs.uta.edu, zyang@uta.edu, wlee@uta.edu

Abstract – Load participation is vital for the Smart Grid development. As an effective tool to improve reliability, stability, and financial efficiency of the power grids, Demand Response (DR) has brought significant financial and technical benefits to power systems. As one of the price-based DR programs with less control costs, the Time-of-Use (TOU) program has been applied as default rate structure by many utility companies. To avoid financial risks and make the most profit out of the market, utility companies treat TOU as an effective strategy to change customers' electricity consumption patterns. As reported in many literatures, existing TOU programs are not effective as expected in many developed countries due to the complexity of human behaviors and disparities of residential customers. To examine whether to obtain different outcomes of TOU on the residential customers in developing countries, actual utility usage data from residential consumers in Shanghai, China are analyzed in this paper. The result shows current TOU in Shanghai, China has similar trends as TOU in developed countries. With high penetration level of renewable energy, an effective TOU program is urgently needed in the utility industry. In recent years, a creative TOU pricing structure that has been introduced at Electrical Reliability Council of Texas (ERCOT) deregulated market, and it shows that the introduced "zero pricing" strategy has significant impact on customers' consumption patterns. The purpose of this research is to examine the key reasons that underlying ineffectiveness/effectiveness of TOU programs at residential level.

Index Terms --Demand Response, Demand-Side Management, EROCT, Electricity Market, Retail Market, TOU, Smart Grid

5.1 INTRODUCTION

With the advancement of technology and power systems, the concept of Smart Grid has been formalized around the world. Load participation such as Demand Response (DR) has been widely implemented by power industries. According to U.S. Department of Energy (DOE) [1-2], DR is defined as "changes in electric usage by end-use customers from their normal consumption patterns in response to changes in the price of electricity over time, or to incentive payments designed to induce lower electricity

use at times of high wholesale market prices or when system reliability is jeopardized". There are mainly two types of DR programs in the United States, including time-based DR and price-based DR [1]. As a price-based DR, TOU has been applied by many utility companies as an approach to reduce the demand during the peak-time and to improve the utilization efficiency of power grids [3].

In the U.S., research on TOU can be traced back to 1970s. At that time, studies were conducted to focus mainly on whether TOU pricing affects customers' total electricity usage, how TOU pricing affects utility consumption patterns, and how much TOU can benefit utility companies and end-users. During that time, the major obstacle for applying the TOU program was that advanced metering infrastructure (AMI) technology had not been well developed. Therefore, the TOU program was only experimented by a small number of customers [4, 5]. According to a recent study by Lawrence Berkeley National Laboratory, 98% of customers in the U.S. were charged with a flat rate in 2012 due to the lack of AMI, but by 2014, more than 50 million advanced meters had been installed by utility companies which covered almost half of the homes in the country [5]. Meanwhile, AMI is also largely equipped in other developed countries such as Italy, Sweden, Canada, and Australia [6]. As a result of high penetration of AMI in developed countries, the implementation of TOU programs has been stimulated significantly for residential customers. Nevertheless, many studies have shown that TOU at residential level in developed countries are not effective as expected [3-4 and 7-9].

With the increasing penetration of AMI globally, TOU has also been applied in some developing countries at residential level. Comparing with developed countries, people in developing countries should be more sensitive to the price of the electricity due to the higher electricity bill to income ratio. To study the effectiveness of TOU in developing countries, data from Shanghai, China is analyzed in this paper as a case study from different aspects such as income levels, housing sizes, and number of residents in a single house. The results are compared with the one of the TOU programs in the Electric Reliability Council of Texas (ERCOT) market. Study shows that properly implementing TOU programs with creative strategy has the potential to bring considerable benefits to transmission line companies, utility companies and residential customers.

For the rest of the paper, current TOU program in a developing country (Shanghai, China) is analyzed in Section 5.2. The need of effective TOU programs is discussed in Section 5.3. Significance of zero price and zero-pricing TOU in Texas are presented in Section 5.4. Section 5.5 assesses zero-pricing TOU benefits for residential customers and utility companies. Conclusion of this study is presented in Section 5.6.

5.2 TOU IN A DEVELOPING COUNTRY (SHANGHAI, CHINA)

This session examines how the current TOU program would affect residential customers in a developing country with different objective factors, including income levels, size of house, and number of residents in one house. Monthly peak and valley electricity consumption of different groups of customers are studied [10]. A TOU program has been applied to residential customers in Shanghai since 2001. The profile of TOU program in Shanghai is shown in Table 5-1. The information of residential utility consumption data from 956 households over the past three years in Shanghai is presented in Table5-2.

The results indicate that, consistent with what one would expect, the total monthly electricity consumption is higher for the family that has higher income, larger house size, and more family members living in that house. However, there is no significant usage shift from peak time to valley time across different groups of consumers, suggesting that the current TOU program is not effective for local residents despite their differences in income, household size, and housing size.

TABLE 5 - 1. TIME-OF-USE RATES IN SHANGHAI [11]

Multistep	Usage (kWh/Year)	Time	Price ($/kWh)
Step 1	0-3120 (included)	Peak	$0.09
		Valley	$0.04
Step 2	3120–4800 (included)	Peak	$0.1
		Valley	$0.05
Step 3	Above 4800	Peak	$0.15
		Valley	$0.07

Peak Time: 6:00 AM to 9:59 PM; Valley Time: 10:00PM to 5:59 AM

TABLE 5 - 2. Profile of Residential Data in Shanghai

Data Type	Monthly Residential
Data Period	Jan 2009 to April 2016
Number of Valid Customers	965 customers
Objective Factors	Income level, Size of house, Number of residents

To better understand how customers' behavior would be affected by TOU rates, the ratio between the monthly electricity usage in valley time and the total monthly usage is used for showing how different customers react to the TOU rates in Shanghai, China. valley ratio (VR) is defined in (1).

$$\text{VR} = \frac{\text{Monthly Usage in Valley Time (kWh)}}{\text{Monthly Total Usage (kWh)}} \quad (1)$$

5.2.1 VR for Different Income Levels

In this part, income levels have been categorized into 8 groups from less than $3,000 per year to more than $36,000 per year. Average VR for each group is listed in Table 5-3, which shows that customers used around 28% of electricity during the valley time regardless their income levels. Due to the space limitation, only the lowest and the highest income levels are shown in this paper. Probability Density Function (PDF) of VR for each group is shown in Fig. 5.1. and Fig. 5.2. From both figures shown below, majority of customers' VR is around 0.3, which means, for most consumers, electricity consumption of valley time is around 30% of their total monthly usage for both income levels. As the result, most consumers still use large amount of electricity during the peak time regardless of their income levels.

TABLE 5 - 3. Average Valley Ratio for Different Income Levels

Annual Income (USD)	Average VR
Less than 3,000	0.2736
From 3,000 to 7,000	0.2818
From 7,000 to 11,500	0.2746
From 11,500 to 14,500	0.2805
From 14,500 to 22,000	0.2866
From 22,000 to 29,000	0.2638
From 29,000 to 36,000	0.2938
Greater than 36,000	0.3176

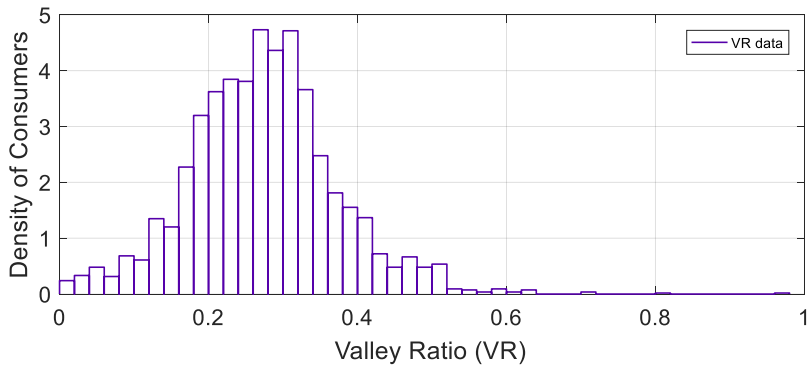

Fig. 5. 1 PDF of VR for customers whose income is less than 3,000USD per year

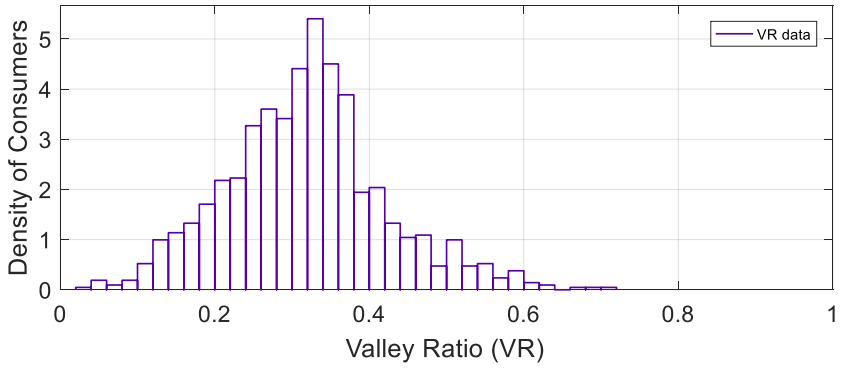

Fig. 5. 2 PDF of VR for customers whose income is greater than 36,000RUSD per year

5.2.2 VR for Different Housing Sizes

In this part, average VR for each group is listed in Table 5-4, which shows that customers used around 27% of electricity during the valley time regardless their housing sizes. Due to the limitation of the space, only PDF of VR for the smallest and the largest housing sizes presented in Fig. 5.3. and Fig. 5.4. respectively. From both figures shown below, majority of customers' VR is around 0.3, which means, for most consumers, electricity consumption of valley time is around 30% of their total monthly usage for both housing sizes. As the result, most consumers still use large amount of electricity during the peak time regardless of housing sizes.

TABLE 5 - 4. Average Valley Ratio for Different Housing Sizes

Housing size (m^2)	Average VR
Less than 10	0.2921
From 10 to 30	0.2857
From 30 to 50	0.2764
From 50 to 70	0.27
From 70 to 100	0.2726
From 100 to 150	0.2839
Greater than 150	0.253

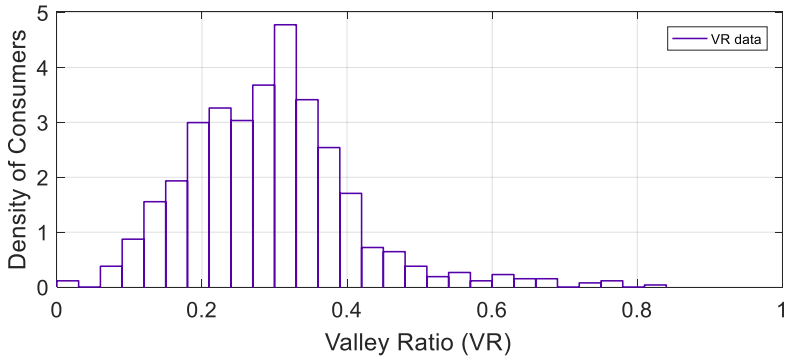

Fig. 5. 3 PDF of VR for customers whose housing size is less than 10m^2

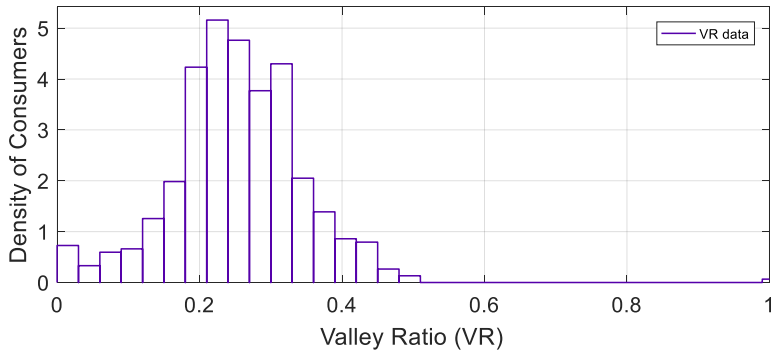

Fig. 5. 4 PDF of VR for customers whose housing size is greater than 150m^2

5.2.3 VR for Different Number of Residents in One House

In this part, average VR for each group is listed in Table 5-5, which shows that customers used around 27% of electricity during the valley time regardless the number of residents under single household. Due to the limitation of the space, only PDF of VR for the lowest and the largest number of residents in one house is presented in Fig. 5.5. and Fig. 5.6. respectively. From both figures shown below, majority of customers' VR is around 0.3, which means, for most consumers, electricity consumption of valley time is around 30% of their total monthly usage for both housing sizes. The result illustrates that most consumers still use large amount of electricity during the peak time regardless of number of residents of one household.

TABLE 5 - 5. VR for different number of residents

Number of Residents	VR
1	0.2847
2	0.2796
3	0.2725
4	0.271
5	0.2711

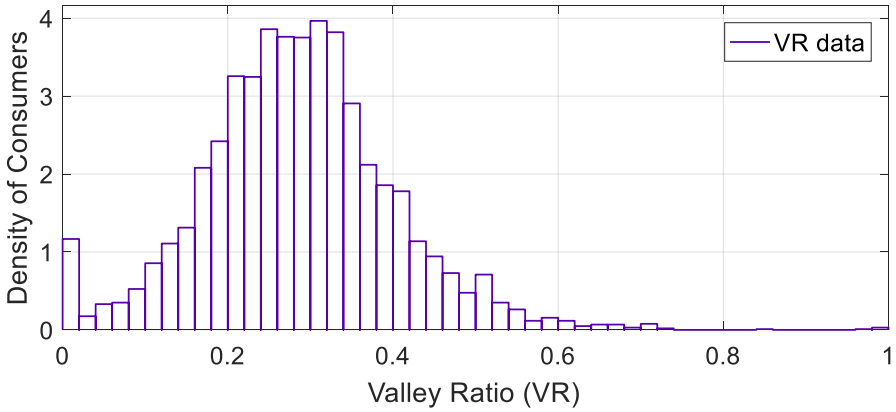

Fig. 5. 5 PDF of VR for A House Having 1 Resident

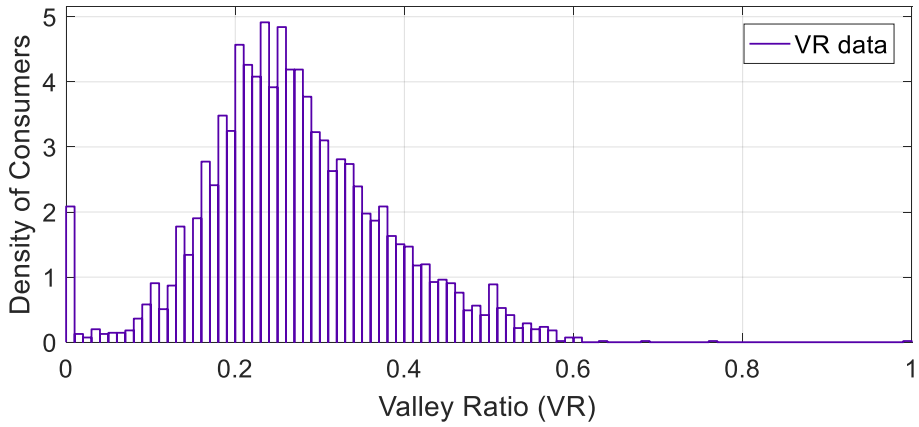

Fig. 5. 6 PDF of VR for A House Having 5 Residents

5.2.4 VR for All Customers

PDF of all the customers' VR from January 2009 to April 2016 is plotted in Fig. 5.7, which shows most customers' VR is less than 0.3. Extremely large portion of customers' electricity usage is still consumed during peak time after TOU has been applied. The percentage of customers whose VR is greater than 50% each month is plotted in Fig. 5.8. From Fig. 5.8, less than 10% of customers consume more than half of their monthly electricity at valley time.

As the result, it is clear that TOU did not change residential customers' monthly electricity usage pattern noticeably in Shanghai, China. Most customers' electricity usage is still from peak period regardless their income level, house size and other objective factors.

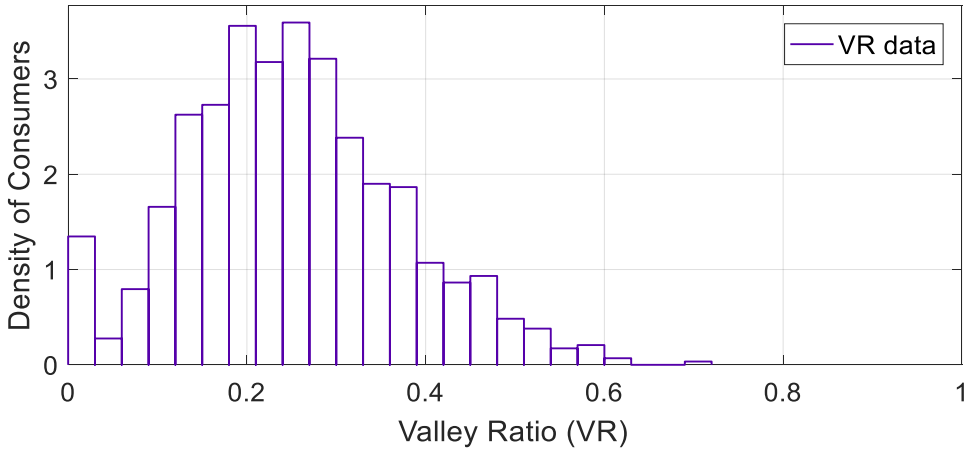

Fig. 5. 7 PDF of Valley Ratio for Residential Customers in Shanghai

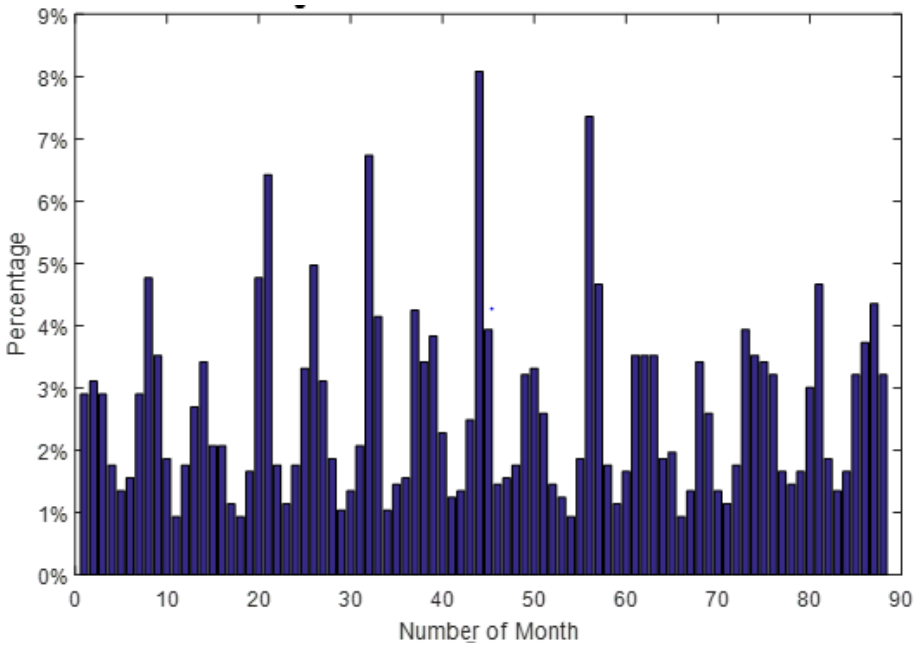

Fig. 5. 8 The percentage of customers whose VR is greater than 50%

5.3 THE NEED OF EFFECTIVE TIME-OF-USE (TOU) PROGRAMS

Increasing the effectiveness of TOU programs becomes paramount for both researchers and marketing practitioners, especially for those working in the renewable energy sectors. For example, as one of the fastest growing renewable energy resources, enormous amount of wind energy infrastructures has been installed all around the world [12]. According to Global Wind Energy Council (GWEC), the total installed wind capacity in the world reaches 432.883 GW by the end of 2015. As the largest installed wind capacity nation, China has 145 GW installed by 2015. The U.S. and Germany are the 2nd and 3rd largest wind capacity installed nations, with 74GW and 45GW installed respectively [13]. Due to the high penetration of the wind power, market price has become more volatile than ever in many electricity markets due to the unpredictability of the wind power. Exceeded wind power generation with less demand would unavoidably cause negative electricity prices in power markets, which means customers would be paid for consuming electricity during the negative price periods. Serious negative price in electricity market of Germany has happened often due to exceeded wind supply [14]. Electricity market in Denmark is also suffering the negative price situation caused by high penetration of wind generation [15]. As the largest wind generation state in the U.S., Texas is now suffering the negative prices in The Electric Reliability Council of Texas (ERCOT) market. As an example, in Fig. 5.9. [16], the price in ERCOT real time market could be from almost negative 100$/MWh to more than 3000$/MWh at the same time in different locations. At the same time, installed capacity of photovoltaic (PV) has increased exponentially

in last 10 years [17]. In California, due to the large PV capacity has been installed in recent years, negative prices also happened more frequently in California Independent System Operator (CAISO) market [18]. As an example, CAISO net generation and Real-time hourly price in March 11th, 2017 is shown in Fig. 10 [19], and negative price lasted hours during the daytime. Severe negative price would cause certain issues on reliability of power systems and operations on power markets [12]. Therefore, how to utilize energy in an efficient way (instead of a pure conservative way) is becoming a new challenge for power industries. An effective TOU program would be one of the options to change customers' usage of electricity, so that the demand of the system would be adjusted.

In Italy, for example, TOU has been applied as a default rate for all residential customers since July 1^{st,} 2010 [20]. In Ontario, Canada, 90% of residential customers have enrolled in TOU programs [21]. In the United States, various TOU programs are offered in different states. For the 13 states where electricity retail market is available, customers could choose different electricity providers based on their preferences [22]. Despite the prevalence of TOU, many studies have shown that the effectiveness of the current TOU programs are not as expected due to the futile TOU pricing design [3-4, 7-9 and 23-24].

Many studies have shown that TOU at residential level in developed countries have extremely limited impacts [3-4 and 7-9]. A white paper provided by Electric Power Research Institute (EPRI) shows that the key reason underlying the ineffective response at demand side is that the TOU price difference is less than the price threshold of customers [3]. In other words, the critical factor for an efficacious TOU program is pricing [7]. As evidence, the authors in [7] modelled the impact of TOU rates for 2,000 residential customers in BC, Canada and found that a larger ratio between peak-price and off-peak price increases the response of demand significantly. In [8], effectiveness of TOU pricing on demand side in different countries was analyzed. As a general conclusion from this study, the impact of price on residential customers' usage behaviors is contingent upon other factors, such as education and metering technologies. Recent research also examines the current TOU program using longitudinal data [24]. For example, the finding of a study on six-year historical utility usage among 38 single-family households in Sweden indicates that the current TOU program is not effective enough. Higher incentives for customers are needed to make demand side more responsive. Other studies also show that pricing is a vital factor for the success of TOU programs [25-27]. A potential problem of these studies is that they mainly use price elasticity to quantify the effectiveness of TOU. Due to the complexities of human behaviors and geographical diversities, price elasticity tends to vary across different groups of consumers [3], which makes it hard to compare the effectiveness of TOU across different studies.

Under the current market policies and the surge of renewable energy development, it is necessary to have different price structure to increase the effectiveness of TOU programs. In this paper, TOU programs in both a developing country (Shanghai, China) and a developed country (Texas, USA) were analyzed and compared by using real residential data. Effectiveness and potential benefits of zero pricing TOU to customers and utilities were also assessed.

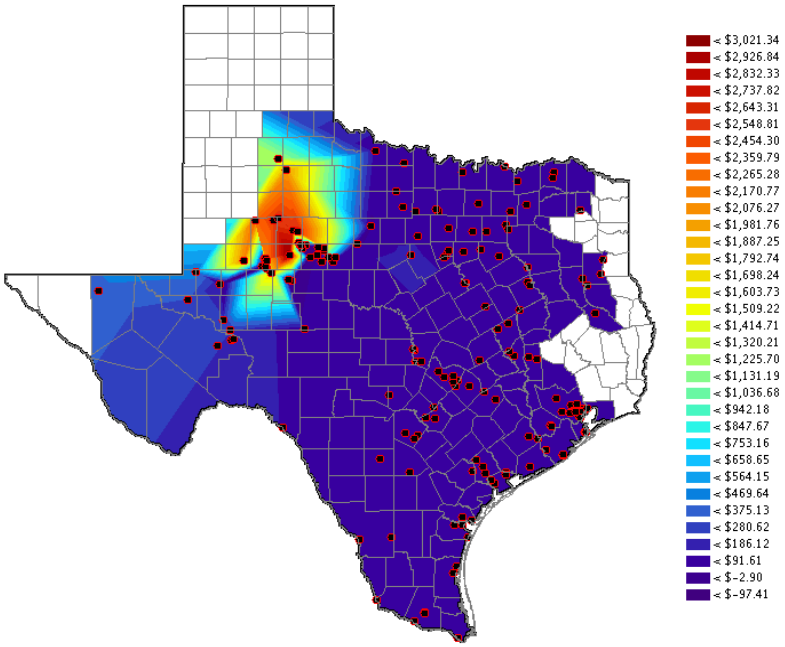

Fig. 5. 9 Locational Marginal Price (LMP) of ERCOT at 11:15, Oct. 08, 2012 [16]

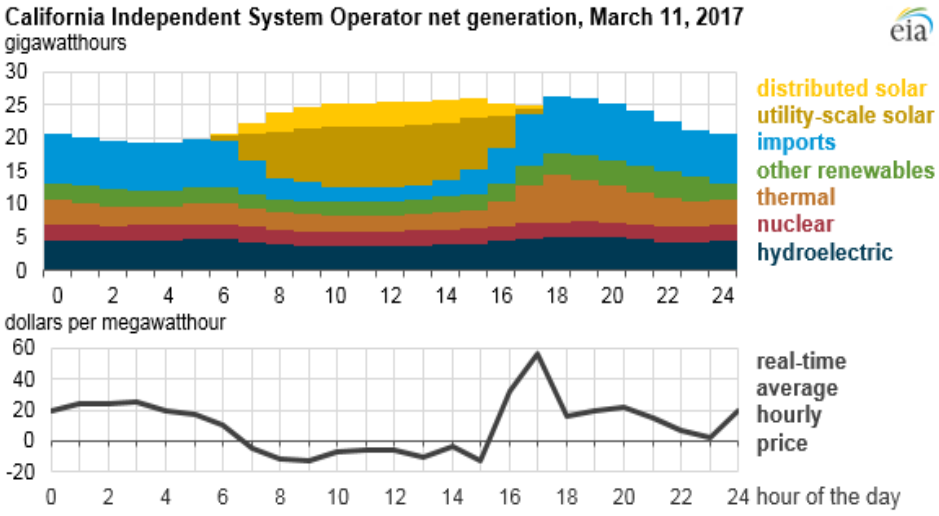

Fig. 5. 10 CAISO Net Generation and Average Hourly Price [19]

This study shows that due to the unique psychological properties related to this special price point, zero-price could be considered as a very effective tool in TOU programs in the future progress of power grids. Properly implementing zero pricing into TOU programs with scientific strategy has the potential to bring considerable profit for utility companies in the future.

5.4 SIGNIFICANCE OF ZERO-PRICE AND ZERO-PRICING TOU IN TEXAS

5.4.1 Zero-Price

Recent research shows that zero-price has special meanings to consumers. A major reason is that consumers tend to perceive free products as having a much higher utility than the difference between benefit and cost. In their studies [28], Shampanier, Mazar, and Ariely provided consumers with two sets of choices. In one set, the choice is between a free product and a superior product at the price of $A. In the other set, the products are the same, but the first option is priced at a low amount $B, rather than $0, whereas the second option is priced at $(A+B), as shown below:

Set 1: Option 1 (free) vs. Option 2 ($A);

Set 2: Option 1 ($B) vs. Option 2 ($A+$B).

Given that both sets have exactly the same price difference ($A), rational choice theory predicts that there is no difference in the relative preference of these two options. Contrary to this prediction, Shampanier et al. show that in both sets, Option 1 is preferred. However, the relative preference for Option 1 is much higher when it is free than it is priced at a small amount of $B. According to Shampanier et al., this is mainly due to the special meaning associated with zero-price. As a result, the utility that consumers obtain from a small positive amount to zero is non-linear. “Free” promotions tend to evoke a non-transactional mindset; however, non-zero price promotions often induce cost-benefit decisions [29]. Similarly, Hossain and Saini argue that zero-price tend to put individuals into an affective mood, leading to a salient affect-as-information effect [30].

We expect that the zero-price effect is stronger when the product has a lower level of involvement, such as electricity. According to Fisher, electricity is a low-involvement product, since the costs do not consist of a major component of a household’s budget [31]. On top of that, electricity consumption is often invisible. Different from visible products such as organic food, electricity consumption does not reflect one’s lifestyle [32]. As a result, consumers view electricity as a necessary, but a mundane product with which specific features do not matter much [31].

The Elaboration Likelihood Model [33] sets up a great platform for us to understand the zero-price effect. The ELM suggests that involvement is a key determinant of how information is processed and what

type of information is used in making choices. High involvement decisions (e.g., costly purchases) often lead consumers to deliberately and consciously process those message elements that they believe are relevant in meaningfully and logically evaluating available choices. By contrast, for low-involvement decisions, individuals engage in little or no elaborate processing. When elaboration likelihood is low, consumers' decision making is not based on the careful cost-benefit calculation, but rather on: (a) the issue or object being associated with positive or negative cues, which have no intrinsic link to the attitude stimulus (e.g., an attractive model would likely serve as an argument for the merits of a beauty product, but would more likely constitute a peripheral cue for an oven [34];) or, (b) the recipient drawing a simple inference based on various cues in the persuasion context (e.g., the more arguments for a recommendation, the better it must be[35];). Translating these findings into our study context, we posit that the positive affect evoked by zero-price is likely to be treated a diagnostic cue to drive consumers' decision on utility consumption plan.

5.4.2 Zero-Pricing TOU in Texas

In Texas, electricity retail market has been opened to residential customers since 2002 [13]. According to Public Utility Commission of Texas [13], there were around 6 million residential customers in retail electricity market by the end of 2014. In most areas of Texas, customers could choose any electricity plans from more than 300 retail electric providers based on their preferences from www.powertochoose.com. In 2012, a utility company in Texas became the first retail electricity provider (REP) to offer free electricity during the night time in the U.S., and the plan is called "Energy Free Nights" [36]. Currently, the "Energy Free Nights" plan offers 9 hours' free electricity which could start from 8PM, 9PM or 10PM based on customers' preferences. Except for the free hours, electricity is 13.2 cent per kWh in rest of the time. So far, many customers enrolled in "Energy Free Nights" plan have changed their utility consumption patterns. As indicated in the news of *New York Times* [37], an elementary school teacher, a cosmetologist, and a business manager of a law firm were reported as examples of how "Energy Free Nights" changed their energy consumption patterns. As enrolled customers, all three of them would wait until the free hours to start running their major electric appliances. Similarly, *Dallas Morning News* [38] features an 85 years old "Energy Free nights" enrolled customer who stays up until the free hours to start dishwasher and washing machine. Due to the high privacy concern of the utility companies in the U.S., it is extremely difficult to acquire residential data from local utilities. Fortunately, two current "Energy Free Nights" enrolled customers—who differ in income levels, housing sizes and social status— agreed to share their personal electricity usage data so that effects of zero-pricing TOU could be clearly presented. The usage profiles of customer A and B are shown in Fig. 5.11 and Fig. 5.12, respectively. Based on their usage

profiles, both customers consume more than 50% of their electricity during the free hours regardless their income levels, housing size and other objective factors. Profile of customer A and B are shown in Table 5-6. This proofs that zero-price does have special meanings to consumers.

TABLE 5 - 6. Profile of Customer A and B

Objective Factors	Customer A	Customer B
Annual Income Level ($)	$20,000	$200,000
Yearly Energy Consumption (kWh)	Approximately 3000 kWh	Approximately 17000 kWh

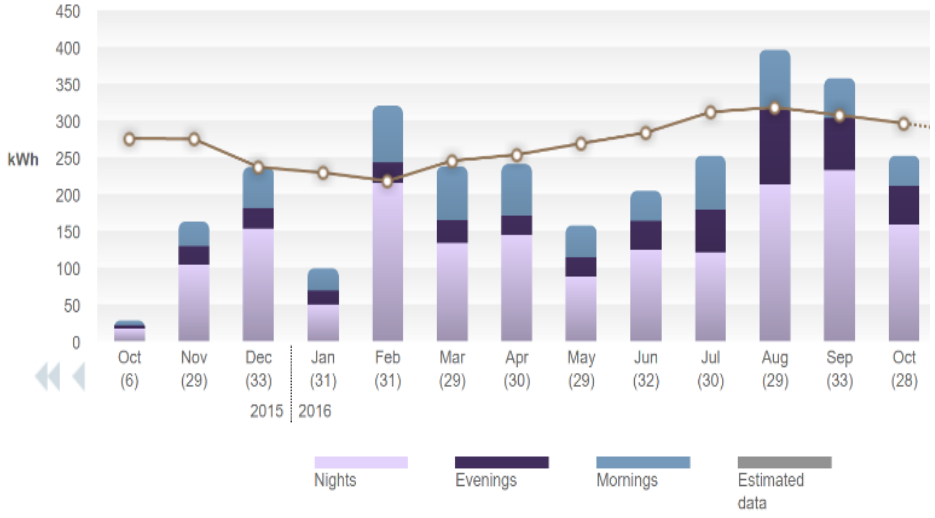

Fig. 5. 11 Monthly usage of customer A

Fig. 5. 12 Monthly usage of customer B

5.5 ASSESSMENT OF ZERO-PRICING BENEFITS

In this part, financial benefits for both utility companies and residential customers from zero-pricing TOU are evaluated. Residential data from a utility company in Shanghai (China) are used, and market price data from the ERCOT market.

5.5.1 Benefits for Residential Customers

To assess the financial benefits for customers, electricity rate of daytime is assumed as 2 times as current rate, and the percentage of bill saving is shown in Table 5-7.

TABLE 5 - 7. Monthly Percentage of Bill Savings

VR	Monthly Percentage of Bill Saving
50%	0%
60%	20%
70%	40%
80%	60%
90%	80%

Financial benefits for customers in Shanghai with zero-pricing TOU is evaluated. The new rates for zero-pricing TOU in Shanghai are assumed in Table 5-8. The average bill saving for each customer in Shanghai is shown in TABLE 5-9.

TABLE 5 - 8. Assumed Zero-Pricing Rates in Shanghai

Multistep	Usage (kWh/Year)	Time	Price ($/kWh)
Step 1	0-3120 (included)	Peak	$0.184
		Valley	0
Step 2	3120–4800 (included)	Peak	$0.2021
		Valley	0
Step 3	Above 4800	Peak	$0.2916
		Valley	0

TABLE 5 - 9. Average Bill Savings Annually for each customer in Shanghai in USD

VR	2009	2010	2011	2012	2013	2014	2015
60%	$9	$9	$10	$10	$10	$10	$10
70%	$44	$48	$50	$51	$54	$45	$47
80%	$80	$87	$89	$93	$97	$81	$84
90%	$115	$125	$129	$134	$140	$117	$121

To evaluate the zero pricing TOU financial benefit for residential customers, data from a utility company in New York City is evaluated in this study. As one of the districts where has the highest residential electricity rate in the U.S., residential customers pay approximately 19 cents per kWh in NYC. Thus, helping residential customers in NYC to reduce electricity bill is more significant. The residential data profile in NYC is shown in Table 5-10. The PDF of valley ratio (VR) for 300 residential customers is shown in Fig. 5.13., which shows most customers' VR is less than 0.4. In this case, TOU period is assumed to be the same as TOU period in Shanghai, China. In this data set, TOU has not been applied.

TABLE 5 - 10. Profile of Residential Data in NYC

Data collection duration	Jan 1st, 2012 to December 31st, 2014
Data type	Residential Level Real Power Energy Consumption
Data unit	kWh
Data sampling frequency	15 minutes
Number of customers	Approximately 300 (Exact number may vary each month)
Number of data per day per customer	96

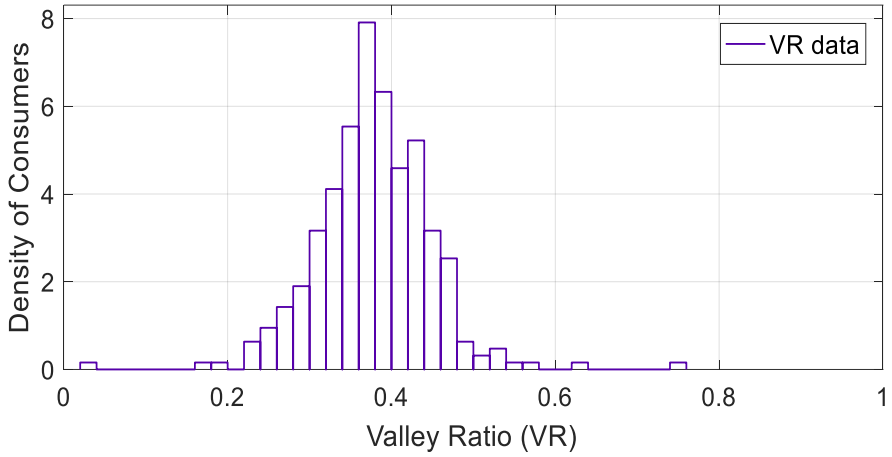

Fig. 5. 13 PDF of Valley Ratio for Residential Customers in NYC

In the assessment, peak time rate is assumed 38 cents per kWh. By using the practical data from a utility company in NYC, every customer's average annual bill saving is shown in Table 5-11. Benefits for customers directly related to the electricity rate during the peak time and amount of usage during the free time.

TABLE 5 - 11. Average Bill Savings Annually for each customer in NYC

VR	2012	2013	2014
60%	160 USD	153 USD	147 USD
70%	321 USD	306 USD	293 USD
80%	480 USD	459 USD	440 USD
90%	642 USD	612 USD	587 USD

5.5.2 Benefits for Utility Companies

Different markets have different incentive policies regarding peak reductions and demand response programs. Zero-pricing TOU has been offered in Texas for years. Currently, there are more than 100,000 residential customers enrolled in the "Energy Free Nights" plan [37] [39]. In this study, benefit for utility companies would be calculated under the current ERCOT market.

In Texas, due to the extremely high demand of power from air-conditioning in summer months, ERCOT applies Four Coincident Peaks (4CPs) charge to all energy consumers whose peak demand is higher than 700 kW. Specifically, 4CP is defined as the highest 15-interval demand in June, July, August and September [40]. As a utility company, avoiding 4CP could not only avoid spike price in spot market but also significantly reduce the 4CP charge which is charged for transmission service in the entire next

calendar year [41]. According to historical data from ERCOT, all 4CPs happened around 5PM in the last 10 years [42]. As one example to show how zero pricing TOU could effectively change consumers' consumption patterns, customer B's hourly load profile of a week in summertime is shown in Fig. 5.14. It shows customer B' demand changed from less than 2kW to more than 10kW once zero-pricing period started. Thus, applying the zero-pricing TOU program, utility companies would be able to shift large amount of demand to later time, and the annual saving from 4CPs is defined by ERCOT as:

$$Annual\ Savings(USD) = 4CP\ reduction(kWh) \times 4CP\ Tariff \times 12 \text{ [40]}$$

In this study, the financial benefit for utility companies is calculated with the current 4CP tariff rates as per Public Utility Commission of Texas [43]. According to [39], more than 100,000 residential customers have enrolled in the "Energy Free Nights" TOU program, and the 4CP tariff rates for the utility company is $3.485 per 4CP kW in 2016 [43]. The financial benefit for utility company from 4CPs is shown in Table 5-12. It shows a large amount of cost for transmission service in 2017 could be reduced if zero-pricing TOU is used.

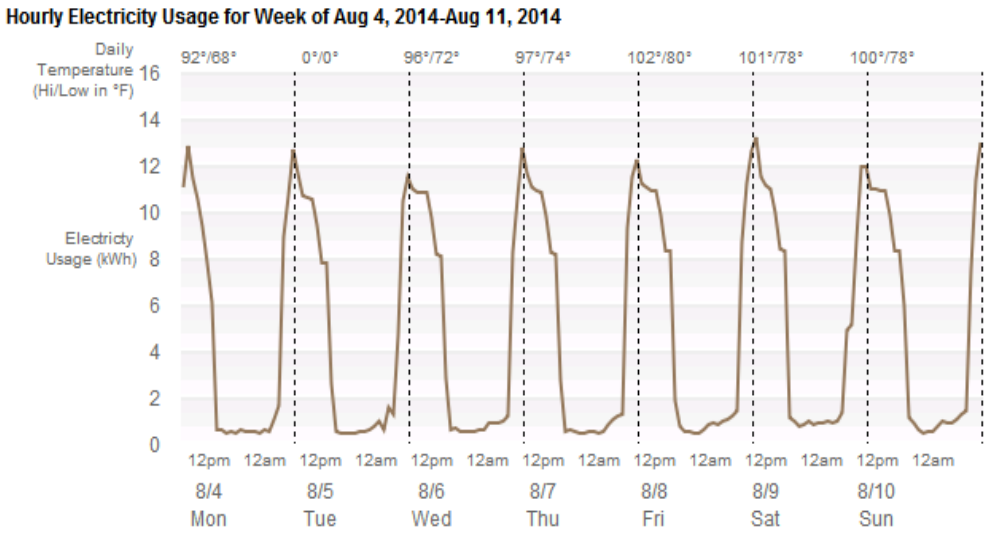

Fig. 5. 14 Customer B's Hourly Load Profile for a Week in August

TABLE 5 - 12. Savings on Transmission Charge in 2017 for The Utility Company

Average Reduction of Each Customer (kW)	The Total Savings in 2017 (USD)
0.5 kW	$ 2,091,000
0.6 kW	$ 2,509,200
0.7 kW	$ 2,927,400
0.8 kW	$ 3,345,600
0.9 kW	$ 3,763,800
1 kW	$ 4,182,000

5.6 CONCLUSION

This study uses zero-pricing TOU as an example to validate that residential customers' consumption patterns will be affected by a creative/special TOU pricing strategy. Such TOU pricing strategies could change customers' consumption patterns remarkably so that effectiveness of TOU at residential level could be improved effectively. Creative/special TOU pricing such as zero-pricing strategies could not be only applied into TOU programs but also be considered for other price-based Demand Response programs such as critical-peak pricing (CPP) and real-time pricing (RTP) to make demand side more responsive. Especially, with the increasing penetration of renewable energy resources, special/creative pricing strategies such as zero-pricing, negative-pricing and dynamic-pricing can be implemented based on the local renewable generation and consumers demand characteristics by utility companies/load service entities (LSEs). All in all, special/creative TOU pricing strategies can be considered as an effective way to improve effectiveness of price-based DR.

5.7 REFERENCES

[1] "Benefits of Demand Response in electricity markets and recommendations for achieving them," U.S. DOE., Feb. 2006.

[2] A. Mohsenzadeh, M. H. Kapourchali and C, Pang, "Impact of smart home management strategies on expected lifetime of transformer," *2016 IEEE Power and Energy Society Transmission and Distribution Conf and Expo*.

[3] B. Neenan, and J. Eom, "Price elasticity of demand for electricity: a prime and synthesis," Elect. Power. Res. Inst., Palo Alto, CA:2007, 1016264, Jan. 2008.

[4] J. A. Hausman and D.A. Wise, "Social experimentation," in *The residential electricity time-of-use pricing experiments: what have we learned?.* University of Chicago press, 1985, pp. 11-54.

[5] P. Cappers, et al. “Time-of-use as a default rate for residential customers: issues and insights.” Lawrence Berkeley National Laboratory., Berkeley, CA, LBNL-1005704, June. 2016.

[6] “Advanced metering infrastructure,” Nat. Energy. Tech. Lab., Feb. 2008.

[7] M. A .R. Muzmar, M. P. Abdullah, M. Y. Hassan, and F. Hussin, “Time of use pricing for residential customers case of Malaysia,” in *proc. 2015 IEEE Student Conf on Research and Development*., pp. 589-593.

[8] K. H. Tiedemann and I. M. Sulyma. Modeling the impact of residential time of use rates, BC Hydro., Burnaby, BC, [Online]. Available: https://www.aeaweb.org/conference/2010/retrieve.php?pdfid=384

[9] Available knowledge on demand elasticity price impact. Inst. Energy. Eng. Spain. [Online]. Available: http://www.demandresponse.eu/html_der/papers/CIGRE%20WG%20C6_WP5_web.pdf

[10] L. Zhao, Z. Yang and W. Lee, “Effectiveness of zero pricing in TOU demand response at the residential level,” presented at the IEEE 53rd I&CPS. Conf, Ontario, Canada, 2017.

[11] *Time-of-use rate in Shanghai.* [Online]. Available: http://sh.sina.com.cn/news/z/jietidianjia/

[12] H. Y. S. Tao, A. K. Srivastava, R. L. Pineda, and P. Mandal, “Wind power generation impact on electricity price in ERCOT,” in *Proc.* IEEE Power Engineering Society General Meeting, San Diego, CA, USA, Jul. 2012.

[13] D. L. Nelson, K. W Anderson, B. M. Marquez, and B. H. Lloyd. (Jan, 2015.). Scope of competition in electric markets in Texas. Public Utility Commission of Texas., Austin, TX. [Online]. Available: https://www.puc.texas.gov/industry/electric/reports/scope/2015/2015scope_elec.pdf

[14] M. Nicolosi, “Wind power integration and power system flexibility–An empirical analysis of extreme events in Germany under the new negative price regime,” *Energy Policy,* vol. 38, pp. 7257-7268, 2010.

[15] M. H. Bashi, G. R. Yousefi, and C. L. Bak, “High penetrated wind farm impacts on the electricity price: the Danish case,” in *Proc. 2016 IEEE 16th International Conf on Environment and Electrical Engineering.*, pp. 1-5.

[16] M. Liu, W. Lee, and L. Lee, “Financial Opportunities by Implementing Renewable Sources and Storage Devices for Households Under ERCOT Demand Response Programs Design,” *IEEE Trans. Industry Applications*, vol. 50, no. 4, pp. 2780-2787, 2014.

[17] *Solar Industry Data.* [Online]. Available: http://www.seia.org/research-resources/solar-industry-data

[18] *California ISO Q4 2016 Report on Market Issues and Performance*. [Online]. Available: http://www.caiso.com/Documents/2016FourthQuarterReport-MarketIssuesandPerformanceMarch2017.pdf

[19] *Rising Solar Generation in California Coincides with Negative Wholesale Electricity Prices*. [Online]. Available: https://www.eia.gov/todayinenergy/detail.php?id=30692#tab1

[20] S. Maggiore, M. Gallanti, W. Grattieri, and M. Benini, "Impact of the enforcement of a time-of-use tariff to residential customers in Italy," in *Proc. 22nd International Conference on Electricity Distribution.,* 2013, pp. 1-4.

[21] A. Faruqui. "Time-variant pricing (TVP) in New York," 2015. [Online]. Available: http://www.brattle.com/system/publications/pdfs/000/005/146/original/Time-variant_pricing_in_New_York.pdf?1427837905

[22] M. J. Morey and L. D. Kirsch. (2016, Feb.). Retail choice in electricity: what have we learned in 20 years?. Elect. Mkt. Res. Foundation. Madison, WI. [Online]. Available: https://www.hks.harvard.edu/hepg/Papers/2016/Retail%20Choice%20in%20Electricity%20for%20EMRF%20Final.pdf

[23] S. Fan and R. Hyndman, "The price elasticity of electricity demand in south Australia," *Energy Policy,* vol. 39, pp. 3709-3719, 2011.

[24] Y. Huang, "Estimating response to price signals in residential electricity consumption," Master. Thesis, Dept. Earth. Sci,. Univ. Uppsala, Uppsala, Sweden, 2013.

[25] S. Borenstein, "To what electricity price do consumers respond? Residential demand elasticity under increasing-block pricing," 2009. [Online]. Available: http://faculty.haas.berkeley.edu/borenste/download/NBER_SI_2009.pdf

[26] A. Faruqui, R. Hledik, and J. Palmer. (Jul, 2012.). Time-varying and dynamic rate design. The Brattle Group., [Online]. Available: http://www.raponline.org/wp-content/uploads/2016/05/rap-faruquihledikpalmer-timevaryingdynamicratedesign-2012-jul-23.pdf

[27] J. M. Potter, S. S. George, and L. R. Jimenez. (Sep, 2014.). Smart pricing options final evaluation. Sacramento Municipal Utility District and Nexant., Sacramento, CA. [Online]. Available: https://www.smartgrid.gov/files/SMUD_SmartPricingOptionPilotEvaluationFinalCombo11_5_2014.pdf

[28] K. Shampan'er and D. Ariely, "Zero as a special price: the true value of free products," *Marketing Science* 2007, 26: 742–757. 10.1287/mksc.1060.0254.

[29] S. Chandran and V. Morwitz, “The Price of ‘Free’-Dom: Consumer Sensitivity to Promotions with Negative Contextual Influences.” *Journal of Consumer Research*, vol. 33, no. 3, 2006, pp. 384–392. [Online]. Available: https://www.jstor.org/stable/10.1086/508439

[30] M. T. Hossain and R. Saini, “Free indulgences: enhanced zero-price effect for hedonic options,” *International Journal of Research in Marketing*, vol. 32, pp. 457-460, Dec. 2015.

[31] C. Fischer, “Influencing electricity consumption via consumer feedback: a review of experience,” [Online]. Available: http://www.eceee.org/library/conference_proceedings/eceee_Summer_Studies/2007/Panel_9/9.095/

[32] B. Birzle-Harder and K. Götz, “Grüner Strom - eine sozialwissenschaft liche Marktanalyse,” [Online]. Available: http://www.isoe.de/publikationen/publikationdetail/?tx_refman_pi1%5Brefman%5D=1048&tx_refman_pi1%5Bcontroller%5D=Refman&tx_refman_pi1%5Baction%5D=detail&cHash=fef4f4ecdc1860e171ab938d6bbe8395

[33] R. E. Petty and J. T. Cacioppo, “The elaboration likelihood model of persuasion,” in *Advances in Experimental Social Psychology*, 1st ed., vol. 19, Academic Press. Inc, 1986, pp. 123-192.

[34] G. J. Gorn, “The effects of music in advertising on choice behavior: a classical conditioning approach,” *Journal of Marketing*, vol. 46, pp. 94-101, 1982.

[35] R. E. Petty and J. T. Cacioppo, “The effects of involvement on responses to argument quantity and quality: central and peripheral routes to persuasion,” *Journal of Personality and social psychology*, vol. 46, pp. 69-81, 1984.

[36] *Energy free nights*. [Online]. Available: http://freenights.txu.com/

[37] C. Krauss and D. Cardwell, “A Texas utility offers nighttime special: free electricity,” *The New York Time*. Nov 8, 2015. [Online]. Available: http://www.nytimes.com/2015/11/09/business/energy-environment/a-texas-utility-offers-a-nighttime-special-free-electricity.html

[38] J. Osborne, “Night, weekend electricity plans gaining a following,” *The Dallas Morning News.* Jun, 2013. [Online]. Available: http://www.dallasnews.com/business/energy/2013/06/12/night-weekend-electricity-plans-gaining-a-following

[39] J. Camp and D. Parkinson, “Virtual assistant drives self-service adoption at TXU energy,” *Electric Light & Power.* Oct 27, 2015. [Online]. Available: http://www.elp.com/articles/print/volume-93/issue-5/sections/customers/virtual-assistant-drives-self-service-adoption-at-txu-energy.html

[40] *Demand Response in ERCOT,* [Online]. Available: http://www.ercot.com/content/wcm/training_courses/104/ercot_demand_response_2014_ots.pptx.

[41] J. Zarnikau and D. Thal, "The response of large industrial energy consumers to four coincident peak (4CP) transmission charge in the Texas (ERCOT) market," *Utility Policy,* vol. 26, pp. 1-6, 2013.

[42] *ERCOT Four Coincident Peak Calculations.* [Online]. Available: http://www.ercot.com/mktinfo/data_agg/4cp

[43] *Public Utility Commission of Texas Comparison of Utilities' Generic T&D Rates.* [Online]. Available: http://www.puc.texas.gov/industry/electric/rates/trans/tdgenericratesummary.pdf

CHAPTER 6

POTENTIAL OF THE COMMERCIAL SECTOR TO PARTICIPATE IN THE DEMAND SIDE MANAGEMENT PROGRAM

POTENTIAL OF THE COMMERCIAL SECTOR TO PARTICIPATE IN THE DEMAND SIDE MANAGEMENT PROGRAM [5]

Long Zhao, Yuhao Zhou, Franklin L. Quilumba, Wei-Jen Lee

L. Zhao, Y. Zhou, F L. Quilumba, and W. Lee, "Potential of the commercial sector to participate in the demand side management program," *IEEE Trans. Ind. Appl.,* vol. 55, Nov/Dec. 2019. pp. 7261-7269.

Potential of the Commercial Sector to Participate in the Demand Side Management Program

Long Zhao Yuhao Zhou* Franklin L. Quilumba Wei-Jen Lee

Student Member, IEEE Student Member, IEEE Member, IEEE Fellow, IEEE

University of Texas at Arlington, 701 S Nedderman Dr, Arlington, TX 76019, USA

long.zhao@mavs.uta.edu, yuhao.zhou@mavs.uta.edu*, quigufrale@ieee.org, wlee@uta.edu

Abstract -- The demand side management (DSM) has been conceived to improve the efficiency and flexibility of the power grids. Currently, different types of DSM programs such as demand response, the efficiency of power delivery, HVAC improvements and distributed energy storage have been developed and implemented by different utility companies. Since DSM is not a one-size-fit all program, detailed consumers' consumption data are required to both develop and improve effective DSM programs for different consumers. The rapid expansion of the advanced metering infrastructure (AMI) in recent years has produced an enormous amount of data which can be utilized by utility companies for the DSM applications. Based upon the consumption characteristics of different types of consumers, various DSM programs can be developed and applied accordingly. This paper analyzes and studies the practical smart meter data of commercial consumers from New York City considering the potential of commercial consumers' participation for DSM applications, and it provides a better understanding of the power consumption pattern of commercial consumers in the urban area. Both utility companies and commercial consumers could benefit from this study to develop and participate in DSM programs respectively.

Index Terms—AMI, Demand Response (DR), Demand Side Management (DSM), Energy Storage, Smart Meter, Time-of-Use (TOU).

6.1 INTRODUCTION

Demand Side Management (DSM) is considered as a tool to reshape the load and to improve the reliability, efficiency, and security of the power grid [1-7]. Various types of DSM programs have been developed for the power systems and adopted by different utility companies. Electricity consumers could also benefit from participating in the DSM programs. The authors in [1] developed a day-ahead demand side management using symbiotic organisms search algorithm, and both utility bill and peak load for residential, commercial and industrial types of consumers can be reduced. In [8], the authors developed game-theoretic demand-side management with storage devices for the future smart grid. In [9], an enhanced Arrow-d'Aspremont-Gerard-Varet (AGV) mechanism is developed for DSM in the smart grid to maximize the social welfare.

According to the United States Environmental Protection Agency (EPA), commercial sector consumed 35% of the total electricity in 2013, which is approximately the same as the residential sector's 37% of total electricity consumption [10]. However, electricity consumption of individual customer in the commercial sector is much higher than the residential sector. By successfully applying the DSM program on the same number of electricity consumers, the commercial sector has much more impacts on the power grid than the residential sector. Therefore, implementing an effective DSM program to commercial sector would affect the overall system significantly. Currently, different types of DSM programs have been proposed and developed for commercial consumers. In [11], DSM program called building energy management system is developed for a commercial building. The simulation result shows that peak power can be reduced from 25% to 30% with this DSM program. In [12], a DSM optimization model is proposed considering Time-of-Use and rooftop PV generation, and the simulation result shows that 25% of utility bill can be reduced for commercial customers. The authors in [13] proposed a medium-term operation model for the industrial customer, which could help the industrial customer to reduce the power consumption and electricity bills. However, to better investigate the benefits of the commercial sector in DSM programs and to further study the potential of the commercial sector in the DSM programs, the detailed practical data is required.

With the development of the smart grid, advanced metering infrastructure (AMI) has been largely installed in current power systems to enable the new demand side management opportunities for utility companies [14]. By 2014, more than 58 million smart meters have been applied in the US power grids and more than 800 million smart meters will be installed globally by 2020 [14]. Fig. 6.1 to 6.3 provide a sample on what information a smart meter can offer.

Fig. 6. 1 Monthly Consumption Pattern of a Customer

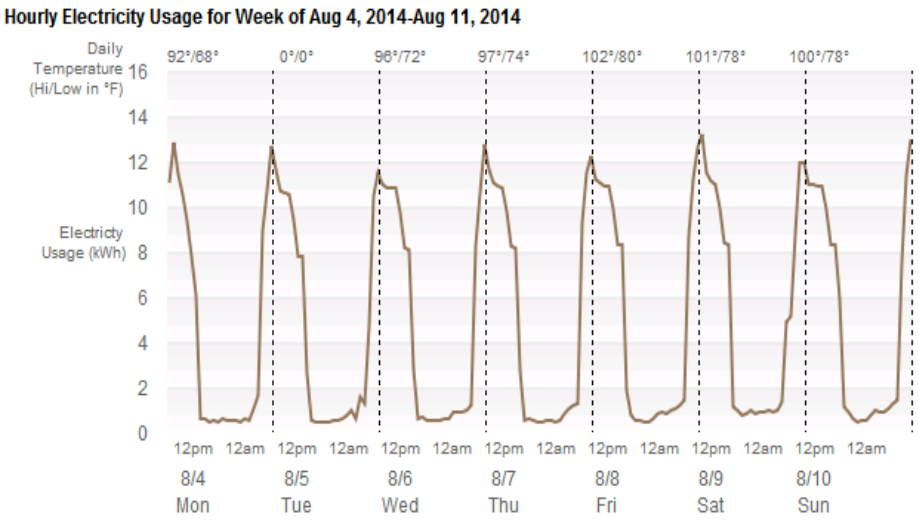

Fig. 6. 2 Hourly Consumption Pattern of a Customer

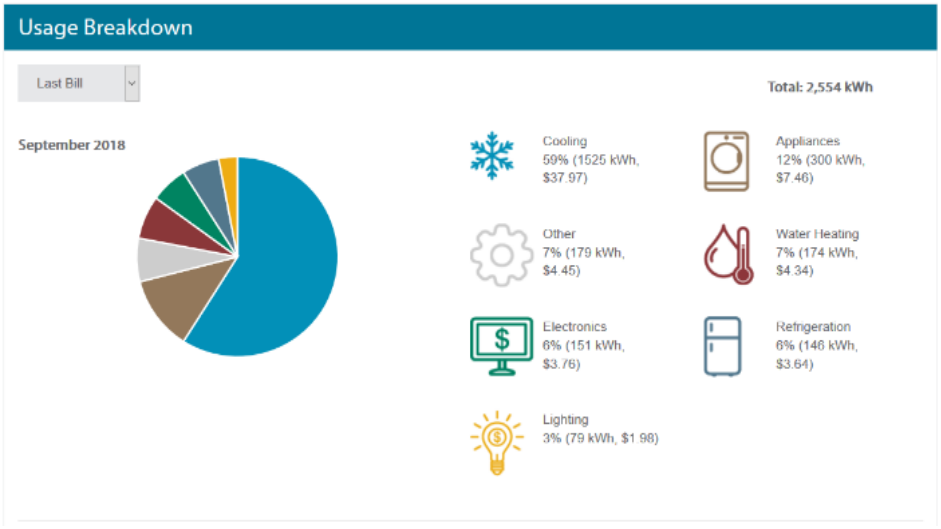

Fig. 6. 3 Breakdown of the Consumption of a Customer

With the detailed data from smart meters, both utility companies and customers can have a better understanding about their power consumption patterns which could help them to benefit from the DSM programs in both economic and technical perspectives.

Electricity rate is a critical factor to study the potential of participation in DSM programs. Generally, the higher electricity rates are, the more benefits participants may receive from DSM programs. New York City is one of the places in the U.S. where it has the highest electricity rates [15]. Participating in the DSM programs in NYC for commercial consumers may bring remarkable economic benefits. In this

paper, the potential of the commercial sector to participate in the DSM program is studied with the practical smart meter data from NYC.

The rest of the paper is organized as follows. Research structure is presented in Section 6.2. Power demand of commercial consumers in NYC is analyzed in Section 6.3. In Section 6.4, financial analysis for one of the current DSM programs in NYC for commercial consumers is performed. Section 6.5 discussed a strategy to improve the effectiveness of DSM programs for commercial consumers in NYC. The conclusion of this study is stated in Section 6.6.

The main contributions of this study are listed below.

- The potential of the commercial sector to participate DSM program is evaluated with real AMI data.
- Practical analysis and results are presented to provide better understanding for DSM developers and DSM commercial participants.
- A hybrid method of using different DSM programs is proposed accordingly to enhance the financial benefits and potential for commercial sector to participate in DSM programs.

6.2 RESEARCH STRUCTURE AND METHODOLOGIES

In this study, the real AMI data from commercial consumers in NYC is utilized. To show the potential for commercial consumers to participate in the DSM program, AMI data is analyzed with probability theory, and probability density function (PDF) is adopted to illustrate the analyzed results. Economic analysis is also performed based on the current DSM program in NYC. To improve the potential for commercial sector to participate in DSM program, a hybrid DSM program is proposed and discussed in this study. The main structure of this research is shown below.

In Section 6.3, three parameters are analyzed with probability theory to illustrate the characteristic of power consumption for each commercial consumer.

In Section 6.4, economic analysis for commercial sector in NYC is presented based on the current local TOU program. Daily incremental cost and beneficial peak-time consumption percentage of using current local TOU are evaluated.

In Section 6.5, A hybrid strategy considering both energy storage and TOU program is proposed to enhance the potential and financial benefits to participate in DSM programs for commercial sector in NYC. Cost of energy storage and current local TOU program rates are applied for the analysis.

To better illustrate the analysis results of a large amount of AMI data, discret probability density function (PDF) which is defined in (1) is used with probability histogram.

$$1 = \sum_{i=1}^{n} p_i \cdot (x_i - x_{i-1}) \quad (1)$$

p: density of the sampled data

i: the number of the sampled data

x: Bin Width of the histogram

n: total number of sampled data

Considering the total number of the sampled data varies in different years, to minimize the difference between the area under the empirical probability distribution and the area under the theoretical probability distribution, Freedman-Diaconis rule is applied to decide the sampled data intervals which is the width of the bins to be used in the histogram. The Freedman-Diaconis rule is defined in (2)

$$Bin\ Width = 2 \times \frac{IQR(X)}{\sqrt[3]{n}} \quad (2)$$

$IQR(X)$: Interquartile range of the data.

n: the number of observations in sample X.

6.3 DEMAND ANALYSIS OF COMMERCIAL CONSUMERS

As one of the most commonly applied DSM programs, Time-of-Use (TOU) has been adopted by many utility companies to reduce the demand during peak-hours [16]. The current TOU rates in NYC for commercial consumers are shown in Table 6-1[17].

TABLE 6 - 1. Commercial Consumers TOU Delivery Rates

Month	Peak	Off-Peak
	8:00 AM to 10:00 PM	10:00 PM to 8:00 AM
June 1st to Sept 30th	29.38 cents/kWh	1.08 cents/kWh
All other Months	14.47 cents/kWh	1.08 cents/kWh

As shown in Table 6-1, the rates of the peak hours from June 1st to September 30th are much higher than all other months. In this study, around 4000 commercial consumers' electricity consumption data were collected by smart meters every 15 minutes from 2012 to 2014. Considering the significance of the TOU rates impacts on the commercial consumers, the data of June, July, August, and September from 2012 to 2014 are used in this study.

To analyze the consumption behaviors of the commercial consumers in each month from June to September, daily power consumption, the percentage of power consumption in peak hours and daily load profile for all consumers are analyzed. Probability density function is a method that is used to show the

probability distribution of a continuous random variable [18]. Considering a large number of collected data, PDF is applied to better illustrate the consumption behaviors of commercial consumers.

6.3.1 Power Consumption of Commercial Consumers

To study the consumption behavior of the commercial consumers, the daily power consumption of each consumer in June, July, August, and September from 2012 to 2014 are calculated. PDF of each month is plotted from Fig. 6.4 to Fig. 6.7, Respectively.

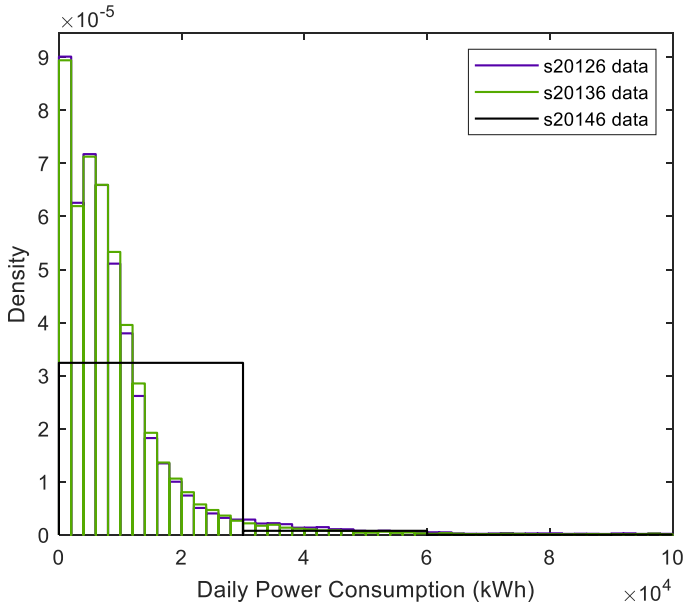

Fig. 6. 4 PDF of Daily Power Consumption for all Consumers in June (2012-2014)

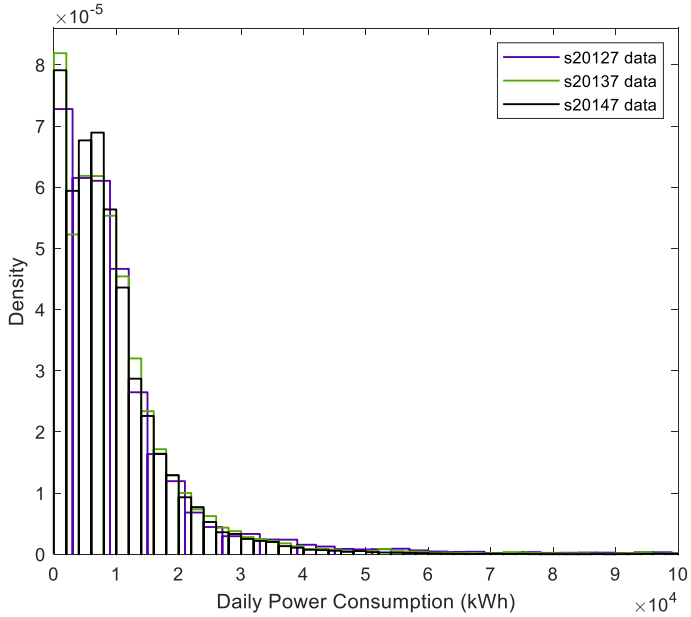

Fig. 6. 5 PDF of Daily Power Consumption for all Consumers in July (2012-2014)

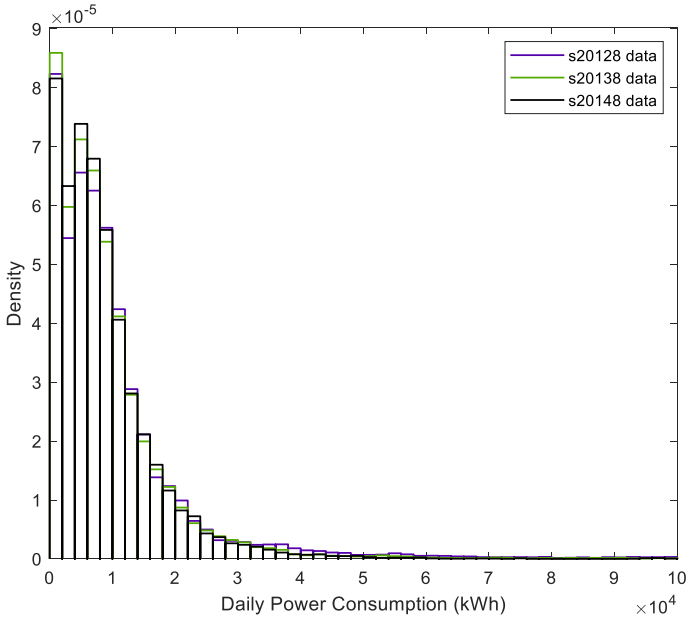

Fig. 6. 6 PDF of Daily Power Consumption for all Consumers in August (2012-2014)

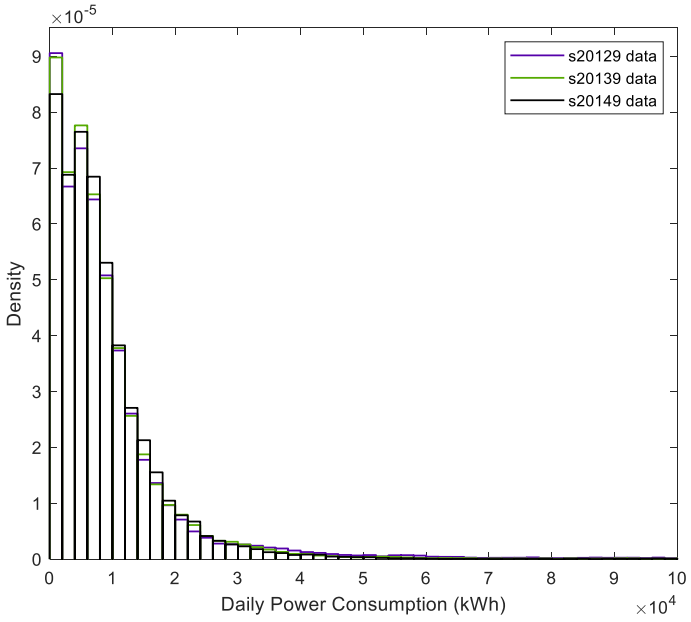

Fig. 6. 7 PDF of Daily Power Consumption for all Consumers in September (2012-2014)

Based on Fig. 6.4 to Fig. 6.7, the PDFs of daily power consumption for all consumers in June, July, August, and September have similar distribution patterns. Most commercial consumers' daily electricity consumption is less than 3,000 kWh. The highest daily consumption range among all consumers is between 0 kWh to 2,000 kWh. Comparing with the average daily residential electricity consumption of 29kWh for every consumer in the U.S. [19], each commercial consumer consumes much more electricity

every day. Thus, DSM program for each commercial consumer has much more impacts on power grids.

6.3.2 Peak Power Consumption Percentage

To analyze the benefits of the current DSM program TOU rates on the commercial consumers, daily power consumption during the peak hours are analyzed in this study. Power consumption from 8 AM to 10 PM for each consumer is calculated. Meanwhile, the percentage of peak power consumption in each day is also analyzed.

To show the peak power consumption from June to September in 2012, 2013 and 2014, PDF of peak power consumption ratio for each month is plotted. Peak power consumption ratio (PR) is defined in (3).

$$PR = \frac{Daily\ Peak\ Power\ Consumption}{Daily\ Power\ Consumption} \qquad (3)$$

PR of June, July, August, September from 2012 to 2014 are plotted in Fig. 6.8, 6.9, 6.10, and 6.11 respectively.

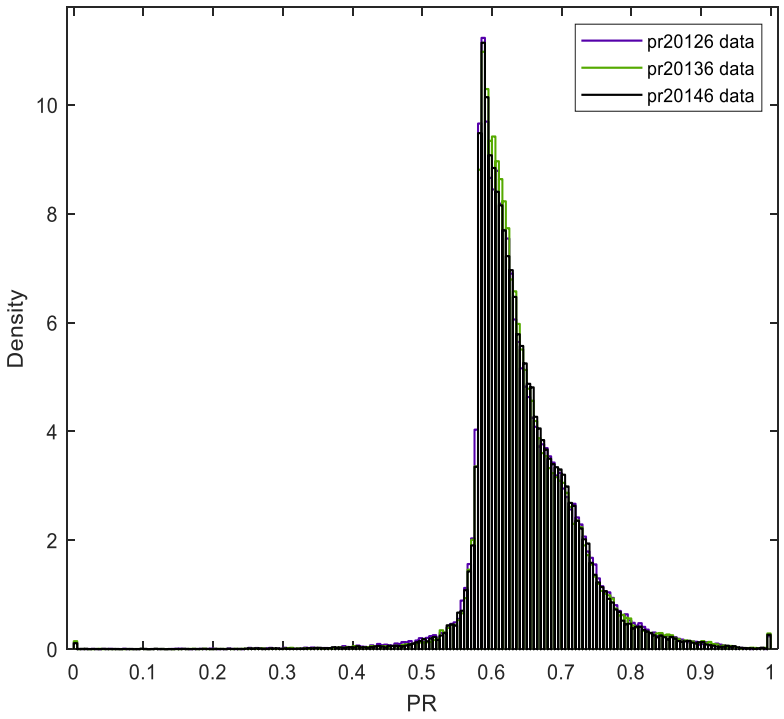

Fig. 6. 8 PR of June (2012-2014)

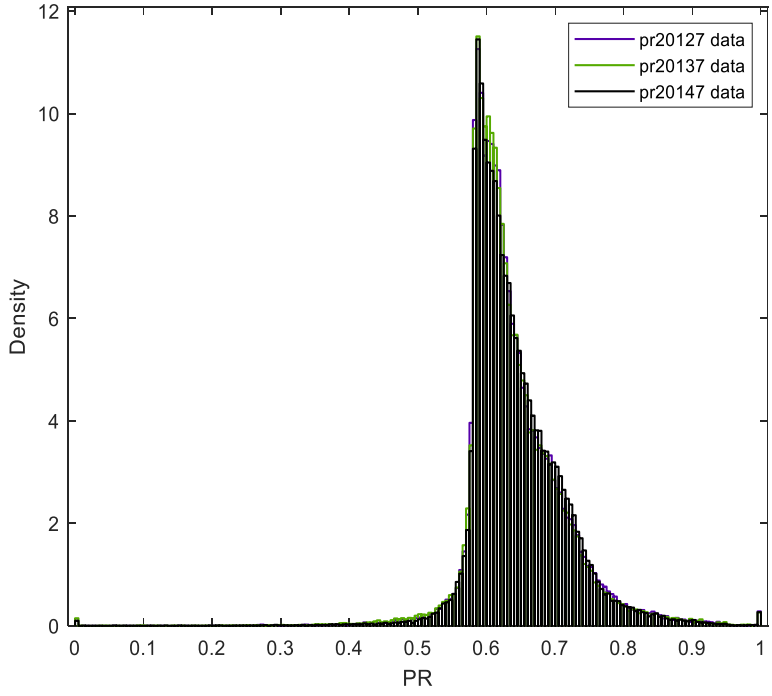

Fig. 6. 9 PR of July (2012-2014)

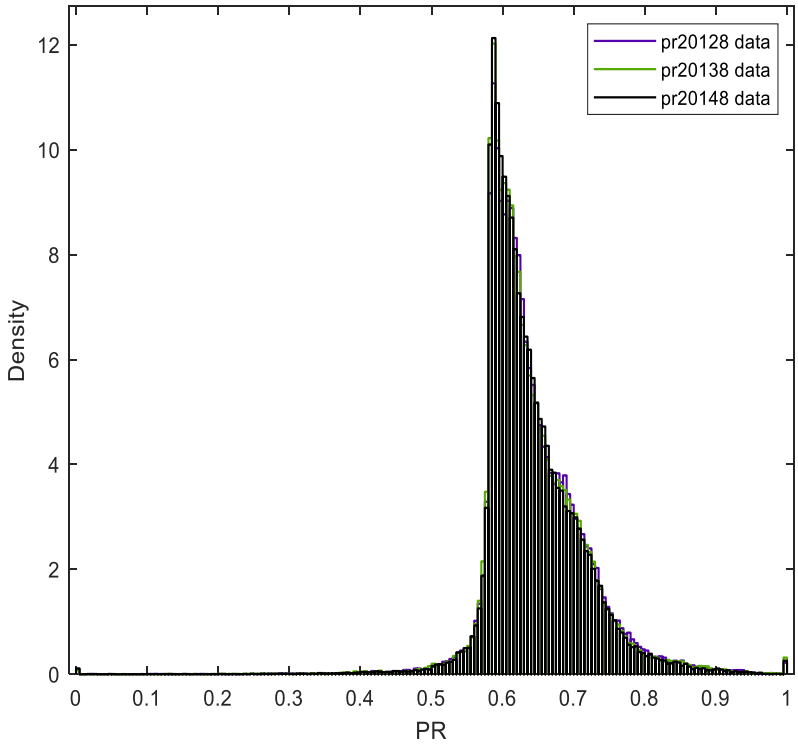

Fig. 6. 10 PR of August (2012-2014)

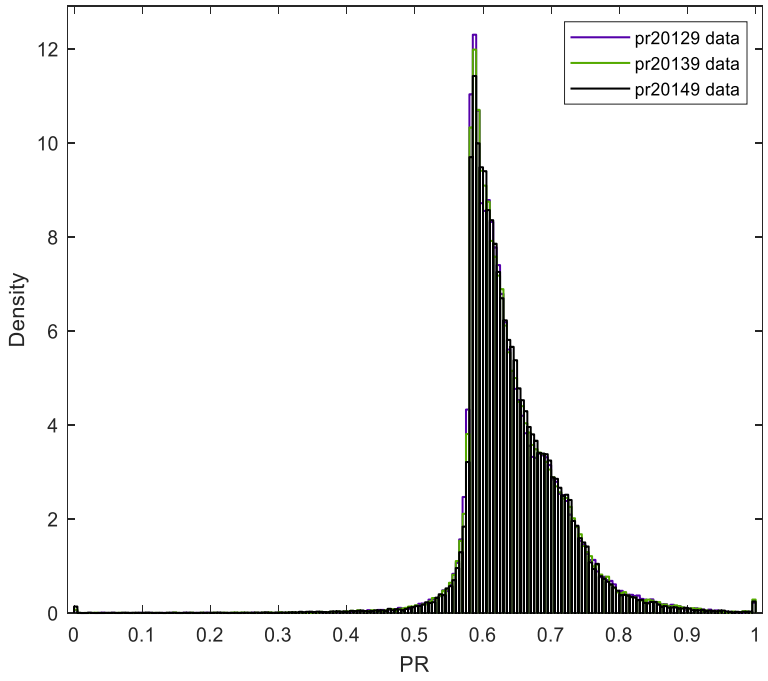

Fig. 6. 11 PR of September (2012-2014)

The figures shown above indicated that most of the commercial consumers consumed more than 50% energy during the peak hours in a day.

6.3.3 PDF of Derivatives of Daily Load Profile

The derivative is a method that shows the rate of change for a given function or continuous data. In power systems, the electricity consumption behaviors can be seen from the load curve. Therefore, it is critical to understand how the load curve changes and to find the demand characteristics of consumers.

In this case, derivative of the daily load profile for each customer is calculated as (4).

$$dp = \frac{E_n - E_{n-1}}{T} \qquad (4)$$

dp: Derivatives of load profile for every 15 min.

E: Energy consumption of every 15 min in kWh.

T: Step size. *T*=1 in this case.

n: Number of 15 min.

To clearly show the derivatives of all consumer in June, July, August, and September from 2012 to 2014, probability density function (PDF) is applied for the *dp* in each month. The PDF of derivatives for all consumers in June, July, August, and September from 2012 to 2014 are plotted in Fig. 6.12, Fig. 6.13,

Fig. 6.14 and Fig. 6.15 respectively.

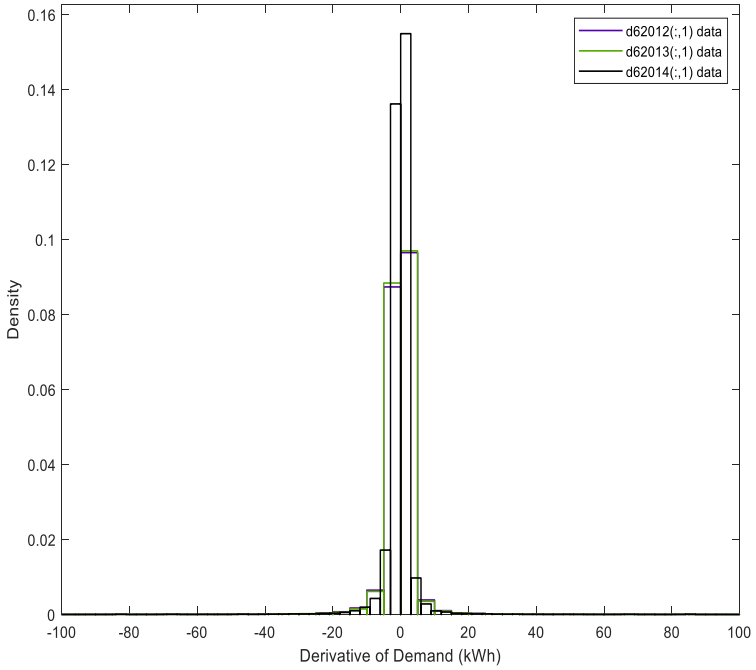

Fig. 6. 12 PDF of *dp* in June (2012-2014)

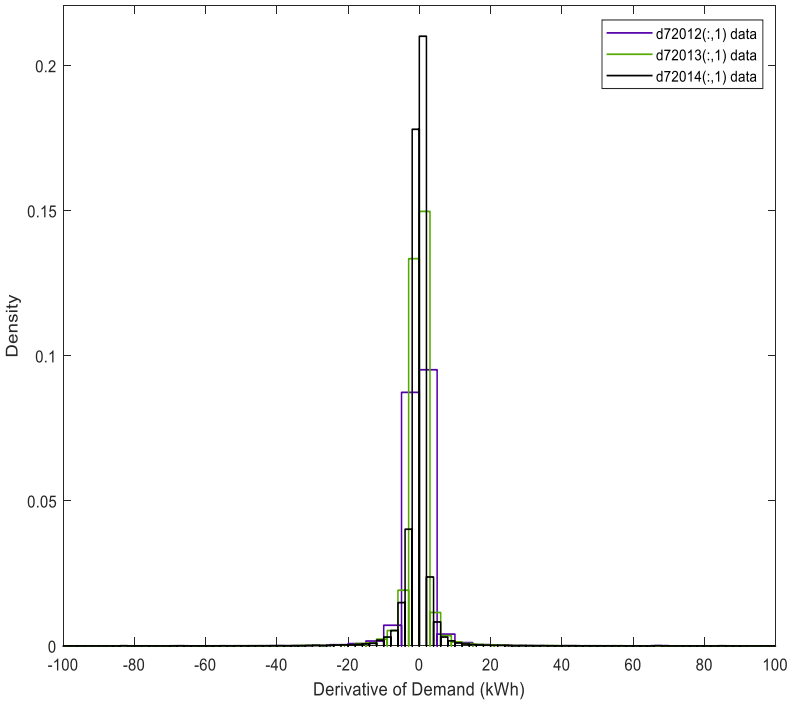

Fig. 6. 13 PDF of *dp* in July (2012-2014)

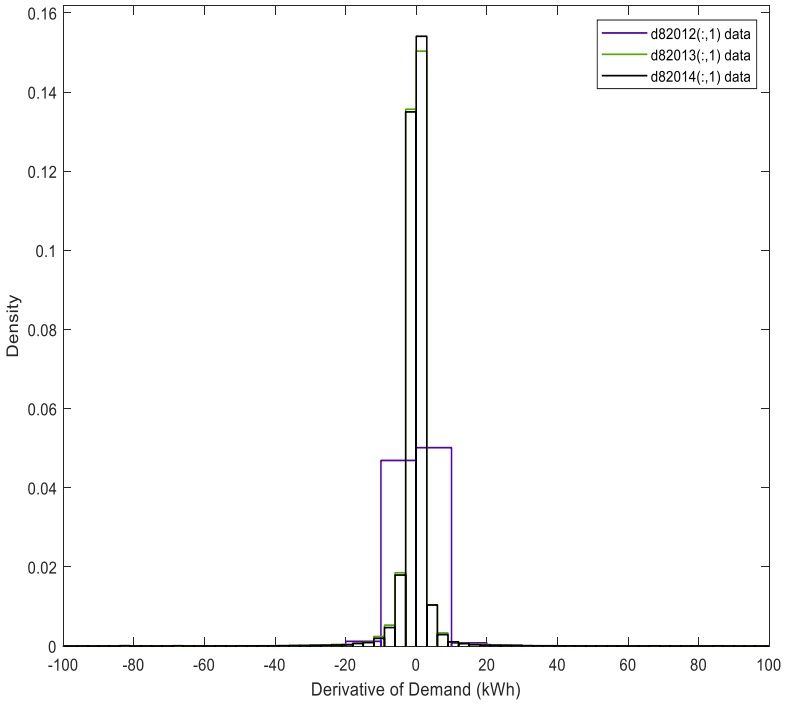

Fig. 6. 14 PDF of *dp* in August (2012-2014)

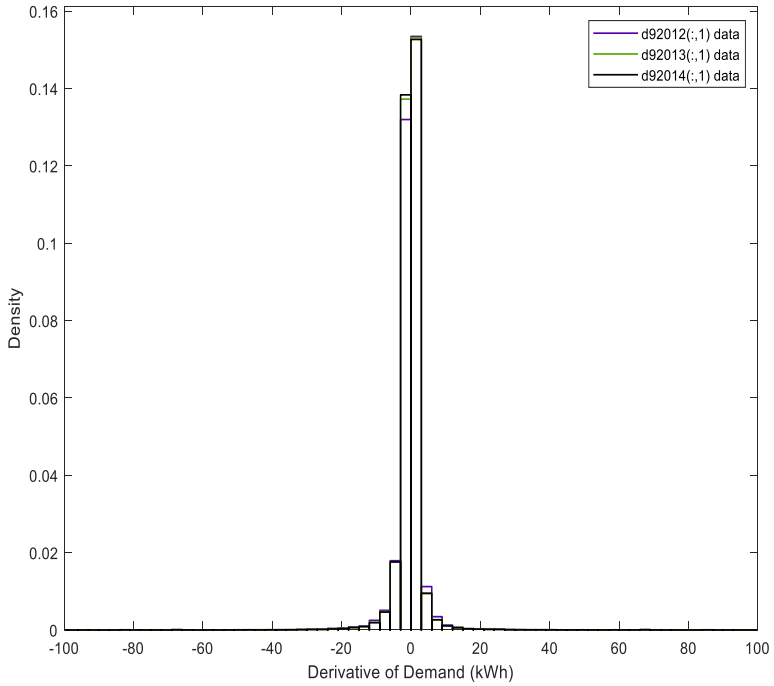

Fig. 6. 15 PDF of *dp* in September (2012-2014)

Based on the results as shown from Fig. 6.12 to Fig. 6.15, the majority of *dp* are close to 0 kWh. In other words, most commercial consumers' daily power demands have low demand deviations. According to the analysis results of the collected smart meter data for commercial consumers, one can see that:

- Most commercial consumers consumed less than 2,000 kWh electricity daily.
- More than 50% of energy was consumed during the peak hours.
- Most of the commercial consumers have relatively constant daily power demand.

6.4 FINANCIAL ANALYSIS OF THE DSM PROGRAM

In section 6.2, commercial consumers' power demands were analyzed from 3 perspectives with a statistical analysis method. It shows that most of the commercial consumers consumed more than 50% to even 90% of total daily energy consumption during the peak hours. Considering this power consumption characteristic of commercial consumers, electricity bills would be increased significantly for commercial consumers to use TOU rates. Using commercial consumers TOU delivery rates shown in Table I and standard delivery rates shown in Table 6-2, daily increased electricity costs for each commercial consumer are calculated using (5).

TABLE 6 - 2. Commercial Consumers Standard Delivery Rates

Month	Peak	Off-Peak
	8:00 AM to 10:00 PM	10:00 PM to 8:00 AM
June 1st to Sept 30th	12.46 cents/kWh	12.46 cents/kWh
All other Months	10.46 cents/kWh	10.46 cents/kWh

$$DIC\ (\$) = (0.2938 \times DPPC + 0.0108 \times OPC) - 0.1246 \times DPC = 0.1692 \times DPPC - 0.1138 \times OPC \quad (5)$$

$$DPC = DPPC + OPC$$

0.2938: TOU electricity rate of the peak hours ($/kWh)

0.0108: TOU electricity rate of the off-peak hours ($/kWh)

DIC: Daily Incremental Cost ($)

DPPC: Daily Peak Power Consumption (kWh)

OPC: Daily Off-Peak Power Consumption (kWh)

DPC: Daily Power Consumption (kWh)

The DIC for June, July, August and September are plotted in the following Figures.

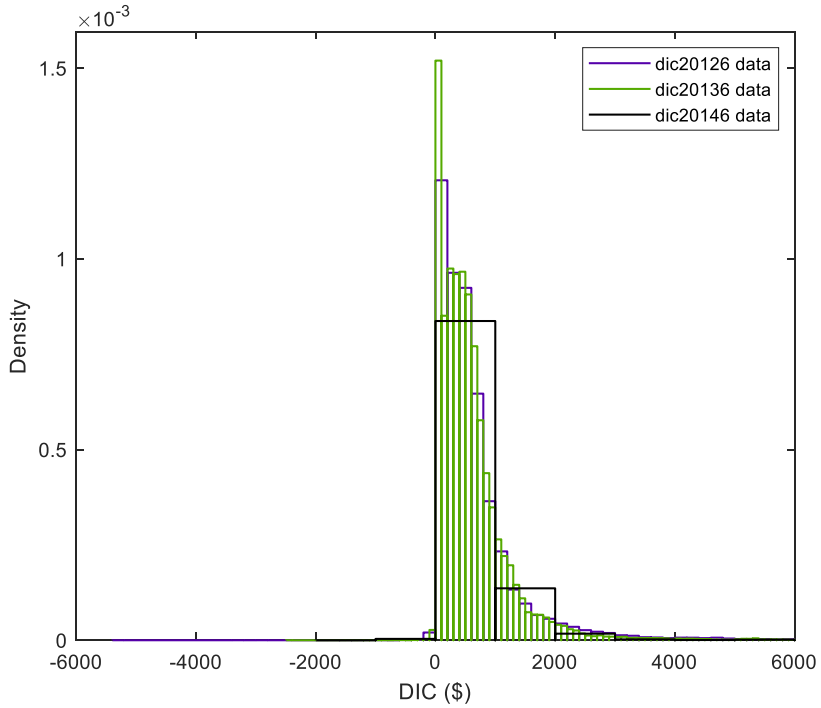

Fig. 6. 16 PDF of DIC in June (2012-2014)

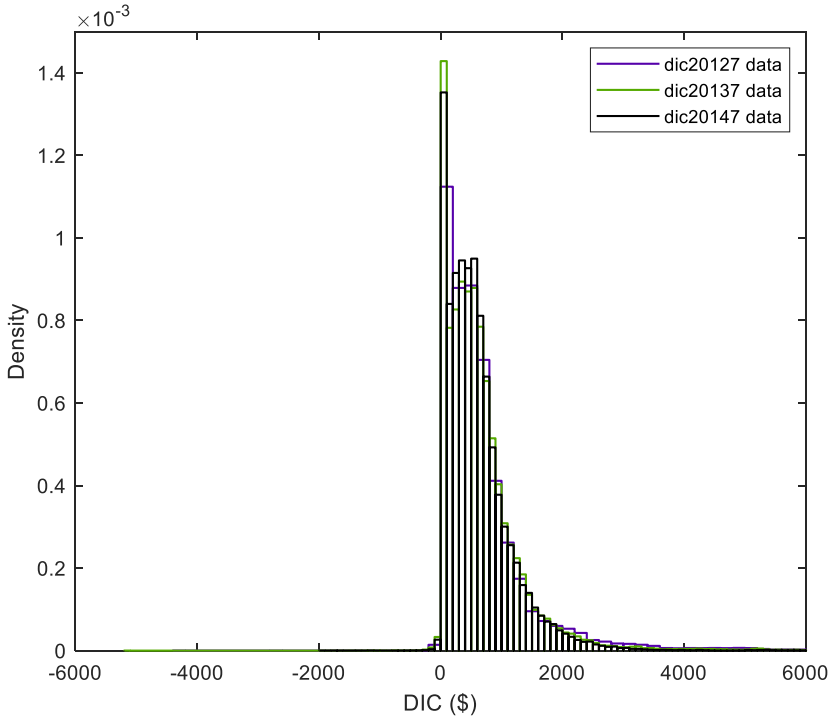

Fig. 6. 17 PDF of DIC in July (2012-2014)

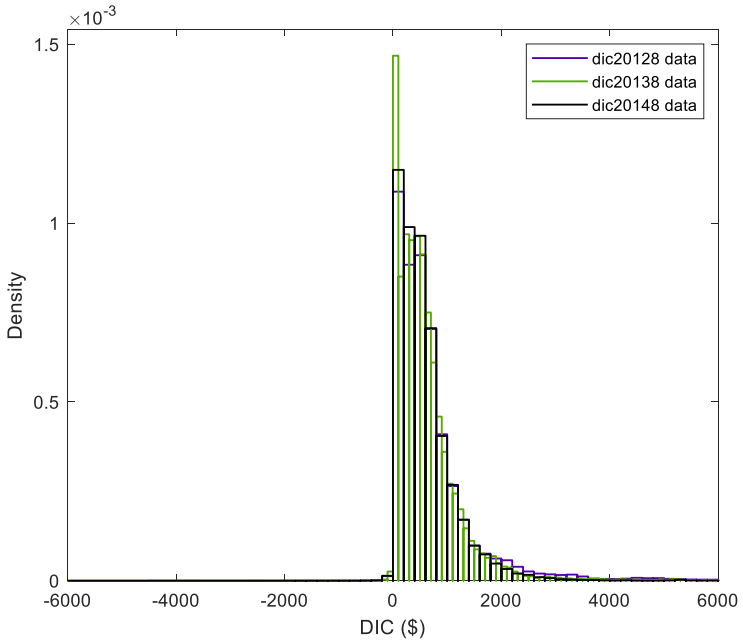

Fig. 6. 18 PDF of DIC in August (2012-2014)

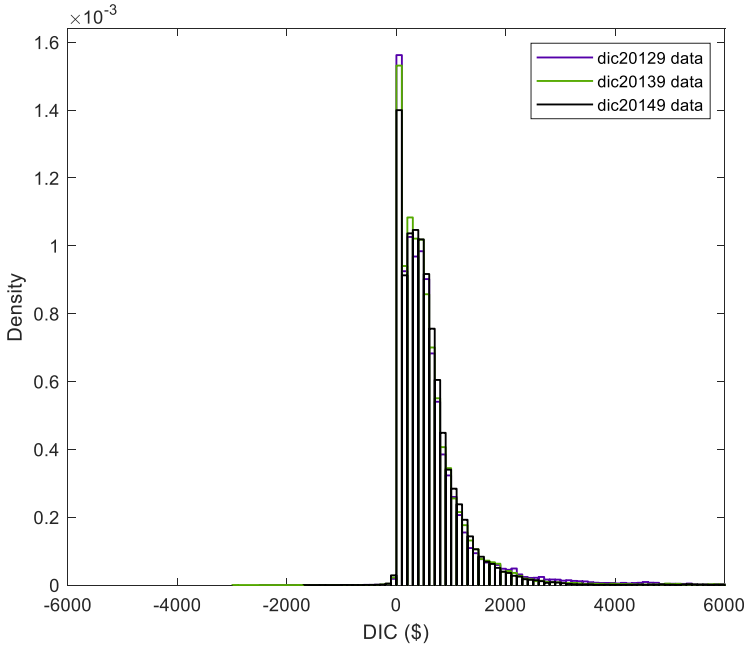

Fig. 6. 19 PDF of DIC in September (2012-2014)

Based on the figures shown above, DIC for commercial consumers in June, July, August, and September can be increased notably by applying TOU rates. Therefore, without changing the consumption patterns, commercial consumers must pay more on their daily electricity bills by using the TOU program

in NYC. Therefore, commercial consumers are not able to benefit from the current TOU program in NYC. To benefit from the current TOU programs, the PR threshold is calculated using (6).

$$DPC \times 0.1246 = DPPC \times 0.2938 + OPC \times 0.0108 \quad (6)$$

$$\frac{DPPC}{DPC} \times 100\% = 40.21\%$$

In (4), each commercial consumer's daily power cost is calculated based on the DPC and commercial consumers' standard delivery rates. To find the PR threshold for the same commercial consumer, daily power cost should be the same as the cost when TOU rate is applied.

Comparing with the standard delivery rates, commercial consumers need to use less than 40.21% of total daily power consumption during the peak hours so that they can benefit from the current TOU program. Based on the results shown in Fig. 6.8 to Fig. 6.11, most commercial consumers need to shift a large percentage of total power consumption from peak hours to off-peak hours. However, due to the consumption characteristics of the commercial consumers, shifting the power demand might affect the normal business operations. Thus, it is quite challenging to change electricity consumption patterns for most commercial consumers.

To utilize the current TOU program in NYC, other DSM programs could be considered to work with the current TOU program and to reduce the electricity cost for commercial consumers.

6.5 HYBRID DSM PROGRAM

As one of the DSM applications, energy storage has been developed for decades [20, 21]. However, high cost is the main obstacle to largely implement energy storage for most end users. Nevertheless, for current TOU rates, peak time delivery fees are 27 times more than off-peak rates, thus benefits of energy storage in DSM program can be enhanced. To analyze the potential of commercial consumers to participate in DSM programs, energy storage and current TOU programs are analyzed with the practical smart meter data.

In this study, energy storage and current TOU rates in NYC are applied to study the potential for commercial consumers to participate in DSM programs. As the results are shown in the previous section, without changing the consumption patterns, commercial consumers are not able to benefit from the current TOU program. As the challenge for the commercial consumers, electricity demand shift could affect the normal business operations and cause unnecessary financial losses. Therefore, energy storage

can be considered in the DSM programs for commercial consumers without changing the power consumption patterns. To utilize TOU rates and to apply energy storage in DSM programs, the cost of energy storage needs to be considered. According to a recent study by U.S. Energy Information Administration (EIA), long duration energy storage costs 399 $/kWh [22].

Using current TOU rates in NYC and considering the energy storage degradation costs, if all daily peak power consumption can be supplied by the energy storage, payback time of energy storage is calculated in (7).

$$DPPC \times 399\,\$/kWh + DPPC \times Degradation\ Cost\ \$/kWh = DPPC \times (0.2938 - 0.0108)\,\$/kWh \times Days$$

$$Days = \frac{399\,\$/kWh}{0.283\,\$/kWh - Degradation\ Cost\ \$/kWh} \qquad (7)$$

As shown in (7), the days to receive the payback of energy storage will be affected by energy storage degradation cost.

Once the energy storage payback is covered, comparing with the standard delivery fees, the daily financial savings for commercial consumers can be calculated in (8).

$$Financial\ Savings\ (\$) = DPC \times 0.1246 - DPC \times 0.0108 - DPPC \times Degradation\ Cost \qquad (8)$$

Therefore, the more daily peak power consumption can be supplied by energy storage the more financial benefit the consumers can receive.

Without considering degradation cost, the commercial consumers would take around 1057 days which is less than 3 years to receive the energy storage payback, and PDF of financial benefits for each consumer is calculated and plotted in Fig. 6.20 to 6.23.

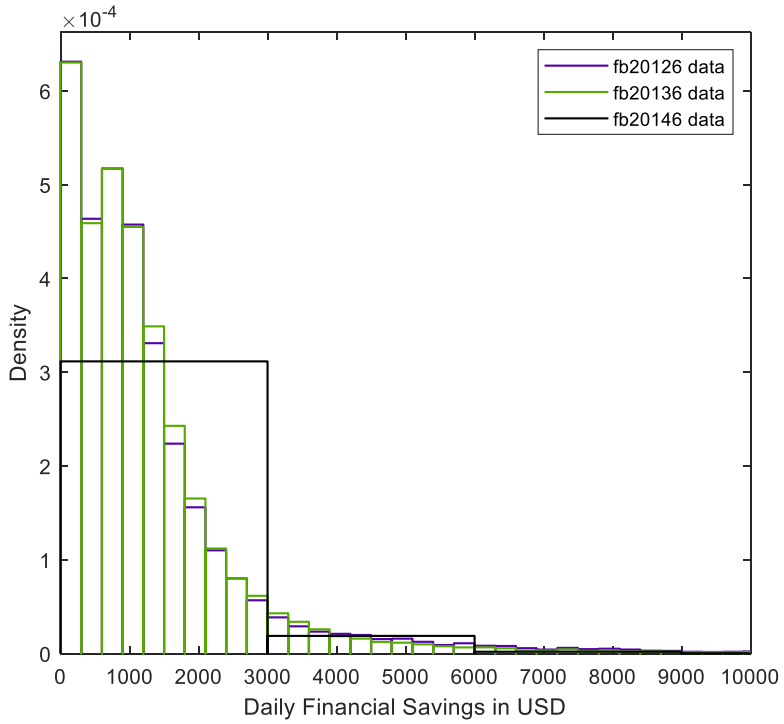

Fig. 6. 20 Daily Financial Savings in June (2012-2014)

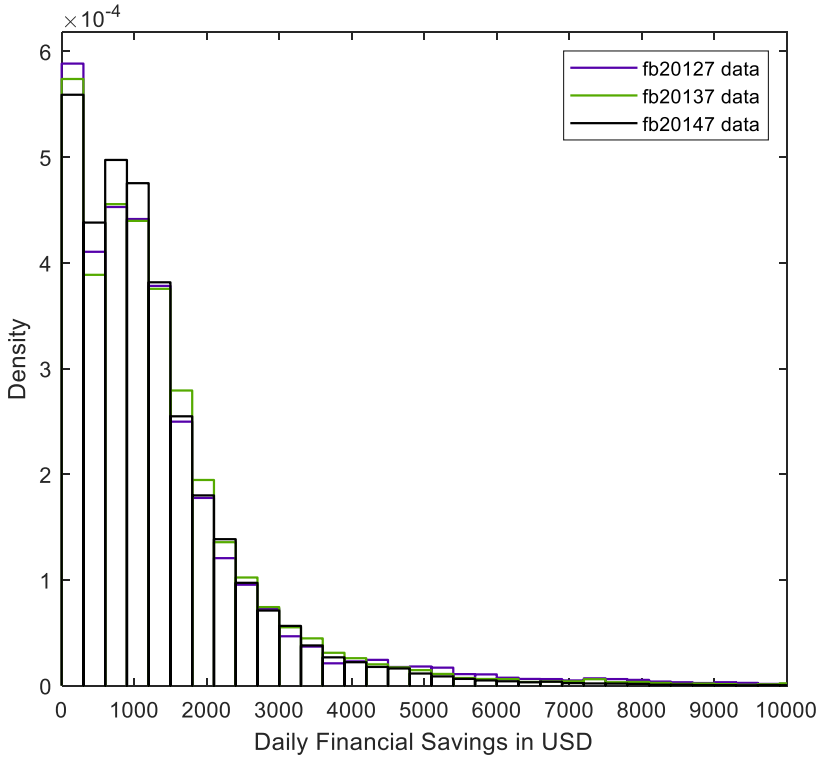

Fig. 6. 21 Daily Financial Savings in July (2012-2014)

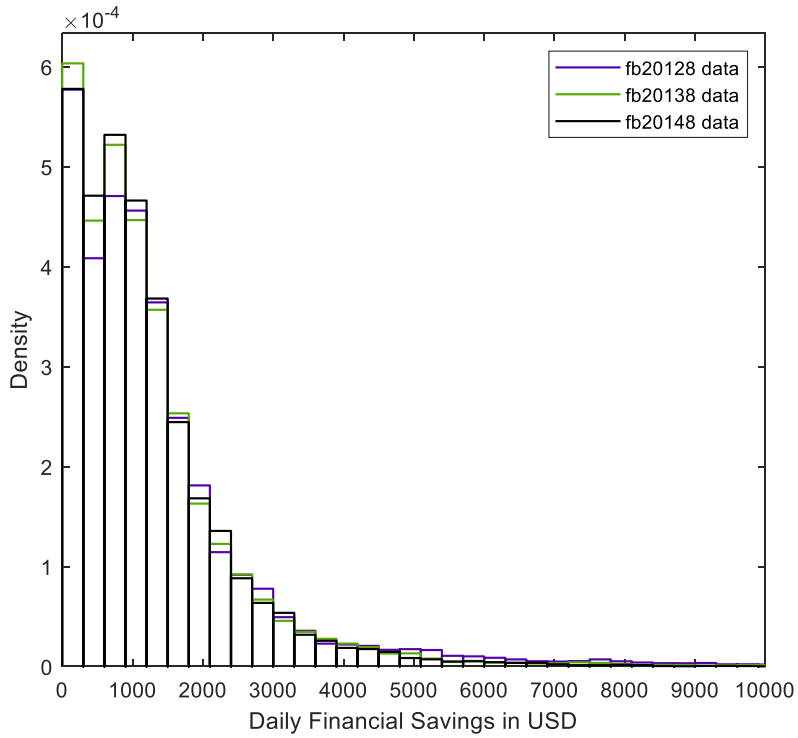

Fig. 6. 22 Daily Financial Savings in August (2012-2014)

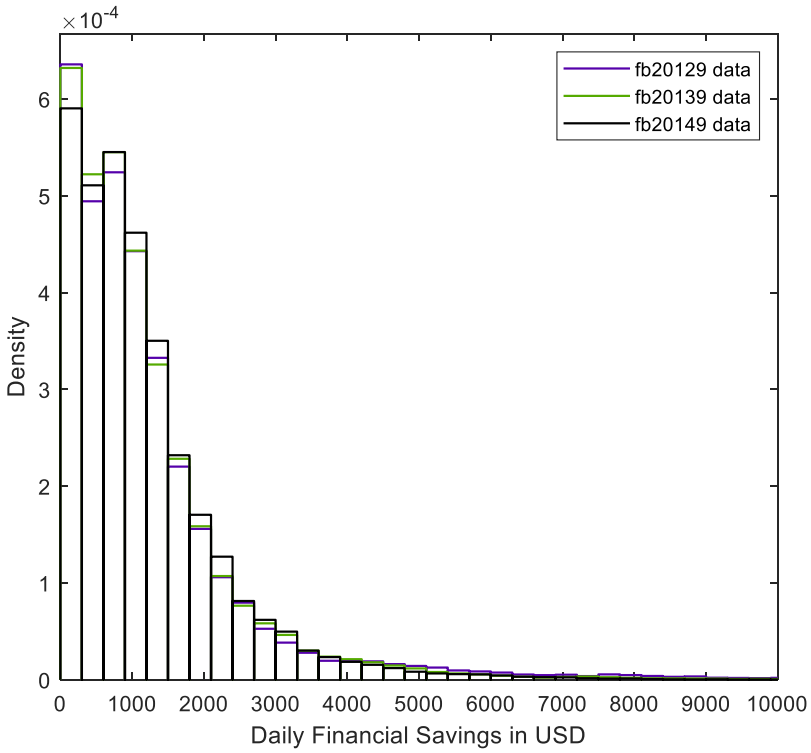

Fig. 6. 23 Daily Financial Savings in September (2012-2014)

As shown above, daily financial benefits from the current TOU program are considerable by applying energy storage. However, the payback time and degradation cost also need to be considered by commercial consumers. Moreover, the financial benefits to participating DSM program for commercial consumers are affected by the TOU rates, energy storage costs and daily peak power consumptions. The more energy can be supplied by storage unit during the peak hours, the more benefits hybrid DSM program could bring to hybrid customers.

6.6 CONCLUSION

In this paper, the potential of commercial consumers to participate in DSM program is studied based on the real smart meter data. The analysis results of the practical data showed most of the commercial consumers have relatively constant daily power demands. Thus, commercial consumers' electricity costs were increased significantly by participating in the current TOU program in NYC. Considering the power demand of commercial consumers, solo load shifting would affect the normal commercial business operations, which would reduce the benefits of DSM application for commercial consumers. Therefore, DSM program for commercial consumers is studied with the energy storage besides current TOU rates. According to the study results, the initial cost of energy storage, energy storage degradation cost and TOU rates would affect the benefits of DSM programs for commercial consumers. However, DSM has a great potential to benefit commercial consumers by applying energy storage and TOU rates at the same time. Especially with the decreasing costs of energy storage, benefits for commercial consumers to participate in DSM programs would be enhanced.

6.7 REFERENCES

[1] V. M. Niharika, "Day-ahead demand side management using symbiotic organisms search algorithm," *IET Generation, Transmission & Distribution*, vol. 12, pp. 3487-3497, Aug. 2018.

[2] P. Samadi, H. Mohsenian-Rad, R. Schober, and V. W. S. Wong, "Advanced demand side management for the future smart grid using mechanism design," *IEEE Trans. Smart Grid,* vol. 3, pp. 1170-1180, Sep. 2012.

[3] D. Huang and R. Billinton, "Effects of load sector demand side management applications in generating capacity adequacy assessment," *IEEE Trans. Power Syst.,* Vol. 27, pp. 335-343, Feb. 2012.

[4] G. Tsagarakis, R. C. Thomson, A. J. Collin, G. P. Harrison, A. E. Kiprakis, and S. McLaughlin, "Assessment of the cost and environmental impact of residential demand-side management," *IEEE Trans. Ind. Appl.*, vol. 52, pp. 2486-2495, May/Jun. 2016.

[5] P. Palensky and D. Dietrich, “Demand side management: demand response, intelligent energy systems, and smart loads,” *IEEE Trans. Ind. Appl.*, vol. 7, pp. 381-388, Aug. 2011.

[6] S. Faddel and O. A. Mohammed, “Automated distributed electric vehicle controller for residential demand side management,” *IEEE Trans. Ind. Appl.*, vol. 55, pp. 16-25, Jan/Feb. 2011.

[7] L. Martirano, E. Habib, G. Parise, G. Greco, M. Manganelli, F. Massarella, and L. Parise, “Demand side management in microgrid for load control in nearly zero energy buildings,” *IEEE Trans. Ind. Appl.*, vol. 53, pp. 1769-1779, May/Jun. 2017.

[8] H. M. Soliman and A. Leon-Garcia, “Game-theoretic demand-side management with storage devices for the future smart grid,” *IEEE Trans. Smart Grid,* vol. 5, pp. 1475-1485, May. 2014.

[9] J. Ma, J. Deng, L. Song, and Z. Han, “Incentive mechanism for demand side management in smart grid using auction,” *IEEE Trans. Smart Grid,* vol. 5, pp. 1379-1388, May. 2014.

[10] *Electricity Customers.* [Online]. Available: https://www.epa.gov/energy/electricity-customers

[11] L. Martirano, G. Parise, G. Greco, M. Manganelli, F. Massarella, M. Cianfrini, L. Parise, P. d. L. Frattura, and E. Habib, “Aggregation of users in a residential/commercial building managed by a building energy management system (BEMS),” *IEEE Trans. Ind. Appl.*, vol. 55, pp. 26-34, Jan/Feb. 2019.

[12] H. O. Alwan, H. Sadeghian, and Z. Wang, “Decentralized demand side management optimization for residential commercial load,” in *Proc. 2018 IEEE International Conf on Electrol/Information Technology (EIT)*, pp. 0712-0717.

[13] Z. Ding, P. Sarikprueck, and W. Lee, “Medium-term operation for an industrial customer considering demand-side management and risk management,” *IEEE Trans. Ind. Appl.*, vol. 52, pp. 1127-1135, Mar/Apr. 2016.

[14] J. Corbett, K. Wardle, and C. Chen, “Toward a sustainable modern electricity grid: the effects of smart metering and program investments on demand-side management performance in US electricity sector 2009-2012,” *IEEE Trans. Eng. Mgmt.*, vol. 65, pp. 252-263, Apr. 2018.

[15] B. Sanderson, “Con Edison prices are the highest by any US utility,” [Online]. Available: https://nypost.com/2015/03/07/con-edison-prices-are-the-highest-by-any-us-utility/

[16] L. Zhao, Z. Yang, and W. Lee, “The impact of Time-of-Use (TOU) rate structure on consumption patterns of the residential customers,” *IEEE Trans. Ind. Appl.*, vol. 53, pp. 5130-5138, Nov/Dec. 2017.

[17] *Time-of-Use Rates*. [Online]. Available: https://www.coned.com/en/save-money/energy-saving-programs/time-of-use

[18] *Using the Probability Density Function (PDF).* [Online]. Available: https://support.minitab.com/en-us/minitab-express/1/help-and-how-to/basic-statistics/probability-distributions/supporting-topics/basics/using-the-probability-density-function-pdf/

[19] *How Much Electricity Does an American Home Use?* [Online]. Available: https://www.eia.gov/tools/faqs/faq.php?id=97&t=3

[20] V. A. Boicea, "Energy storage technologies: the past and the present," *Proc. IEEE,* vol. 102, no. 11, pp. 1777-1794, Nov. 2014.

[21] H. K. Nguyen, J. B. Song, and Z. Han, "Distributed demand side management with energy storage in smart grid," *IEEE Trans. Parallel and Distributed Systems,* vol. 26, pp. 3346-3357, Dec. 2015.

[22] U.S. Battery Storage Market Trends. U.S. Energy Information Administration., Washington, DC. [Online]. Available: https://www.eia.gov/analysis/studies/electricity/batterystorage/

CHAPTER 7.

USING SPECTRUM OF THE LIGHT FOR HIGH SPEED ARCING FAULT DETECTION

USING SPECTRUM OF THE LIGHT FOR HIGH SPEED ARCING FAULT DETECTION[6]

Long Zhao, Igor Matsuo, Yuhao Zhou, Wei-Jen Lee

L. Zhao, Y. Zhou, K. Chen, S. Rau and W. Lee, "Using spectrum of the light for speed arcing fault detection," *IEEE Ind. Appl. Mag.,* vol. 26, May/Jun. 2020. pp. 29-36.

Using Spectrum of the Light for High Speed Arcing Fault Detection

Paper No. ESW2018-41

Long Zhao[1] Yuhao Zhou[1] Kun-Long Chen[2] Shiuan-Hau Rau[3] Wei-Jen Lee[1]

Student Member IEEE Member, IEEE Fellow, IEEE

Electrical Engineering Department, University of Texas at Arlington, Arlington, TX, 76019, USA[1]

College of Electrical Engineering and Automation, Fuzhou University, Fuzhou, Fujian, 35011, China[2]

Shermco Industries, Inc, Irving, TX, 75061, USA[3]

Abstract – Unlike short circuit faults in power systems, arcing faults produce intense light during the events. Light sensing technology has been developed as a part of arc faults detection since 1980's. Currently, optical fiber and point sensors are 2 types of light sensors which have been applied along with the simultaneous over-current mechanism for arc flash relays. Due to the characteristics of light sensors, sensitivity and reliability of the relay may be affected by the ambient light. This paper proposes a new approach for arc flash fault detection by using the spectrum of the light. Electromagnetic radiation means different element would emit spectra with unique wavelengths when their atoms are excited. Therefore, elements can be identified if specific emission spectrum is detected during the excitation period. In general, Copper and Aluminum are commonly used for conductors. By examining the spectrum of the light, arc flash can be accurately and quickly detected. In the experiment of this study, copper and aluminum are applied as conductors. The light spectrum for both materials is measured and recorded by an optic spectrometer during the arcing incidents. The results show that accuracy and reliability of the light-based arc flash fault detection operation can be improved by using the proposed method.

Index Terms — Arc flash, Detection, Fault, Relay, Spectrum.

7.1 INTRODUCTION

Besides thermal energy, a large amount of radiant energy is released with pressure, sounds, and light during arc flash incidents [1]. It could cause severe damages to the power system equipment and operators who are close by, and many studies have used different ways to solve this issue [2-5]. Since the incident energy released by arc flash fault is proportional with fault duration, reducing the clearing time becomes the vital part for arc flash protection design [6]. Due to the high speed of the light sensing, light sensor has been applied to arc flash relay to reduce the tripping time. Light sensing technology for arc flash protection has been developed since 1980's [7]. The first- and second-generation light sensing arc flash relay were implemented in the 1990s and 2000s respectively [1]. With the development of the light

sensing technology, light sensing arc flash relay has been largely applied to power systems at different voltage levels [6-7]. Currently, optical fiber and point sensors are the most common light sensors that are integrated into arc flash protection systems. Both optical fiber and point sensors are used to detect the intense light during an arc flash fault [7].

Even the tripping speed of arc flash detection has been improved significantly [6], reliability and accuracy of the current light sensor mechanism could still be affected by ambient light and light pollution. Some studies show that current light sensing technology in arc flash fault protection system could be accidentally tripped by other light sources [7-9]. Meanwhile, light point sensors are very sensitive to the light directions. Because of the complexity of the arc flash fault, it is quite difficult to locate the effective spot for point sensors in the arc fault detection system. To improve the reliability and accuracy of tripping process, this paper proposes a method that utilizes light spectrum instead of light intensity to detect the arc flash fault.

Study of electromagnetic radiation has been developed for many years, and it also has been widely applied in different applications. The concept of electromagnetic radiation is that different element would emit spectra with unique wavelength when their atoms are excited. Therefore, the element can be identified if its emission spectrum is detected during the excitation period. Because each element has a unique energy level, different elements would emit different spectrums with identical wavelengths. Therefore, by identifying the emitted wave spectrum, the arc flash faults can positively be detected without being affected by other light sources. In this paper, the identical spectra of arc flash are acquired with different experiments, and the arcing fault detection algorithm is developed based on the identical spectra of arc flash. The rest of the paper is organized as follows: Spectrum measurement for arc flash with copper, aluminum, and other different light sources are presented in Section 7.2. Section 7.3 introduces the spectrum-based fault detection algorithm. The conclusion of this paper is shown in Section IV.

7.2 ARC FLASH SPECTRUM MEASUREMENT

7.2.1 Arc Flash Test

In this study, arc flash experiments were created with different types of conductors. To measure the spectrum during the arc flash event with different types of conductors, a spectrum measurement station for arc flash is built as shown in Fig. 7.1. In this station, one variable transformer (0V to 140V) and one step-up transformer (1:125) are implemented to create arc flashes for spectrum measurements. The spectrometer in this study uses coaxial optical fiber sensor which has higher precision and wider detection angles as shown in Fig. 7.2 [10-11].

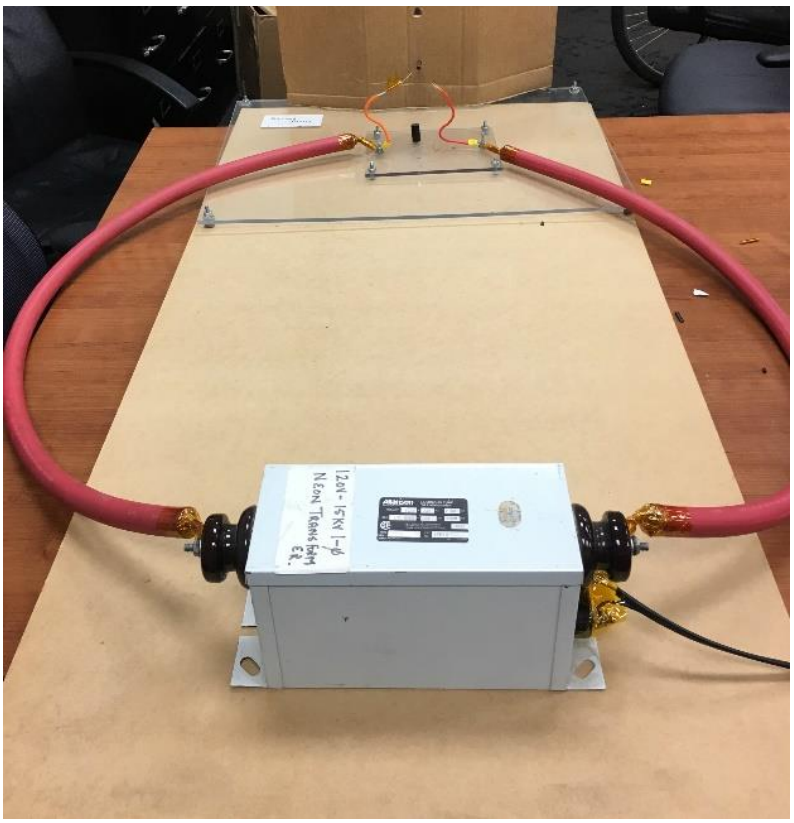

Fig. 7. 1 Arc Flash Spectrum Measurement Station

Fig. 7. 2 Coaxial Optical Fiber Sensor [10]

7.2.2 Spectrum Measurement

To identify the characteristics of the spectrum during arc flash event, light spectrum is measured with different conductors as shown in Table7-1.

TABLE 7 - 1. Arc Flash Experiment

Experiment #	Conductor Type	Voltage
1	12 AWG Solid Copper	8750 V
2	40 AWG Solid Copper	12500 V
3	40 AWG Solid Aluminum	12500 V
4	40 AWG Solid Aluminum and Copper	12500 V

1) Experiment 1: In this experiment, 12 AWG solid copper wire is used as arcing conductors. Due to the thickness of the copper conductors and the limited energy of arc flash in this experiment, arc flash happened without conductors burning. Arc flash of experiment 1 is shown in Fig. 7.3. Spectral line of arcing light in experiment 1 is shown in Fig. 7.4.

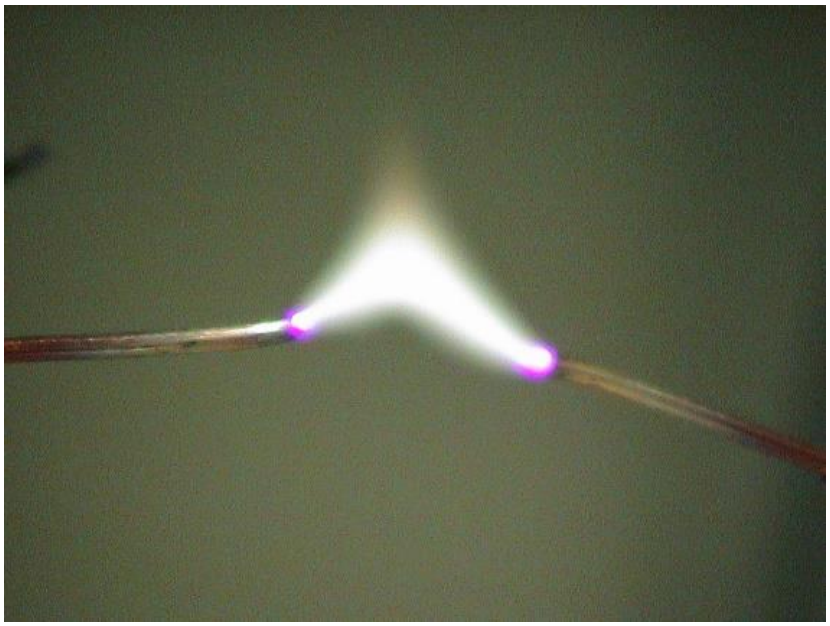

Fig. 7. 3 Arc Flash

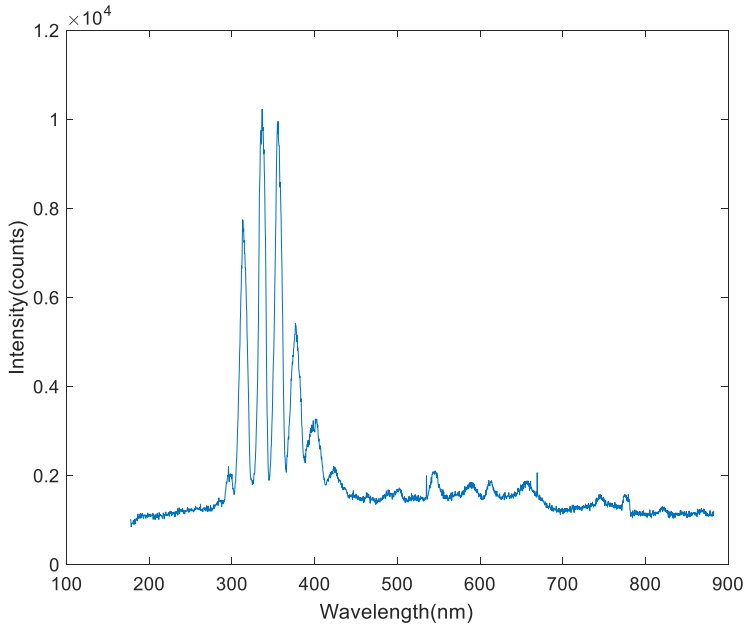

Fig. 7. 4 Spectral Line of Experiment 1

2) Experiment 2: 40 AWG solid copper wire is used as arcing conductors. Copper conductors are burned along with the arc flash. Spectral line of arc flash in experiment 2 is shown in Fig. 7.5.

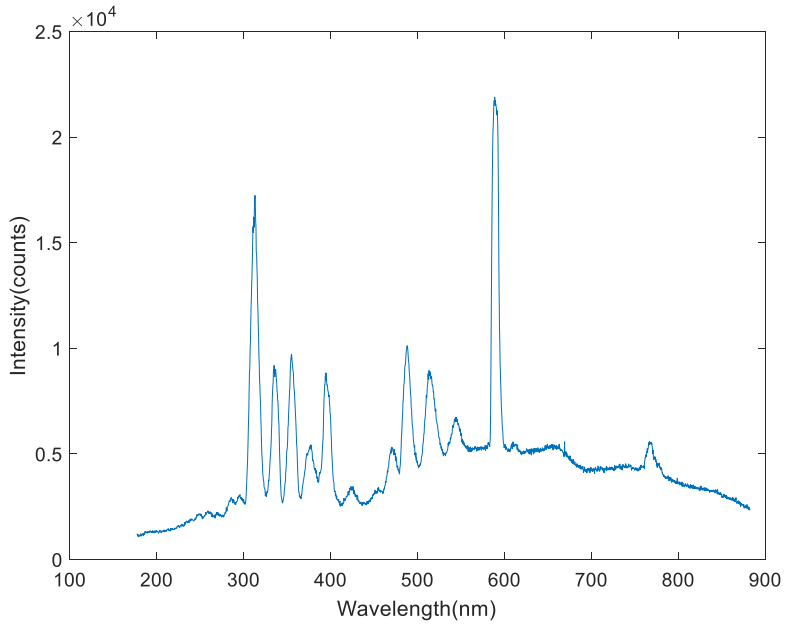

Fig. 7. 5 Spectral Line of Experiment 2

3) Experiment 3: 40 AWG solid aluminum wire is used as arcing conductors. Aluminum conductors are burned along with the arc flash. Spectral line of arc flash in experiment 3 is shown in Fig. 7.6.

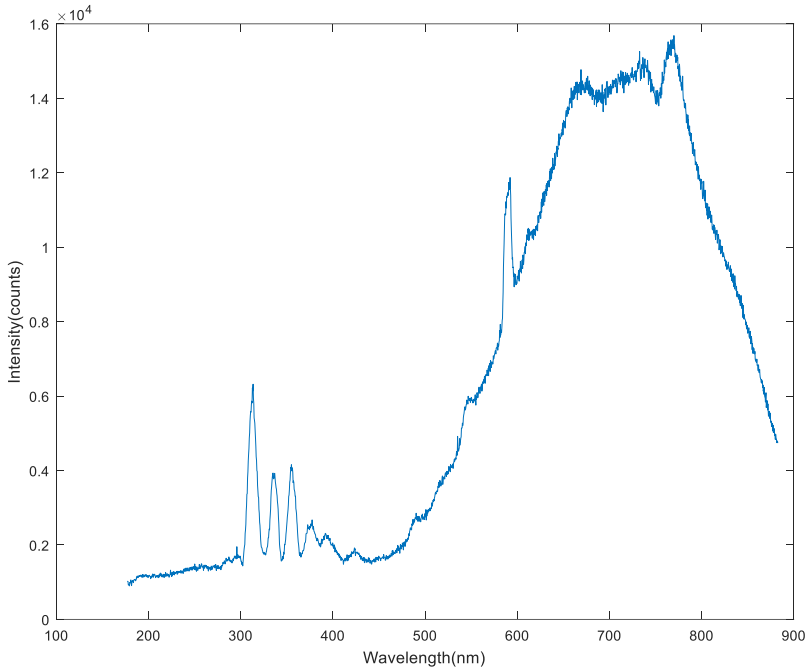

Fig. 7. 6 Spectral Line of Experiment 3

4) Experiment 4: 40 AWG solid copper and aluminum wire are used as arcing conductors. Both conductors are burned along with the arc flash. Spectral line of arc flash in experiment 4 is shown in Fig. 7.7.

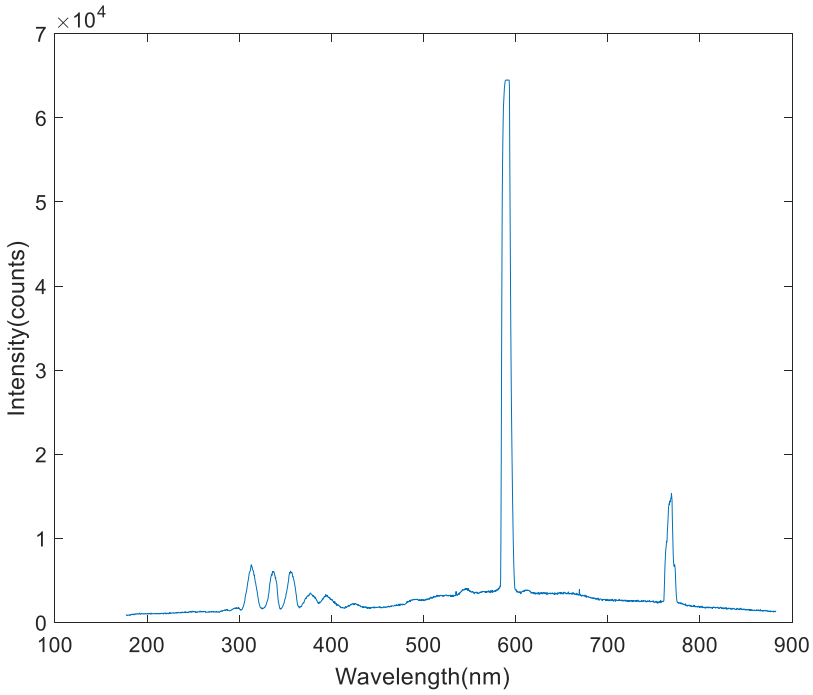

Fig. 7. 7 Spectral Line of Experiment 4

As the reference, Fig. 7.8 [12] shows the light spectrum for different light wavelengths. To show the distinct spectra of arc flash, Fig. 7.9 Shows the spectral line for all experiments. As it is shown, peaks are measured between 300 nm to 400 nm wavelength every time when arc flash happened. According to the study [13], most air fluorescence emission spectra are from ionized nitrogen, and Fig. 7.10 [13] shows the Nitrogen Fluorescence spectrum between 300 nm and 400 nm in dry air. Therefore, the identical spectra of arc flash between 300 nm and 400nm are mostly from ionized nitrogen. To distinguish the spectral line of arc flash from other light sources, spectral line of LED, fluorescent, and daylight under different environments are also measured which are shown from Fig. 7.11 to Fig. 7.13 respectively. In Fig. 7.13, direct daylight indicates spectrometer faces sunshine directly. Indirect daylights were measured under a shadow area by facing different directions. Each one of them was measured around the same time on a clear day.

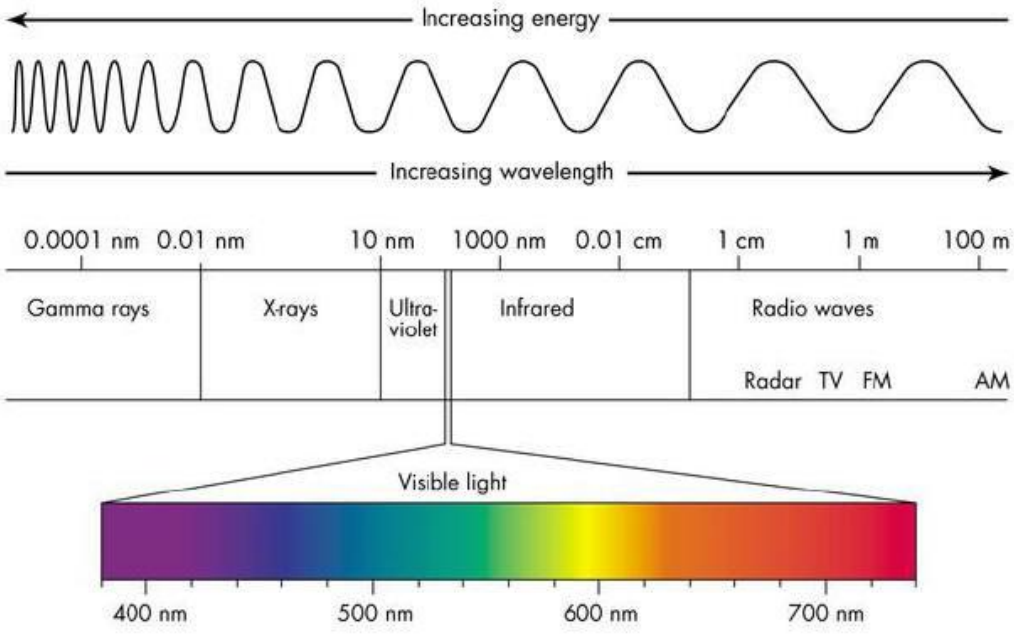

Fig. 7. 8 Light Spectrum [12]

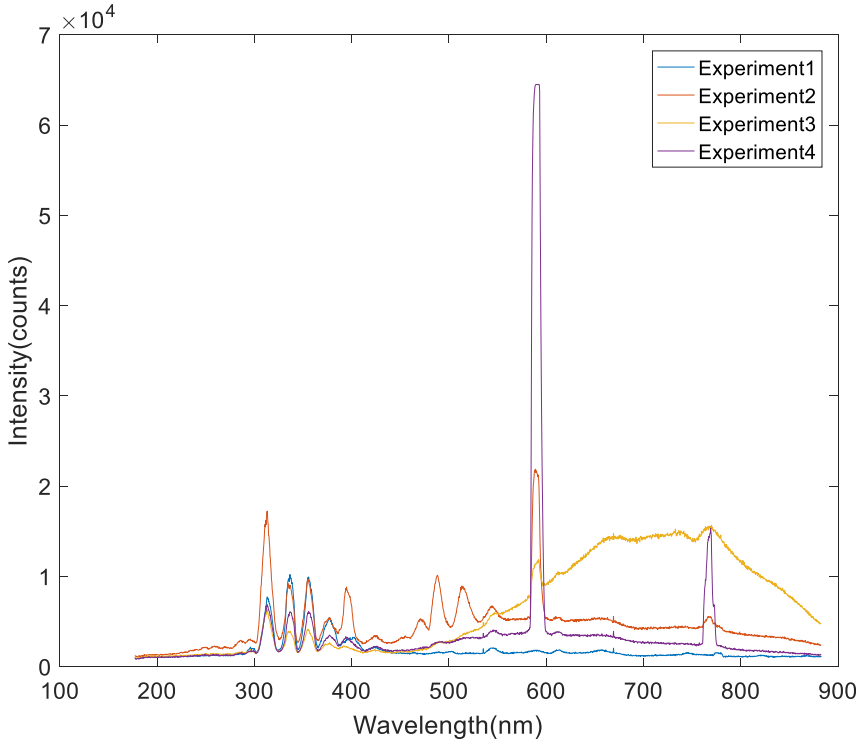

Fig. 7. 9 Spectral Line of Arc Flash for All Experiments

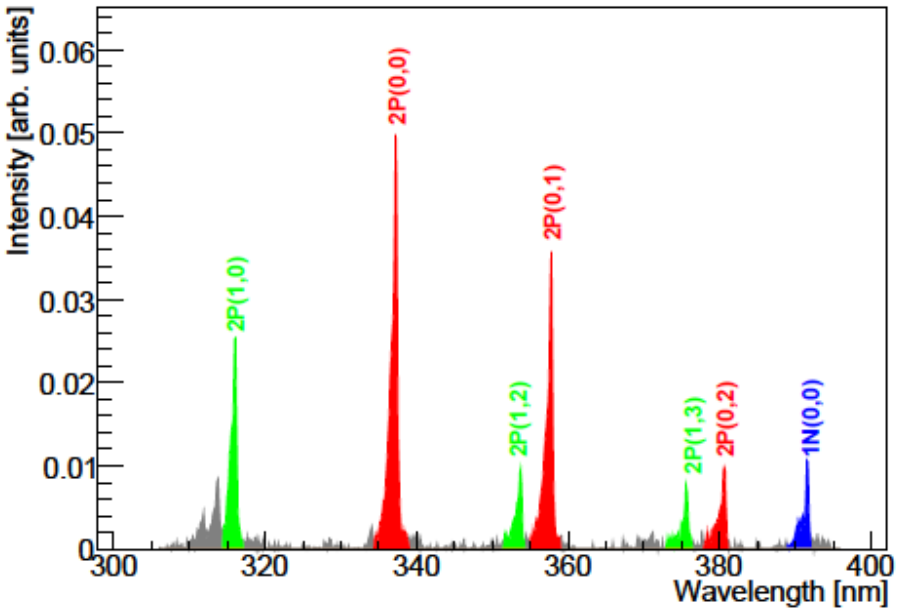

Fig. 7. 10 Nitrogen Spectrum Between 300 nm and 400 nm in dry air at 1013hPa [13]

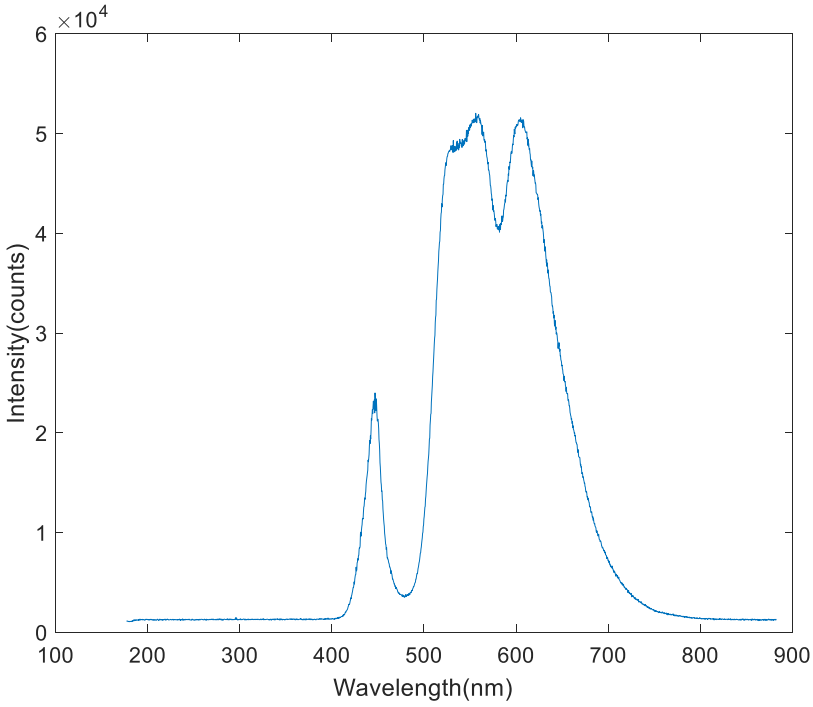

Fig. 7. 11 Spectral Line of LED Light

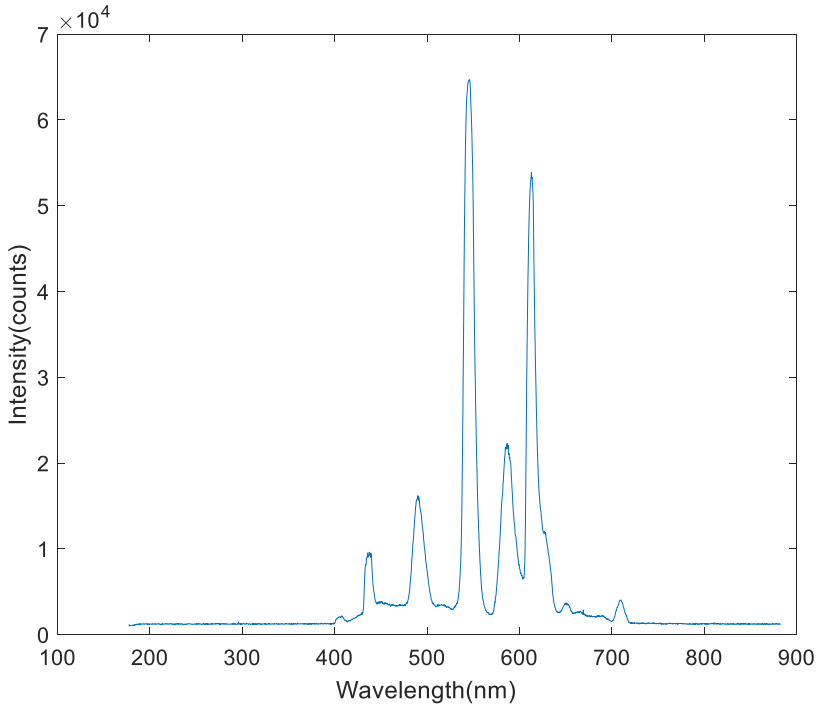

Fig. 7. 12 Spectral Line of Fluorescent Light

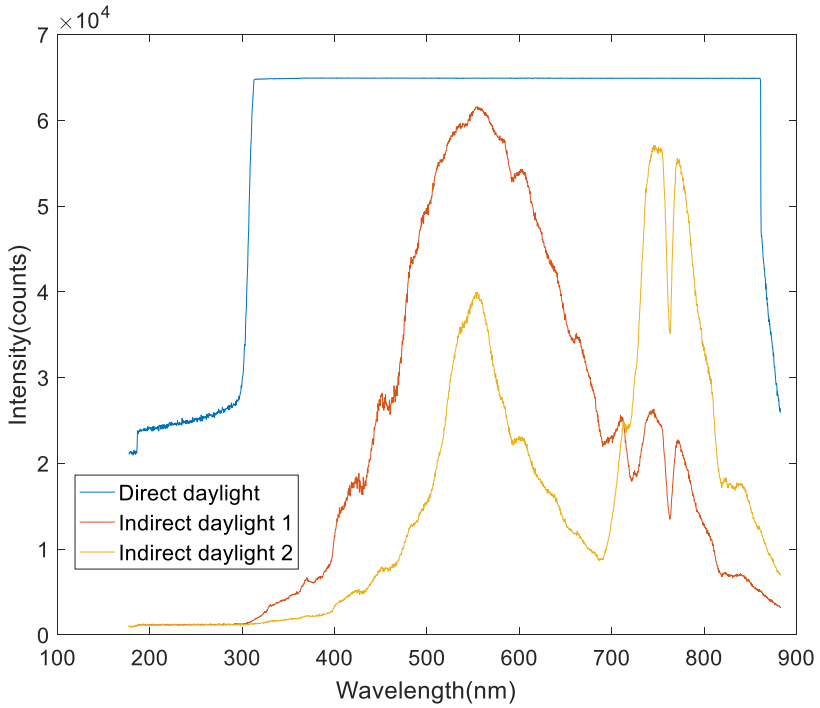

Fig. 7. 13 Spectral Line of Daylight

As it is shown from the spectral lines of different sources, copper and aluminum do emit distinct spectral lines. However, distinct UV pattern from ionized nitrogen is detected during the arc flash events regardless of the material of the conductors. Therefore, the distinct UV signature is considered as a trigger signal in the detection process.

7.3 ARC FLASH DETECTION ALGORITHM

To acquire the sufficient spectra signals from arcing light, a linear silicon CCD array sensor with 200 to 1100 nm range and 0.1 nm resolution is adopted in this study. Most importantly, this detector has 2.4MHz readout rate which could improve the speed of the detection significantly [14-15]. According to paper [6], the arc flash incident energy is proportional to the clearing time. Therefore, this proposed detection method shows the ability to reduce arc flash incident energy so that hazards could be mitigated. As an example of this CCD sensor application, the minimum integration time of the spectrometer that is applied in this study could achieve 1ms compared with 2ms for most light intensity sensors [15]. Due to the wide detection range, the linear CCD sensor has a better response for UV spectrum, which is extremely beneficial for the proposed arc flash detection application [14].

To provide positive arc flash fault detection with spectral data, an arcing fault detection algorithm is developed with General Regression Neural Network (GRNN) in this paper [16]. GRNN has been developed since 1991 for classification and prediction by using training datasets [17]. Because GRNN could be built up with less training samples, it makes GRNN more practical for measurement system applications [18]. To specify the identification of spectra during arc flash events, derivative of spectral line is calculated in (1).

Y: Spectra Intensity (Counts).

X: Wavelength of spectrum (nm).

D: Derivative of intensity to the wavelength of spectra.

$$D = \frac{\mathrm{d(Y)}}{\mathrm{d(X)}} \qquad (1)$$

7.3.1 The Derivative of Spectral Lines of Arc Flashes

Derivatives of spectral lines of all arc flash experiments are presented from Fig. 7.14 to Fig. 7.17.

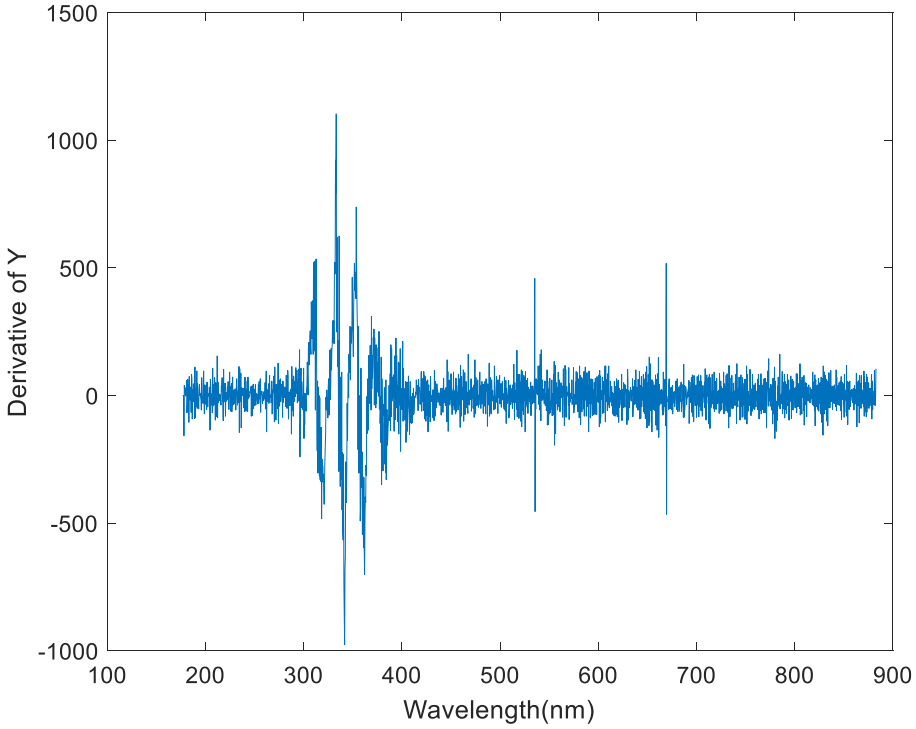

Fig. 7. 14 The Derivative of Y in Experiment 1

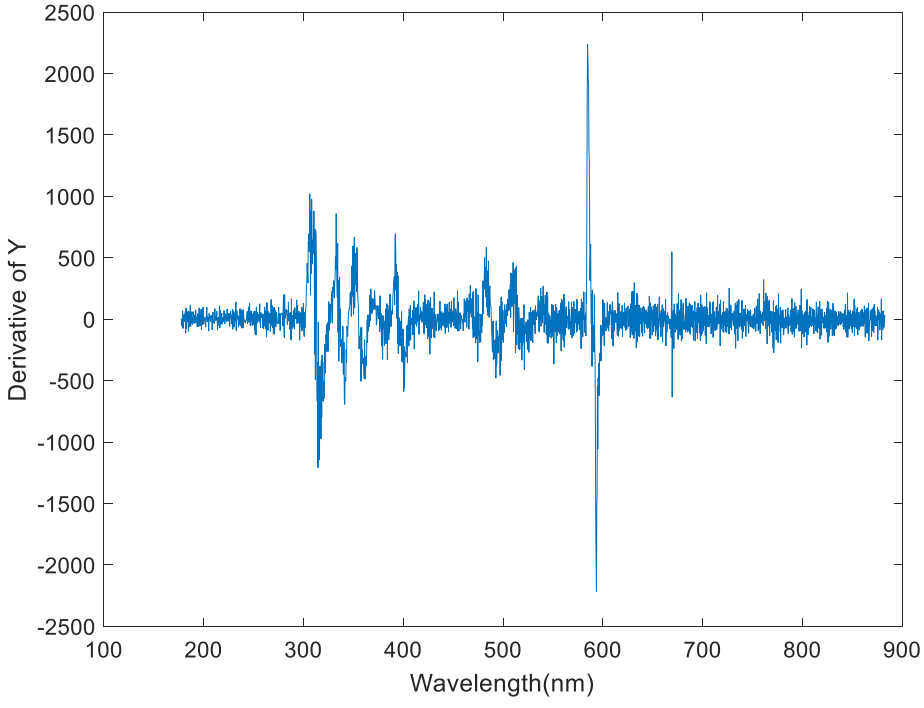

Fig. 7. 15 The Derivative of Y in Experiment 2

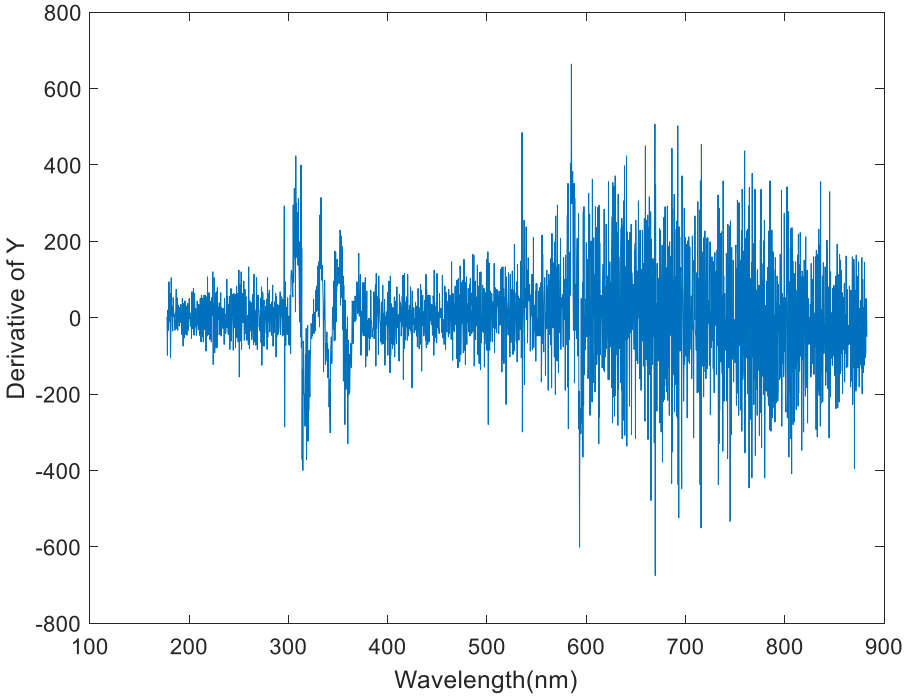

Fig. 7. 16 The Derivative of Y in Experiment 3

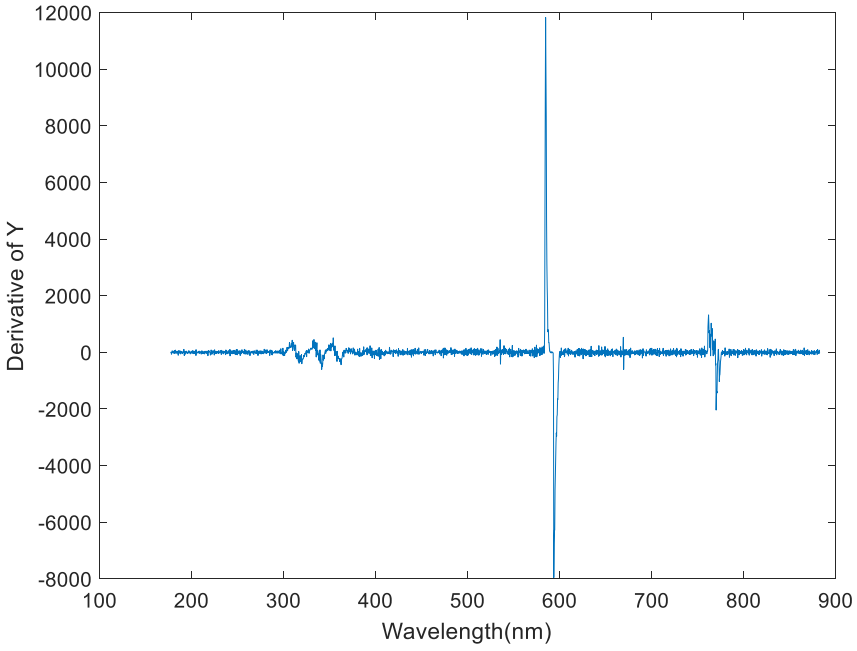

Fig. 7. 17 The Derivative of Y in Experiment 4

7.3.2 The Derivative of Spectral Lines of Ambient Light Sources

To differentiate the arcing lights and the different ambient light sources, derivatives of the spectral line of different ambient light sources are shown in Fig. 7.18 to Fig. 7.22.

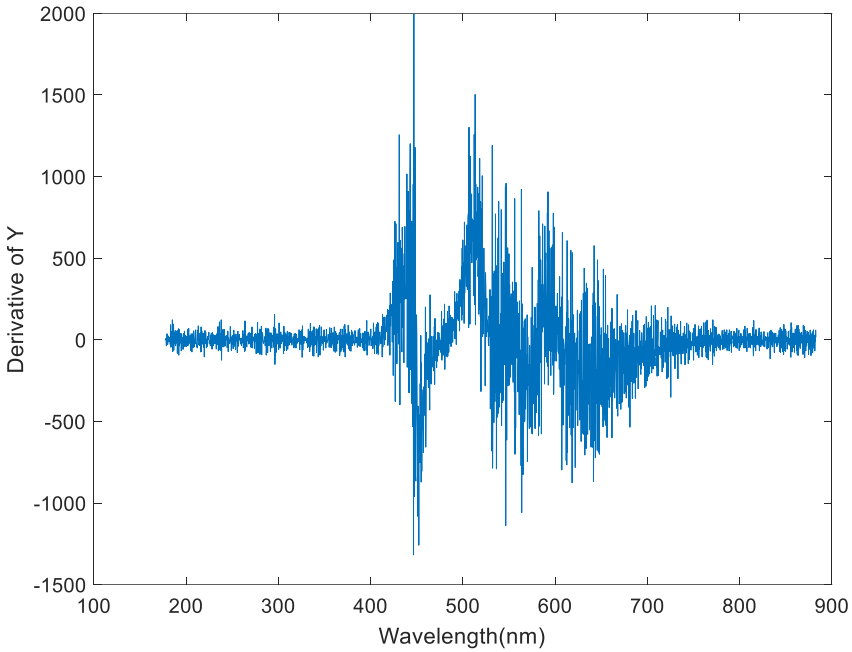

Fig. 7. 18 The Derivative of Y of LED

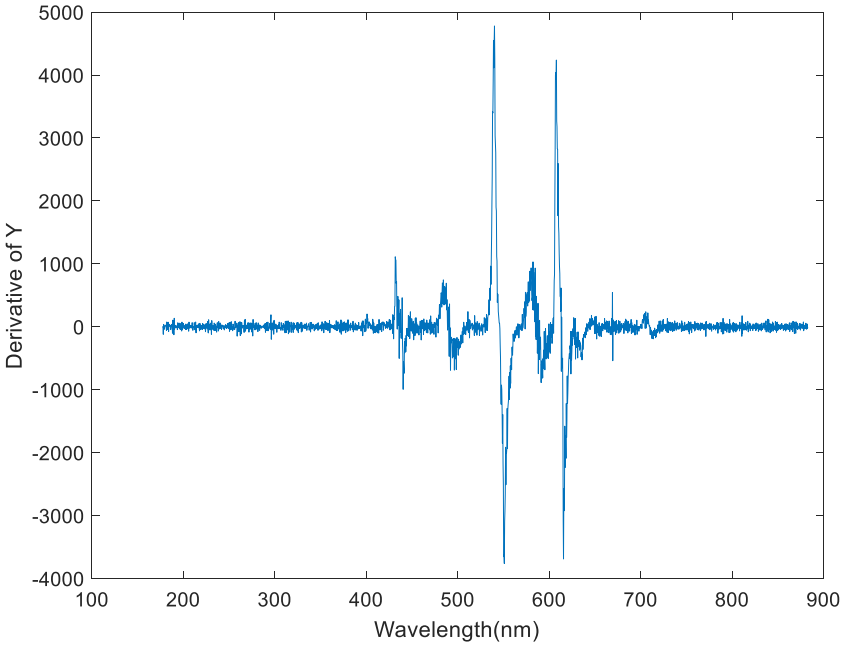

Fig. 7. 19 The Derivative of Y of Fluorescent

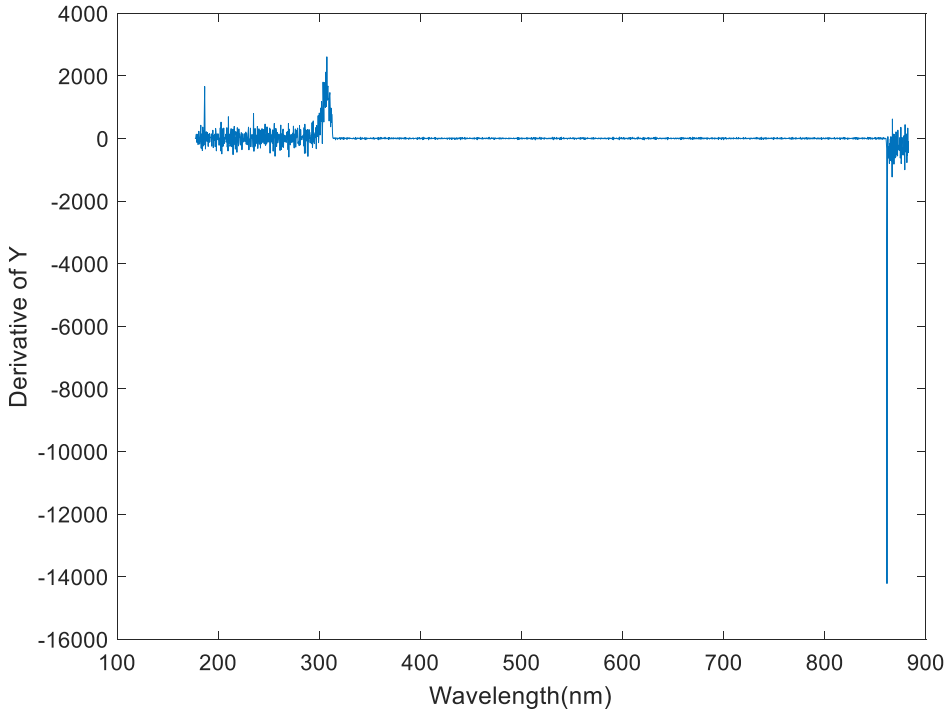

Fig. 7. 20 The Derivative of Y of Sunshine

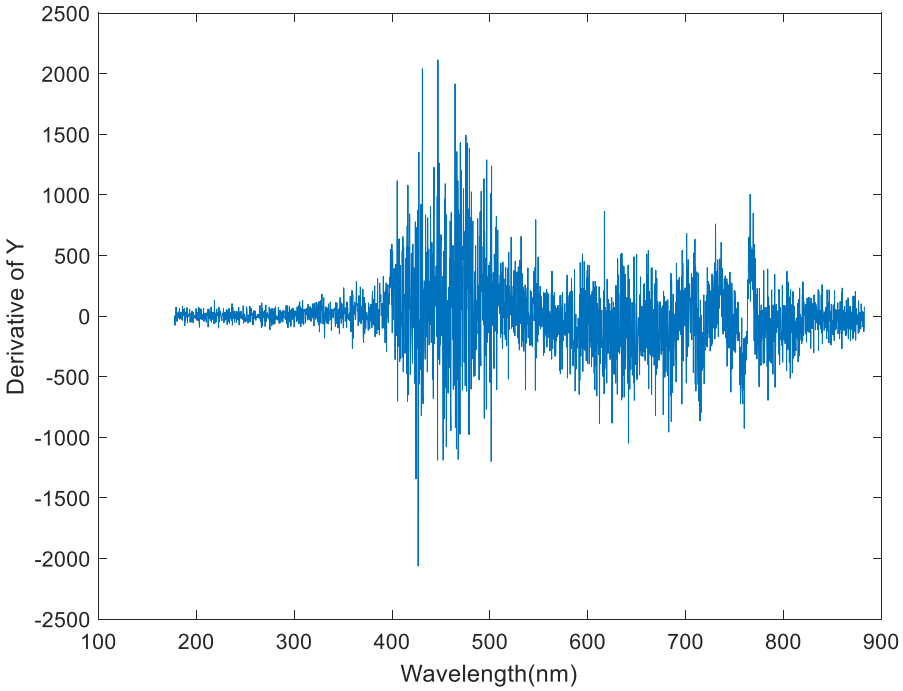

Fig. 7. 21 The Derivative of Y of Indirect Daylight 1(Shadow)

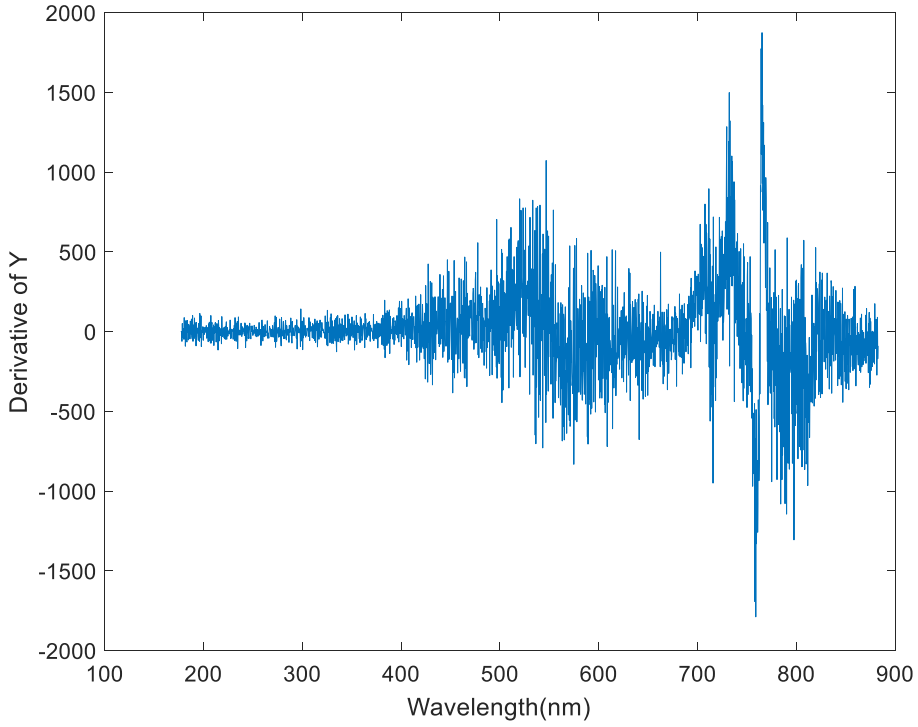

Fig. 7. 22 The Derivative of Y of Indirect Daylight 2 (Shadow)

7.3.3 General Regression Neural Network (GRNN)

As all the figures are shown previously, waveforms between 300nm to 400 nm is considered as a "Signature" spectrum for arc flash faults. To design a program that could identify the derivative of spectrum between 300 nm to 400 nm, GRNN is applied in this paper. Fig. 7.23 shows derivatives of spectra of arc flashes in all 4 experiments from 300 nm to 400 nm. To have the identical waveforms for arc flash detection algorithm, a Savitzky-Golay FIR smoothing filter [19] is implemented to filter out all the noisy data. Smoothed data is shown in Fig. 7.24.

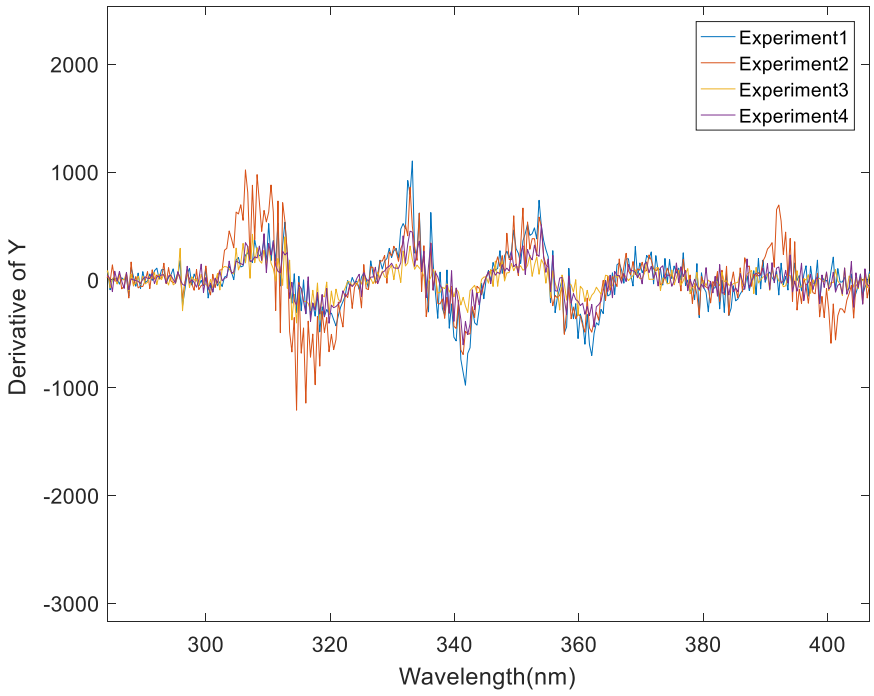

Fig. 7. 23 Derivative of Y from 300 nm to 400 nm

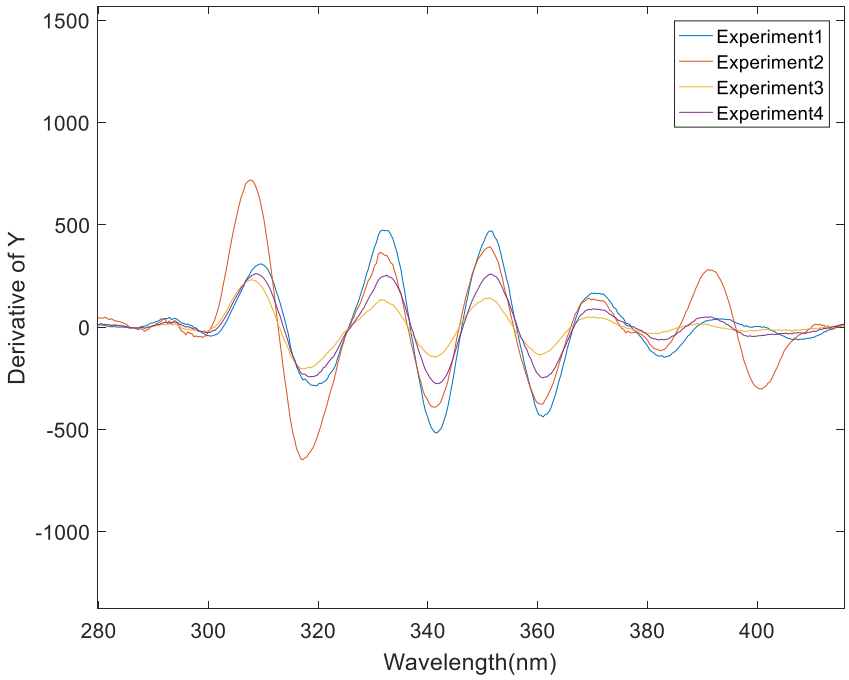

Fig. 7. 24 Filtered Derivative of Y from 300 nm to 400 nm

As shown in Fig. 7.24, smoothed waveforms for different arc flash experiments have similar patterns. General regression neural network (GRNN) is applied to detect the arcing event. In this study, a smoothed derivative of Y from 300 nm to 400 nm of arc flash experiments and other ambient sources are used as training samples. Fig. 7.25 and Fig. 7.26 shows the light spectra based arc flash detection method by using the GRNN.

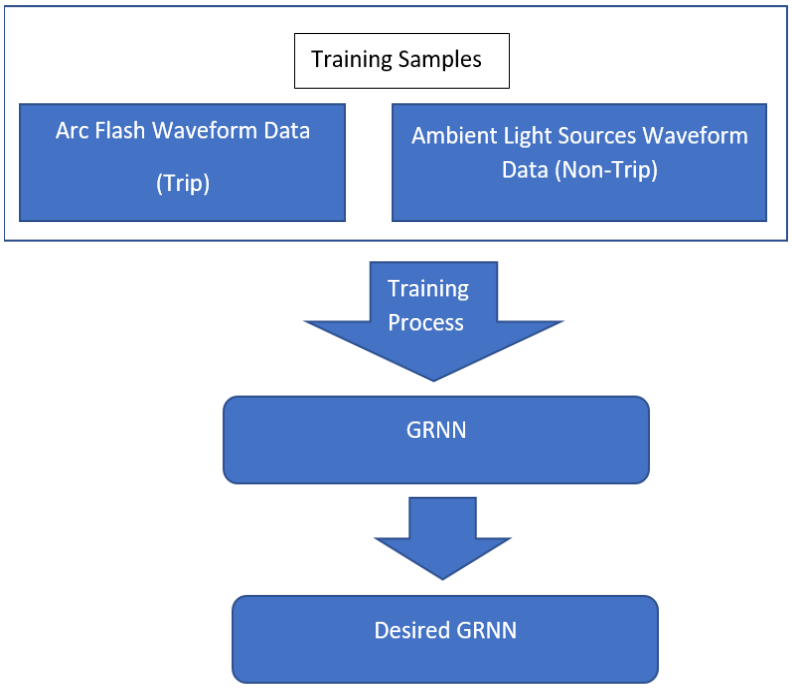

Fig. 7. 25 GRNN Training Process

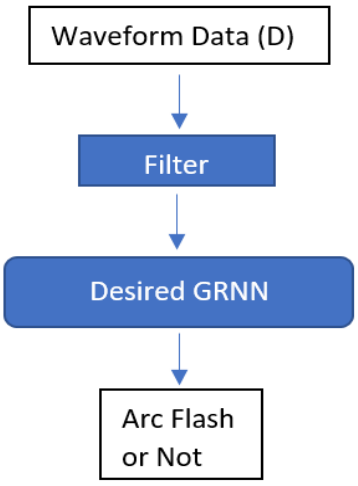

Fig. 7. 26 Detection Process with GRNN

After applying Savitzky-Golay digital filter, the characteristics spectra of arcing light could be identified by using GRNN without being affected by most common ambient light sources, and this could reduce the possibility of erroneous detection significantly. As the result, spectrum-based arc flash detection method shows a great prospect to be developed as an arc flash protection application to improve the speed, accuracy, and reliability of the detection operation.

7.4 CONCLUSIONS

Light spectrum-based arcing fault detection method is proposed in this paper. By using an optic spectrometer, the spectrum of arc flash faults under different circumstances are measured and analyzed. By comparing with the most common ambient light sources, ionized nitrogen spectral line between 300nm and 400nm are considered as potential spectrum signals for arc flash detection operations. With Savitzky-Golay FIR smoothing filter and GRNN, arc flash light spectrum lines could be implemented to provide detection signals. From computer simulation, the proposed spectrum-based arc flash detection method shows a great potential to be developed as an arc flash detection application with improved speed, reliability, and accuracy.

In the future, due to algorithm the identical emission spectrum of different elements, this spectrum-based approach could also be developed for fault identifications if different materials are used in different phases to enhance the operation of arc flash fault detection and protection.

7.5 REFERENCES

[1] Z. Zhang, W. Lee and D. A. Dini, "Grounding and Isolation of Sensitive Measurement Equipment for Arc Flash Testing at High-Power Laboratory," *IEEE Transactions on Industry Applications,* vol IA-51, pp 5281-5287, Nov/Dec 2015.

[2] R. Hasan, R. Mender and L. Steinberger, "Hybrid Arc Flash Protection Within Electrical Calefied Areas," *IEEE Transactions on Industry Applications,* vol IA-52, pp 3548-3556, Jul/Aug 2016.

[3] T. Faber, T.L. Schiazza, P. Megna, "Improvement in Passive Arc Flash Protection Through Limiting Arcing Duration", *Petroleum and Chemical Industry Conference - Record of Conference Papers*, pp. PCIC-2015-13, 2015.

[4] S. Rau, Z. Zhang, W. Lee, and D. A Dini "Arc Flash Visible Light Intensity as View from Human Eyes," *IEEE Transactions on Industry Applications,* vol PP, pp 1-1.

[5] J. C. Das, "Protection planning and system design to reduce arc-flash incident energy in a multi-voltage-level distribution system to 8 cal/cm2 (HRC 2) or less—Part II: Analysis", *IEEE Trans. Ind. Applicat.*, vol. 47, no. 1, pp. 408-420, 2011.

[6] R. A. Wilson, R. Harju, J. Keisala, S. Ganesan, "Tripping with the speed of light: arc flash protection", *Proceedings of the 60th Annual Conference for Protective Relay Engineers*, pp. 226-238, Mar. 27–29, 2007.

[7] G. Roscoe, M. Valdes, R. Luna, "Methods for arc-flash detection in electrical equipment", *Proc. IEEE Petroleum Chem. Ind. Conf. Rec.*, pp. 1-8, 2010.

[8] P. Parikh, D. Allcock, R. Luna, J. Vico, "A Novel Approach for Arc-Flash Detection and Mitigation : At the Speed of Light and Sound", *IEEE Trans. Ind. Appl.*, vol. 50, no. 2, pp. 1496-1502, 2014.

[9] B. Hughes, "Arc-flash detection prevents catastrophic damage", *IEEE IAS Electrical Safety Workshop (ESW)*, 2016.

[10] Premium-grade Reflection Probes, *Ocean Optics*, Available: https://oceanoptics.com/product/premium-grade-reflection-probes/

[11] Dection based on "light" What is a Fiber Optic Sensor ?, *Introductory Guide to Sensors Sensor Basic,* Available: http://www.keyence.com/ss/products/sensor/sensorbasics/fiber/info/

[12] W.J. Lee, Z. Zhang, S.H. Rau, T. Gammon, B.C. Johnson, J. Beyreis, "Arc Flash Light Intensity Measurement System Design", *IEEE Trans. Ind. Appl.*, vol. 51, no. 5, pp. 4267-4274, Sep./Oct. 2015.

[13] T. Waldenmaier, J. Blumer, and H. Klages, “Spectral Resolved Measurement of the Nitrogen Fluorescence Emissions in Air Induced by Electrons,” *Astropart. Phys*, 29, pg. 205-222, (2008).

[14] Spectrometers Fact, Ocean Optics, Available: https://oceanoptics.com/wp-content/uploads/OceanOptics_Spectrometers.pdf

[15] USB2000+ Data Sheet, Ocean Optics, Available: https://oceanoptics.com/wp-content/uploads/OEM-Data-Sheet-USB2000-.pdf

[16] D. Specht, "A general regression neural network," IEEE Transactions on neural networks, vol. 2, 1991, pp. 568-576.

[17] James. Brown, Mohd. Anwar, Gerry. Dozier, "An Evolutionary General Regression Neural Network Classifier for Intrusion Detection", *International Conference on Computer Communication and Networks (ICCCN)*.

[18] General Regression Neural Network (GRNN), *University of Wisconsin,* Available: https://minds.wisconsin.edu/bitstream/handle/1793/7779/ch2/pdf?sequence=14

[19] Savitzky-Golay filter, *MathWorks*, Available: https://www.mathworks.com/help/signal/ref/sgolayfilt.html

CHAPTER 8

GENERAL CONCLUSIONS

8.1 CONCLUSION

In this article-based dissertation, IoT-based applications in power systems are presented in six published research journal papers. Research areas of these applications include monitoring systems in power grids, demand-side management for both residential and commercial consumers, and arc flash protection in electric power systems.

In the first three research papers, IoT-based monitoring systems are developed for power substations at petrochemical facilities, power substations for large power grids, and holistic wind turbine monitoring, respectively. IoT platform provides real-time and remote capabilities for a monitoring system which are extremely critical in power system monitoring. These monitoring systems are developed on Hybrid FPGA-CPU controllers. because of the deterministic and parallel processing capability of FPGA, the overall performance of the monitoring system has been improved in terms of speed and accuracy. Meanwhile, as the hardware programmable device, FPGA enables developers to customize and modify the monitoring objects without purchasing other devices. Therefore, this development provides a cost-effective solution for power industry monitoring. In Chapter 2, the monitoring system for petrochemical facilities, different detection mechanisms including SSO detection are programmed in the system. In Chapter 3, the second monitoring system for power substations, task allocations, and different communication methods are discussed to improve the overall performance of this system. In Chapter 4, the holistic monitoring system for wind turbine provides a novel solution for wind turbine condition monitoring and SSCI detection at the same time. It could avoid the catastrophic failure of the wind turbines and reduce the downtime.

In Chapter 5 and Chapter 6, DSM at residential and commercial levels are discussed. To realize real-time price DSM programs, the IoT platform is required to provide real-time data communication capability. To develop effective online DSM programs, offline DSM needs to be studied first. As one of the most commonly applied DSM programs, TOU has been applied in many countries. In Chapter 5, real smart meter data from Shanghai, China, and New York City, USA are analyzed from different aspects. According to the literature review and data analysis with the smart meter data, we found that current Time-of-Use (TOU) is not as effective as people expect. To improve the effectiveness of TOU, a special pricing mechanism is studied with a marketing psychology perspective. By analyzing the current zero pricing TOU program at Texas, zero pricing TOU program has been found that it has a special impact on consumer's behavior. Both benefits for consumers and utility companies are discussed. In Chapter 6, the DSM potential for commercial consumers is analyzed with real smart meter data and real TOU rates from New York City. In this study, the financial benefit is studied considering the power demand characteristics of

commercial consumers and the application of energy storage. The study shows that DSM has great potential to benefit commercial consumers with energy storage applications. These two research papers could be applied to IoT-based DSM programs in real-time Demand Response.

In Chapter 7, the light spectrum of arcing fault is applied to detection the arc flash events. Comparing with the traditional detection mechanisms, this developed approach improves the accuracy and speed of the detection. When arc flash happens, the nitrogen in the air will be ionized. The ionized nitrogen has identical spectral waveforms which can be used as arc flash detection signals. This study adopted the General Regression Neural Network as the detection algorithm. The result shows that detection accuracy and speed are satisfied. This development can be applied with multiple sensors at different locations using the IoT platform in a protection system for automatic control, monitoring, and event analysis.

8.2 THE FUTURE RESEARCH DIRECTION

In this article-based dissertation, IoT-based applications in power system monitoring, power system demand-side management, and power system protection are presented in 6 published journal articles. As the most important component of smart grid development, IoT provides the platform which enables data transfer without time and location limitations.

In the first part of this research, the application of an IoT-based monitoring system can be expanded to different monitoring and control systems with desired purposes. In future research, more related data such as weather, solar radiation, and power demand can be collected and integrated using this development to improve the overall monitoring. Therefore, efficiency, reliability, and resilience of the power grids can be enhanced.

The second part of this research can be implemented for real-time DSM program design. As one of the most adopted DSM programs, the TOU program was discussed and studied in the published two research papers. For residential consumers, special pricing mechanisms need to be considered to lead consumers' electricity consumption behavior. Based on this research outcome, A location-dependent mathematic model can be developed to improve the effectiveness of real-time price DSM in the future. At the same time, the research result of this study shows that commercial consumers can benefit from participating TOU program considering energy storage. With the development of smart appliances and energy storage, real-time price DSM programs would provide more opportunities for commercial consumers to participate in the electricity market and benefit from it. However, without IoT technology, real-time DSM are not able to be realized.

In the last part of this research, the light spectrum is used for arcing fault identification. Comparing with the traditional detection methods which are using overcurrent relay and light intensity sensor, our

development is more accurate and reliable. Meanwhile, it has great potential to enhance fault detection speed. This research established a fundamental approach for arcing fault detection using the light spectrum. In future research, IoT can be adopted to build a protection network with multiple spectrum detection sensors. Those sensors will be installed at different locations of the system to provide more detailed information for protection engineers to do online and offline event analysis. Meanwhile, light spectrum measurement has been extended to arc fault type identification which has been published in a conference paper.